UNIVERSITY OF SOUTHAMPTON

DEPARTMENT OF ELECTRONICS

OPTICAL FIBRES FOR COMMUNICATIONS:

MANUFACTURE, PROPERTIES AND APPLICATION

BY

STEPHEN ROY NORMAN

A thesis submitted for the degree of
Doctor of Philosophy
March 1981

TABLE OF CONTENTS

UNIVERSITY OF SOUTHAMPTON

ABSTRACT

FACULTY OF ENGINEERING AND APPLIED SCIENCE
DEPARTMENT OF ELECTRONICS

Doctor of Philosophy

OPTICAL FIBRES FOR COMMUNICATIONS: MANUFACTURE, PROPERTIES, AND APPLICATION

by Stephen Roy Norman

The successful application of optical fibres to wideband communications demands the utilisation of fibres exhibiting very low attenuation and high bandwidth at the wavelength of operation. This thesis describes an experimental study of the homogeneous chemical vapour deposition (HCVD) technique, a convenient process for the manufacture of ultra-pure waveguide glasses. Objectives of the programme included the development of technologies which could be adopted by industry for the routine manufacture of high-quality optical fibres. Aspects of the work have included not only optimisation of the HCVD and fibre-drawing processes but also the development of protective coatings which preserve the physical and optical performance of the fibres.

A lathe-based system has been constructed for the manufacture of optical-fibre preforms by HCVD, and evaluation of fibres prepared by HCVD has led to the development of ternary phosphogermanosilicate glasses for use as the core glass in multimode fibres. The fibre drawing operation is described, and, in particular, it is shown that the addition of a fibre diameter measuring system led to important refinements to the preform-manufacturing and fibre-drawing processes.

Multimode graded-index fibres have been produced in lengths in excess of 5km, with numerical apertures up to 0.25, attenuation as low as 0.8 dB/km, and intermodal dispersion as low as 0.3 ns/km; fibres suitable for operation in the 1.3 μm and 1.55 μm regions have been prepared. The versatility of the HCVD process has enabled low-loss monomode fibres to be fabricated. In addition, a monomode fibre having a linear birefringence of less than 3°/m has been manufactured for transducer applications; this represents the lowest value reported to date for the birefringence of an optical fibre.

Techniques have been developed for the application of a surface-protective coating to fibres in-line with drawing. Using a thick primary coating of a thermosetting silicone elastomer, it has been possible to maintain the high inherent strength of freshly-drawn fibres without degrading their optical performance; a median tensile strength of 5.2 GN/m^2 was obtained in 1.0m gauge-length samples. An experimental evaluation of materials suitable for providing a tough outer jacket over primary-coated fibres is described. An extrusion line has been developed for applying thermoplastic jackets, and by using nylon-6 as the jacketing material, it has been possible to provide an excellent degree of microbending resistance and mechanical protection without compromising the fibres' performance.

Suitably protected graded-index fibres have been cabled and installed in a particularly severe environment, where they form part of an optical link transmitting video signals and high bit-rate digital data. The performance of the fibres within the link surpassed initial expectations, and confirmed the capabilities of the fibre-manufacturing technology.

CHAPTER 1: INTRODUCTION

The demand for ever-increasing bandwidth in medium- to long-distance communication systems has led to an exponential growth in the research and development of optical communications systems using optical fibre waveguides as the transmission medium. Such has been the pace of development over the last decade that trial systems have been installed in many countries and are carrying regular telecommunications traffic on a reliable basis. Indeed, plans are already well advanced for the installation of a 140 Mb/s optical fibre network within the U.K. to link the new System X trunk telephone exchanges.[1]

The widespread interest in optical fibre systems stems from the many advantages that they offer compared with conventional metallic cable systems. These advantages centre around the greatly increased bandwidth associated with the use of optical carrier frequencies, potentially ultra-low loss, freedom from electromagnetic interference (EMI), low weight and bulk for a given capacity, and intrinsic safety when operating in hazardous environments. As an illustration of their considerable attractions, compare a digital trunk telecommunications system operating at 140 Mb/s (1920 voice channels) over conventional coaxial cable with an optical fibre system operating at the same bit-rate. The highest quality coaxial conductor currently available is 9.5mm in diameter, and would require repeaters spaced at 2km intervals. In contrast, a graded-index multimode fibre operating at 0.85μm would be able to operate without regenerators over distances of 10km, and in its protected state would be approximately 1mm in diameter. Even at the present day costs of small-scale production of graded-index fibres, the 140 Mb/s optical fibre system is cost-competitive with the coaxial system. Furthermore, by utilising the 1.55 μm wavelength region in which the attenuation of silica-based fibres can reach a minimum of 0.2 dB/km[2], future systems employing single-mode optical fibres could sustain regenerator spacings of the order of 100km[3].

This thesis describes work undertaken during the period 1975 to 1980, during which time the proliferation of developments in optical fibres was ever-increasing. The primary objective of the programme was to develop manufacturing processes which would yield high-quality optical fibres on a routine basis, and which could be adopted on an industrial scale for the manufacture of fibres for use in telecommunications cables. The research programme has therefore been concerned largely with the technological aspects of fibre manufacture, rather than the more fundamental topics of glass technology and waveguide propagation. The thesis reports several aspects of research covering fibre manufacture, characterisation, strengthening of fibres by the application of protective coatings, and incorporation of fibres into a novel cable. To illustrate the capabilities of the processes, an application of graded-index multimode fibres in an optical communications system installed in a particularly severe environment is described. As an off-shoot of the work on fibre manufacture, a particular type of single-mode fibre exhibiting extrememly low polarisation birefringence has been developed, and a brief description of its manufacture and properties are included. The success of the development of the manufacturing processes has led to the transfer of technology to industry where the same techniques are being employed in the large-scale production of fibre. Hence, it is intended that the thesis should not only present results of the research programme, but should also act as a reference for the future use of industry adopting the technology.

1.1 Historical Background to the Research Programme

More than any other development, it was the advent of the laser in the early 1960s that made high-capacity optical communications a real possibility, and the laser's potential in telecommunications was soon recognised. Although initial efforts were directed towards the use of atmospheric optical communications, it was clear that line-of-sight restrictions and atmospheric scattering would severely limit the usefulness of such systems, and attention switched to guided systems in which the optical carrier was constrained within a transparent conduit (or light pipe) containing re-focusing elements appropriately spaced along the length of the pipe. Whilst being technically feasible, the costs of this approach precluded it from serious consideration for most telecommunications systems.

In 1966 Kao and Hockham, in a classic paper[4], proposed that the optical carrier could be transmitted over optical fibres, and that although the attenuation was typically 1 dB/metre at that time, this was due mainly to the presence of transition metal impurities within the glass. They suggested that reduction of the impurity levels would allow attainment of losses much lower than those typically encountered. In another important paper[5], published in 1969, Kao demonstrated that synthetic silica having transmission losses as low as 5 dB/km was commercially available, and soon after single-mode fibres having a core of titania-doped silica in a silica cladding with losses below 20 dB/km were reported[6]. This result prompted developments in many countries and further breakthroughs came with the modified chemical vapour deposition technique developed independently by workers at Southampton University[7] and Bell Laboratories[8].

Although the Bell workers utilised the already known properties of boric-oxide-doped silica to form the cladding of a fibre having a silica core[9], the Southampton work disclosed the discovery of phosphosilicate glass as a suitable material for use as the core of a silica-clad fibre. The logical development of a phosphosilicate-core, borosilicate-clad fibre was to follow from Southampton University[10] in the early stages of the current research programme. At that time it was possible, with care, to manufacture fibres having minimum losses of the order of 3dB/km in lengths of up to 1 km. The process control was inadequate, and it was therefore difficult to guarantee parameters such as core size, core/cladding diameter ratio, refractive index profile, bandwidth and loss. Furthermore, the fibres were not protected from abrasion or chemical attack, and were too weak to be incorporated into a cable structure.

In contrast, at the completion of the present programme, fibres have been drawn in lengths in excess of 5 km, losses as low as 0.8 dB/km have been achieved, and the control of refractive index profile, bandwidth and fibre geometry have been significantly improved. Furthermore, technologies have been developed for protecting the fibres both mechanically and optically, and the manufacturing technology has been adopted on an industrial basis by the world's largest cable-manufacturing group.

1.2 The Main Research Topics

1.2.1 Low-loss Fibre Manufacture

The many methods for the manufacture of low-loss optical fibres generally derive from one of two fundamental approaches to the preparation of high-purity glasses, viz, soft-glass preparation by the melting of raw materials, and preparation of silica-based glasses by a chemical vapour deposition (CVD) process. This study has concentrated solely on the latter because it offers greater versatility in the fibre design and choice of material without the need for a large investment in glass-melting equipment. Using the so-called modified CVD (MCVD) or homogeneous CVD (HCVD) process, fibre is produced in two separate operations, the first involving the preparation of a composite blank or preform having the same geometrical and optical configuration as the resultant fibre. The preform is subsequently elongated at high temperature in a drawing-down operation to form the optical fibre.

1.2.1.1 Preform Manufacture by HCVD

The HCVD process offers a very elegant solution to perhaps the greatest problem facing the successful application of optical fibre communications, namely the preparation of high purity glasses having very low levels of transition metal impurities. By purifying the volatile halides of silicon and other glass forming elements (e.g. phosphorus, germanium and boron) using simple distillation and separation techniques, it is possible to obtain ultra-pure halides having transition-metal impurity levels as low as 10 parts per billion (ppb)[11]. In the HCVD process, vapours of the halides are oxidised at high temperature within a silica tube, and the oxides are deposited as a glassy layer onto the wall of the substrate tube. The silica tube provides a high purity environment for the reaction and the deposited glass therefore has a purity comparable to that of the source chemicals. In addition, by adjusting the composition of the reactant gas stream it is possible to control the rate of deposition and the refractive index of the deposited material[12].

Hence to produce an optical fibre preform, an appreciable thickness of glass having a defined refractive index distribution is built up by the successive deposition of many glass layers of controlled thickness and refractive index[7]. The temperature of the silica substrate is then raised above its softening point and the composite tube collapses under surface tension forces into the solid preform which is later drawn into fibre.

During the course of this study an HCVD system for the routine production of both multimode and monomode-fibre preforms has been developed[12]. The inexpensive system offers great flexibility in the choice of glass composition, deposition rate and deposition temperature. A study of the deposition process has been undertaken and developments in the control of the glass composition and deposition rate have enabled a broad spectrum of fibres to be produced for experimental purposes. Thus long lengths (>5km) of multimode graded-index fibre having losses below 1 dB/km and band-widths in excess of 1.0 GHz km have been manufactured on the same equipment as step-index fibres having a 300 μm core diameter! Similarly, without the need for modification to the equipment, preforms have been produced for drawing into monomode fibres operating in the 0.85 μm and 1.3 μm regions. To assess the repeatability of the process more than twenty multimode graded-index preforms have been produced under similar conditions. The characteristics of the fibres drawn from the preforms have been compared and some of the fibres have been employed in a 5.3km optical fibre link.

Chapter 2 describes the HCVD process in detail and covers the manufacture of both the multimode- and monomode-fibre preforms. Rather than itemising the improvements to the equipment and process technology in a chronological fashion, the chapter discusses the common glass systems which can be manufactured by HCVD, describes the deposition equipment developed by the author, reports the results of a systematic study of the main process variables, and finally illustrates the application of the process to the manufacture of a variety of preform configurations. By presenting the work in this form it is hoped that the reader will obtain an understanding of the process and of the significance of the research programme's contribution to the present 'state of the art'.

1.2.1.2 Drawing of Silica-based Fibres from HCVD Preforms

Fibre drawing is, in principle, a very straight-forward operation and is performed on a purpose-built machine comprised of three sub-units[13]. The preform is gripped in a driven crosshead and is fed into a furnace having a graphite resistance-heating element. The furnace temperature is raised above the softening point of the preform and the fibre is drawn from the end of the preform on to a winding drum having an accurately controlled take-up speed. Important parameters affecting the stability of the operation are the temperature stability of the furnace and the speed stability of the feeding and winding systems. At the outset of this project fibre diameter was maintained at a near-constant value by electronically interlocking the motor controllers for the feeding and winding systems[13]. However, whilst this system operates satisfactorily for a uniform preform, diameter variations along the length of a preform will produce a corresponding variation in the fibre diameter. Hence, an important aspect of the current work has been the addition of a fibre diameter measuring system to the fibre drawing machine and its incorporation in a feedback loop to control the fibre diameter.

As will be shown in Chapter 3 the addition of the diameter measuring system led to the discovery of several sources of fibre diameter noise, and investigations of these effects led to an improved furnace design. Also the importance of preform surface finish was established and led to improvements in the preform manufacturing process. On completion of the study 4km lengths of fibre had been drawn with less than $\pm$ 1 μm diameter variation in an overall fibre diameter of 125 μm, a result previously only possible when drawing fibre from high-quality silica rod. The improvement in fibre diameter control has been accompanied by a reduction in the wavelength-independent excess loss commonly associated with diameter fluctuations, and has led to a reduced variance of attenuation from fibre to fibre.

1.2.2 Characteristics of Fibres Made by the HCVD Process

As outlined above, the HCVD technique has been applied to the manufacture of multimode and monomode fibres having a number of end-uses. The further development of the manufacturing techniques has resulted in a marked improvement in the quality and yield of fibre. Chapter 4 describes the principal optical characteristics of the various types of fibre, and illustrates the results that have been brought about by the optimisation of the waveguide glass systems and the processing conditions.

As a major aspect of this work has been the development of low-loss graded-index fibres for telecommunications, the geometrical and optical characteristics of such fibres are discussed in depth. It is shown that by employing the P_2O_5-GeO_2-SiO_2 glass system as the core glass of graded-index fibres, very high quality fibres can be manufactured having excellent geometrical properties, very low loss over the 0.8 μm to 1.7 μm wavelength region and very high bandwidth at the wavelength of operation. Core ellipticity and core/cladding eccentricity have both been reduced below 1% in graded-index fibres having a 63 μm core in a 125 μm diameter. Numerical apertures of 0.23 are readily achieved without introducing excessive stress into the fibre. Spectral attenuation measurements show that the level of transition metal impurities within the fibres has been reduced to negligible levels, and that in some cases the OH ion absorption peak centred at 0.95 μm has been reduced to less than 0.2 dB/km. Thus attenuation levels of less than 3.0 dB/km at 0.85 μm and less than 1.5 dB/km at 1.06 μm have been achieved; extended measurements into the infrared show that the attenuation falls to even lower levels in the 1.3 μm region where material dispersion effects fall to a minimum, and that the fibres should be capable of 'second' and 'third-window' operation. The P_2O_5-GeO_2-SiO_2 glass system has allowed more accurate refractive index profile control than the P_2O_5-SiO_2 system, and by creating a germania-rich environment in the closure zone during preform collapse, the out-diffusion of dopant from the innermost core layers has been almost eliminated.

Bandwidth measurements on graded-index fibres have been made using time-domain measurement of pulse dispersion in the 0.85 μm region. Intermodal dispersion as low as 0.3 ns/km has been achieved in some fibres, although 1.0 ns/km would be more representative of the mean. Pulse dispersion measurements over a broad wavelength range (0.75 μm to 1.35 μm) are reported for one fibre[15]. The results indicate that the refractive index profile of this fibre cannot be described by a single exponent α in the equation.

$$n(r) = n_1 \left[1 - 2\Delta\left(\frac{r}{a}\right)^{\alpha}\right]^{\frac{1}{2}}$$

where n_1 = refractive index at r = 0
a = core radius
Δ = relative index difference between core and cladding.
α = power law exponent characterising the profile.

More accurate control of the refractive index profile near the core/cladding interface should lead to an improvement in the bandwidth performance of the fibres.

In single-mode fibres designed for telecommunications purposes, bandwidth is limited (to the first order) by material and mode dispersion effects[16]. The system used for the measurement of pulse dispersion in multimode fibres has insufficient resolution for the measurement of material and mode dispersion in relatively short monomode fibres (<3km), and therefore the measurements presented on single-mode fibres are confined to geometrical measurements, attenuation measurements and measurement of normalised frequency, or V-value. It has been found relatively easy to manufacture low-loss monomode fibres for 0.85 μm operation using the HCVD technique[12]. Measurements in the 1.0 μm to 1.7 μm region show that the attenuation level of these fibres is capable of further reduction by the elimination of OH ions within the deposited material and by reduction of the wavelength independent losses in the fibre.

Monomode fibres are also finding applications in instrumentation, where their ability to transmit coherent polarised light is most attractive. In one application [17] the current travelling in a busbar is measured by monitoring the Faraday rotation of polarised light propagating in a monomode fibre wound around the conductor. As the sensitivity of this instrument is limited by the residual birefringence of the fibre, a systematic study of the causes of birefringence has been undertaken and a monomode fibre exhibiting less than 3°/metre linear retardance has been developed[18], and has been incorporated into an operational current measuring system.

1.2.3 Protective Coatings for Optical Fibres

For optical fibres to be successfully incorporated into telecommunications cables without breakage or degradation of optical characteristics, it is necessary to protect them in such a manner that they can withstand the limited tensile loads applied during cabling and be isolated from asymmetric lateral forces which cause microbending losses[19]. Chapter 5 describes a two stage approach to this problem, firstly, to apply a protective 'primary' coating to the fibres in line with drawing so as to preserve their inherent strength, and, secondly, to apply an extruded 'secondary' coating of a thermoplastic material off-line to reduce the fibres' sensitivity to microbending losses[19].

1.2.3.1 Primary Coatings for Optical Fibres

It is well known that the high-temperature fibre-drawing operation can produce a pristine fibre surface free of stress concentrating flaws (Griffiths microcracks) and that freshly-drawn fibres can exhibit strengths approaching 7 GN/m^2. The subsequent introduction of flaws by handling, abrasion, or atmospheric attack will reduce the strength by a factor of 20 or more. Hence to optimise the strength of our fibres, techniques for on-line coating of the fibre have been developed to preserve the pristine surface condition of the newly-drawn fibre and maintain its high initial strength throughout its operational lifetime.

The requirements of the primary coating have been defined and various coating materials have been characterised. It was found difficult to apply solvent-based coatings in reasonable thickness within the normal range of fibre drawing speeds[12]. Although the first-choice material, polyorganosiloxanes, gave most encouraging initial results, problems of solvent evaporation led to the selection of an alternative, solventless, silicone rubber for use as the primary coating. Coatings of up to 80 μm thickness have been applied over long lengths of 125 μm fibre, and it has been possible to achieve a uniform coating which has not affected the fibres' optical performance. Concentricity between fibre and coating has been improved by employing tapered-nozzle coating tips, and by reducing the ratio of the overall coating diameter to the fibre diameter; minimum coating thicknesses of approximately 40 μm are typical.

Significant improvements in fibre strength have been obtained and some preliminary investigations of the flaw distribution have been completed. Tensile strength measurements on samples taken at random from lengths of primary-coated graded-index fibres have shown a bimodal Weibull strength distribution characterised by a high-strength region of modulus 'm' $\sim$25, and a low-strength 'tail' of m $\sim$11.

The low-strength tail gives a rather broad distribution of flaw sizes which is characteristic of fibres drawn in graphite resistance-heated furnaces. Nevertheless, median strengths of 5.2 GN/m^2 in 1.0m lengths of fibre have been achieved; mean breaking loads in excess of 60 N have been obtained in 125 μm diameter fibres, compared with about 6 N in bare fibres subjected to normal handling before testing.

1.2.3.2 Secondary Coatings for Optical Fibres

Gloge has shown[19] that surprisingly small external forces can cause lateral deformation, mode coupling and microbending loss in optical fibres. To cable fibres without significant increase of attenuation it is therefore necessary to isolate the fibre from distortion by the application of a suitable protective jacket. The choice between a tightly adherent jacket or a loosely fitting jacket around the fibre depends very much on the modulus and thickness of both the primary coating and the jacket itself. An experimental evaluation of materials suitable for jacketing of silicone rubber primary-coated, graded-index fibres has been undertaken. It was found that conventional extruders used for insulating metallic conductors were generally too big for use with optical fibres. A new jacketing line incorporating a small extruder was commissioned for use with fibres.

A number of materials have been evaluated for their influence upon fibre transmission properties. Nylon 6 was found to be the most promising material and was selected for further assessment. The effects of the extrusion conditions and secondary coating diameter on attenuation have been assessed. Both the cooling conditions of the extrudate and the colouring of the extrudate by pigmentation have a marked effect upon the low temperature performance of the coated fibre; these effects have been attributed to the influence of cooling and pigmentation upon the degree of crystallinity of the nylon.

Using nylon 6 as a tightly-adherent jacket over the graded-index fibres it has been possible to coat fibres to 0.5mm and 0.7mm overall diameter without degrading the attenuation or bandwidth of the fibres. The variation of attenuation with temperature over the range -40°C to + 60°C has been reduced to less than 0.1 dB/km. Whilst the 0.5mm coated fibre is sufficiently robust for handling and incorporation within a loose cable structure, the 0.7mm diameter secondary coating will offer greater mechanical isolation to the fibre and will also improve the tensile load bearing capabilities of the jacketed fibre.

1.2.4 DINORWIC: An Optical Fibre Field Trial

To demonstrate the capabilities of the graded-index fibres developed at Southampton, Chapter 6 describes a collaborative programme which has been undertaken between Southampton University, Pirelli General Cable Works and the Central Electricity Research Laboratories (CERL) to install an optical fibre communications system in the pumped-storage power station under construction at Dinorwic, North Wales[22]. Initially, the optical fibre link is operating between the head-works of the upper reservoir and a lower terminal building above the station's main control room, a total distance of about 5.3km over severe terrain with a vertical drop of some 500 metres between the two ends. Although only two channels were necessary to transmit video and control signals between the terminals, it was decided to allow scope for further experiments by installing a cable containing four graded-index fibres. The fibres, manufactured at Southampton University by the author, were taken to Pirelli General for jacketing and cabling. Installation was also carried out by Pirelli General whilst the CERL were responsible for the development and installation of the terminal equipment.

The severity of the route and the continuing site construction dictated the need for a robust cable structure offering high tensile strength for drawing the cable into ducts, and a high hoop-strength to protect the fibres from impact. To afford maximum protection to the fibres a cable structure was selected in which the strength members were embedded in the sheath and the fibres were loosely laid within an internal cavity. Several designs employing different degrees of cable reinforcement were considered and a number of trial cables were made before the final design was conceived. The design[23] employs a composite sheath comprising a longitudinally-formed steel-tape with a polyethylene oversheath and offers a good balance of strength and flexibility.

A novel manufacturing technique was developed in which the fibres were driven into the cable cavity at a speed in excess of the cable forming speed. It was thus possible to achieve a significant degree of strain relief by incorporating an excess length of fibre (typically 0.5%) within the cable. Time delay measurements on fibres before and after cabling confirmed the presence of the excess length. Attenuation and pulse dispersion measurements before and after cabling showed no deterioration of properties and in some cases an apparent reduction in attenuation was measured due to the absence of any microbending forces within the cable.

Cable lengths of up to 1600 metres were manufactured and installed without fibre breakage; the mean attenuation of the installed fibres was found to be only 3.6 dB/km at 0.85 μm, well below the 5 dB/km figure set out in the specification. The 5.3 km route was cabled in only five lengths and jointed using the copper-substrate V-groove technique developed by the British Post Office. Considerable difficulty was experienced in making low-loss joints in the dusty environment and end-to-end loss measurements indicated that the joint losses were high. By re-making the joints using the fusion splicing technique the mean attenuation of the jointed link fell from 4.4 dB/km to 3.8 dB/km.

The bandwidth of all four channels was found to be very good (<1ns/km pulse dispersion), and so to carry out a more demanding test on the fibres, two channels were jointed to form a 6.6km loop to which a 34 Mb/s line system was connected. The system[24], developed by Telettra, employs an LED source operating at 900nm and as such has a limited operating margin of 25dB for an error rate of 1 in 10^9; over long lengths the system's performance is also limited by material dispersion. However, the system was successfully operated over the 6.6km link at a bit error rate (BER) of better than 1×10^{-10}. Attenuation measurements on the loop show a 3dB system margin in good agreement with the measured BER. This system is the first 34 Mb/s optical fibre communications link installed within the United Kingdom and its performance compares well with other LED-based 34 Mb/s systems installed in other countries. Its long term stability will be monitored over the next two years, as will the stability of the fibres, cables and joints.

If the results of this practical field trial form a basis for assessment, it can be concluded that the original objectives of the research programme have been met. However, as with any new technology, the initial strides in its evolution leave scope for further steps which introduce refinements in the product. Whilst in Chapter 7 the results of the study are summarised and conclusions are drawn, the areas for future development are identified and a number of research projects are suggested.

1.3 References to Chapter 1

1. Murray, W.J.: "Optical fibres in the Trunk Network', British Telecom presentation to TCMA and TEMA on Strategy for Optical Communications, London Sept. 1980.

2. Miya, T., Terunama, Y., Hosaka, T., and Miyashita, T.: 'Ultimate low-loss single-mode fibre at 1.55 μm', Electron. Lett., 15 (1979), pp 106-108.

3. Nakagawa, K., and Ito, T.: 'Detailed evaluation of an attainable repeater spacing for fibre transmission at 1.3 μm and 1.55 μm wavelengths; Electron. Lett., 15 (1979), pp 776-777.

4. Kao, K.C. and Hockham, G.A.: 'Dielectric fibre surface waveguides for optical frequencies', Proc. IEE, 113 (1966), pp 1151-58.

5. Jones, M.W. and Kao, K.C.: 'Spectrophotometric studies of ultra-low-loss glass', J.Sci.Instr., 2 (1969), pp 331-335.

6. Kapron, F.P., Keck, D.B., and Maurer, R.D.: 'Radiation losses in glass optical waveguides', App. Phys. Lett., 22 (1973), pp 307-309.

7. Payne, D.N., and Gambling, W.A.: 'New silica-based low-loss optical fibre', Electron. Lett., 10 (1974), pp 289-290.

8. French, W.G., MacChesney, J.B., O'Connor, P.B., and Tasker, G.W.: 'Optical waveguides with very low losses', B.S.T.J., 53 (1974), pp 951-954.

9. MacChesney, J.B., O'Connor, P.B., and Presby, H.M.: 'A new technique for the preparation of low-loss and graded-index optical fibres, Proc. IEEE, 62 (1974), pp 1278-79.

10. Payne, D.N., and Gambling, W.A.: 'A borosilicate-cladded phosphosilicate core optical fibre', Opt. Commun., 13 (1975), pp 422-425.

11. E. Merck and Co., Darmstadt, W. Germany: 'Materials for optical fibres, sample assay'.

12. Norman, S.R.: 'The fabrication and properties of optical fibre waveguides', Minithesis, Department of Electronics, University of Southampton, 1977.

13. Payne, D.N. and Gambling, W.A., 'The preparation of glass- and liquid-core optical fibres', Opto-electronics, 5 (1973), pp 297-307.

14. Gambling, W.A., Payne, D.N., Hammond, C.R., and Norman, S.R.: 'Optical communication through fibres', Annual Report 1974-1975, Department of Electronics, University of Southampton.

15. Hartog, A.H.: Private communication.

16. Gambling, W.A., Matsumura, H., and Ragdale, C.M.: 'Mode dispersion, material dispersion and profile dispersion in graded-index single-mode fibres', Microwaves, Optics, and Acoustics, 3 (1979), pp 239-246.

17. Smith, A.M.: 'Polarisation and magneto-optic properties of single mode optical fibre', App. Opt., 17 (1978), pp 52-56.

18. Norman, S.R., Payne, D.N., Adams, M.J., and Smith,A.M.: 'Fabrication of single-mode fibres exhibiting extremely low polarisation birefringence', Electron Lett., 15 (1979), pp 309-311.

19. Gloge, D.: 'Optical fibre packaging and its influence on fibre straightness and loss', B.S.T.J., 54 (1975), pp 245 -262.

20. Morley, J.G., Andrews, P., and Whitney, I.: 'Strength of fused-silica fibres', Symposium on the strength of glass and ways of improving it, Florence 1965, pp 417-445.

21. Olshansky, R., and Maurer, R.D.: 'Tensile strength and fatigue of optical fibres', J.App.Phys., 47 (1976), pp 4497-4499.

22. Osterfield, J.R., Norman, S.R., McIntosh, D.N., Rogers, A.J., Castelli, R., and Tamburello, M.: 'An optical fibre link in a mountainous environment', 29th International Wire and Cable Symposium, Cherry Hill, U.S.A.., Nov. 1980, pp. 202-210.

23. European Patent Application No. 80302477.7, 22-7-1980, 'Optical Fibre Cable'.

24. Castelli, R., Mazzuco, R., and Tamburello, M.: 'Design, manufacture and performance of a 34 Mb/s optical fibre transmission system', Proc. Fifth European Conference on Optical Communications, Amsterdam 1979, pp 22.5-1, 22.5-4.

CHAPTER 2: THE HCVD PROCESS FOR THE MANUFACTURE OF OPTICAL FIBRE PREFORMS

The application of optical fibres to long-distance telecommunication demands the utilisation of glasses having ultra-low attenuation at the wavelength of operation. Early in the development of optical fibres it was clear that the total attenuation was generally high in glasses prepared by conventional melting processes, not due to intrinsic losses, but to absorption by transition metal impurities present in the glass. For several years the major effort in fibre manufacture was directed towards the reduction of impurity levels in the waveguide glasses. Although it was proving difficult to produce ultra-pure glass by melting, fresh impetus was provided by Kao's[1] demonstration that certain synthetic grades of fused silica could exhibit low attenuation. Attention switched from the so-called'soft glasses', prepared by melting, to synthetic, silica-based glasses which might be incorporated with silica into an optical fibre structure. A number of techniques evolved for the manufacture of high-silica glasses [2-6], but of these, the homogeneous chemical vapour deposition (HCVD) technique, [5, 6] was probably the most significant because it provided a versatile process which could be readily adapted to the manufacture of different glasses and optical fibre configurations. The process was adopted by many research centres throughout the world, and today forms the basis of most manufacturing facilities for the production of ultra-low-loss fibres. This chapter describes the development of the process and shows how it has been applied to the manufacture of both multimode and monomode optical fibre preforms. The subsequent drawing of the preforms into fibre and the characteristics of the fibres are covered by ensuing chapters.

2.1 Principles of the HCVD Process

The principle of the HCVD process results from the fact that, at temperatures in excess of 1200°C, silicon tetrachloride vapour reacts spontaneously with oxygen to form a dispersion of silica particles[7].

The reaction can be carried out at high concentration within a silica tube to form a dense fog of silica soot which adheres to the internal wall of the tube; furthermore, the soot can subsequently be fused at high temperature into a clear glass layer. By incorporating a suitable additive or dopant into the reaction it is possible to deposit a glass having a refractive index which is different to that of silica, and which may therefore be combined with silica to form a composite waveguide structure.

Figure 2.1 is a schematic representation of the application of the HCVD process to the manufacture of optical fibres. The fibres are produced in three distinct stages:-

2.1.1 The Deposition Process

A gas stream of oxygen, silicon tetrachloride and dopant vapours is passed through a silica tube along which a hot-zone is traversing in the direction of the gas flow. Provided that the temperature is sufficiently high, when the vapours reach the hot-zone they spontaneously oxidise to form the soot dispersion which, as the reactant concentration is high, is formed homogeneously across the section of the tube. Glassy particles are deposited on the wall of the tube, not only within the length of the hot-zone, but also downstream from it. A certain amount of soot is also transported out of the tube by the reaction by-products, principally chlorine and excess oxygen. If the hot-zone temperature exceeds the softening temperature of the soot particles, they fuse into a clear layer of glass in the region of the hot-zone; material deposited downstream from the hot-zone is fused as the hot-zone approaches. Thus, by traversing the hot-zone along the tube, a single-layer of glass may be deposited, the thickness and refractive index of the glass depending upon parameters such as reactant flow-rate, dopant concentration, traversal rate and deposition temperature. It follows that, by the successive deposition of many layers, it is possible to build up an appreciable thickness of glass having a defined refractive index distribution. Hence, a material of higher refractive index than silica may be deposited to later form the core of an optical fibre in which the silica substrate forms the cladding.

Alternatively, a low-index cladding glass may be deposited prior to the core glass; in this case the silica substrate acts only as a supporting structure in the resultant fibre. Because the silica tube provides a high-purity reaction environment, the deposited glass is likely to have a purity comparable to that of the reactant materials.

2.1.2 Preform Collapse

In the second stage of fibre manufacture, the composite tube of silica and deposited glass is collapsed into a solid rod, or preform, having essentially the same cross-sectional structure as the resultant fibre. Although this operation may be combined with the fibre drawing operation, it is more conveniently performed immediately after the deposition stage. When sufficient glass has been deposited, the reactant gas flow is stopped and the temperature of the traversing hot-zone is raised above the softening point of the silica tube. Surface tension forces then cause the composite tube to contract radially to form the solid preform, figure 2.1b. The preform may then be removed and stored until required for fibre drawing.

2.1.3 Fibre Drawing

In the fibre drawing operation (figure 2.1c), the end of the preform is fed vertically downwards by a precision feed mechanism into the hot-zone of a short furnace which heats the tip of the preform until it flows. A fibre filament is drawn from the molten tip on to a take-up drum.

2.2 Glass Systems for HCVD

Although it is possible to produce optical fibres from only one material [8, 9], it is generally more convenient to utilise a radially concentric core-and-cladding configuration. To form such a fibre having a silica core or cladding, a second material is required which has a different refractive index and is physically and chemically compatible with silica.

There are a great many oxides which can be added to silica to form a binary glass having a different refractive index. These materials may be network formers such as boric oxide (B_2O_3), phosphorus pentoxide (P_2O_5), germanium dioxide (GeO_2), arsenic trioxide (As_2O_3), or they may be network modifiers such as sodium oxide (NaO), calcium oxide (CaO), lead oxide (PbO) or titania (TiO_2). However, to produce the glass in ultra-pure form by HCVD, several pre-requisites must be met. Firstly, a volatile halide or oxyhalide of the proposed additive must exist and preferably be a liquid at room temperature (to assist in purification) and, secondly, this halide must readily oxidise when mixed with oxygen at an elevated temperature below the softening point of silica. The glass should also be compatible with silica and be stable at the fibre drawing temperature ($> 2000°C$). Fortunately all the network formers fulfill these criteria and can with sufficient care be purified using fractional distillation techniques. The common network modifiers on the other hand, being predominantly ionic, form solid halides at room temperature, with the exception of titania, and are therefore unsuitable for fabrication by HCVD. Other materials such as fluorine have been used with some success both at Southampton and elsewhere[11], but do not form part of this study. Of the glass formers, only phosphorus pentoxide, germania and boric oxide have been investigated in this programme, and it seems that the potential advantages of using arsenic trioxide as a dopant do not offset the hazards associated with the source material, arsenic trichloride, since little or no information has been published on fibres made using this material.

2.2.1 Phosphosilicate Glasses

Phosphorus pentoxide is a most attractive candidate for incorporation with silica into a binary glass. When added to silica it increases its refractive index and, although P_2O_5 is strongly hygroscopic, forms a glass which is chemically resistant and does not devitrify. Furthermore phosphorus has two liquid halides, phosphorous trichloride, PCl_3, and phosphorous oxychloride, $POCl_3$ which both readily oxidise at high temperature to form P_2O_5. Of the two halides, PCl_3 is less stable and oxidises to $POCl_3$ at room temperature in the presence of oxygen. $POCl_3$ is therefore a more suitable source material and can be readily purified by distillation at 102°C.

Phosphorus pentoxide is a strong glass former having two isomorphs[12], a low-temperature hexagonal phase and a high-temperature tetragonal phase. The hexagonal form is obtained by melting hexagonal P_2O_5 crystals at 423°C and has a refractive index of 1.490. The tetragonal form is obtained by fusing crystalline, tetragonal P_2O_5 at 580°C and has $n_D = 1.512$. When heated above 500°C the hexagonally co-ordinated glass undergoes a very rapid, irreversible transformation to the more viscous, tetragonal form. Thus, when incorporated with silica at high temperature into a binary glass, the P_2O_5 will be tetragonally co-ordinated and the network liquid will be composed of linking SiO_4 and PO_4 tetrahedra.

When combined together in the HCVD process the oxidation reactions of $SiCl_4$ and $POCl_3$ are of the form:-

$$\begin{aligned} x\ SiCl_4 + xO_2 &\longrightarrow x\ SiO_2\downarrow + 2xCl_2\uparrow \\ 2y\ POCl_3 + 3y/2\ O_2 &\longrightarrow y\ P_2O_5\downarrow + 3yCl_2\uparrow \end{aligned} \qquad (2.1)$$

A phosphosilicate glass of composition $xSiO_2{:}yP_2O_5$ is thus formed having a molar fraction, M , of P_2O_5 in the binary glass, where $M = y/x+y$. Generally, when two pure glasses are mixed, the refractive index of the resulting compound glass varies monotonically between the limiting values of the pure constituents as a function of M[13]. Thus in figure 2.2 the refractive index behaviour of phosphosilicate glass is plotted over the compositional range 0→20 m/o P_2O_5 assuming linear additivity between the constituents. The graph is plotted up to M = 0.20 because it has been found[14] that at higher concentrations of P_2O_5 the glass is physically incompatible with silica due to expansion and viscosity mismatches. It can be seen that a P_2O_5 concentration of 20 m/o produces a 0.75% refractive index difference with respect to silica, corresponding to a maximum numerical aperture of 0.18 in a silica-clad, phosphosilicate-core fibre.

The thermal expansion coefficient of P_2O_5 is $\alpha_T = 140 \times 10^{-7}$ $°C^{-1}$ compared with $\alpha_T = 5.5 \times 10^{-7}$ $°C^{-1}$ for pure silica.

As P_2O_5 is added to SiO_2 the thermal expansion coefficient increases above that of silica until the point is reached where, in a silica-clad, phosphosilicate-core fibre, the tensile stress in the core is such that the glass fractures. This represents one of the major limitations of the phosphosilicate system. A second limitation arises from the fact that the viscosity versus compositional behaviour of phosphosilicate glass is a super-linear function. Thus, in an earlier study,[14] it was found that even small admixtures of P_2O_5 appreciably lower the viscosity of silica, and that this ultimately limits the compatability of phosphosilicate and silica glasses in the HCVD process; at high P_2O_5 levels, the viscosity of the phosphosilicate glass at the collapsing temperature (>1950°C) is so low that it is extremely difficult to maintain core circularity. Nonetheless, the low viscosity of the phosphosilicate system is of great importance in the HCVD process, since, even at low P_2O_5 levels, the soot formed by the gas-phase reaction can be fused into a clear glass layer at temperatures well below that at which the silica tube softens.

2. 2.2 Germanosilicate Glasses

Germania, GeO_2, like phosphorus pentoxide, is a strong glass-former which when added to silica increases its refractive index. In its glassy form, germania has a refractive index of $n_D = 1.610$, considerably higher than that of P_2O_5 ($n_D = 1.512$). Germanium tetrachloride is a liquid at room temperature having a vapour pressure of 66 mm Hg at 20°C, and is therefore well suited to purification by distillation. Furthermore, $GeCl_4$ readily oxidises to GeO_2 when mixed with oxygen at high temperature, although there is some evidence that at temperatures in excess of 1700°C the volatile compound GeO is favoured[15]. By the combined oxidation of $GeCl_4$ to GeO_2 and $SiCl_4$ to SiO_2 it is possible to produce germanosilicate glasses by HCVD according to the reactions:-

$$\left.\begin{aligned} x\,SiCl_4 + xO_2 &\rightarrow xSiO_2\downarrow + 2xCl_2\uparrow \\ y\,GeCl_4 + yO_2 &\rightarrow yGeO_2\downarrow + 2yCl_2\uparrow \end{aligned}\right\} \quad (2.2)$$

Glassy germania is built up of germanium-oxygen tetrahedra in a three-dimensional random network very much like that of silica[16]. The four-valent germanium atom is located at the centre of the tetrahedron with a covalent bond to an oxygen atom at each corner of the tetrahedra as in vitreous silica. Thus in a germanosilicate glass, the GeO_4 tetrahedra substitute directly for SiO_4 tetrahedra and the composite glass is structurally similar to pure silica.

The coefficient of thermal expansion of germania is $\alpha_T = 80 \times 10^{-7}$ $^{\circ}C^{-1}$, approximately half that of P_2O_5, and the viscosity is appreciably higher. Although the central atom-oxygen bond strengths in GeO_2, P_2O_5 and SiO_2 are about 100 kcal $mole^{-1}$, the surprisingly large difference in viscosity between P_2O_5 and GeO_2 is probably due to the fact that in P_2O_5 each PO_4 tetrahedron is bonded to three others instead of four as for GeO_2 (and SiO_2). Although structurally similar to SiO_2, the viscosity of GeO_2 is lower at a given temperature, and a germano-silicate glass would therefore be expected to have a melting point below that of silica; fusion of the glass deposited by HCVD should thus be possible without deformation of the silica substrate.

Figure 2.3 shows the refractive index behaviour of germanosilicate glass over the compositional range $0 \rightarrow 20$ m/o GeO_2, assuming linear additivity between the constituents. In comparison with P_2O_5 (see figure 2.2), it is clear that the refractive index difference resulting from the addition of a certain molar fraction of GeO_2 to SiO_2 is considerably higher than that for the addition of the same molar fraction of P_2O_5 to SiO_2. Thus the theoretical coefficient of refractive index difference is $\Delta n = 15.2 \times 10^{-4}$ $(m/o)^{-1}$ for GeO_2, compared with $\Delta n = 5.4 \times 10^{-4}$ $(m/o)^{-1}$ for P_2O_5. To produce a silica-clad optical fibre of 0.2 NA would therefore require the addition of only 9.0 m/o GeO_2 to silica in the core (25 m/o for a P_2O_5/SiO_2 core). Consequently, from the reduced doping levels (for a particular refractive index difference), the higher viscosity and the reduced expansion, it may be expected that germanosilicate glass would be physically more compatible with silica than phosphosilicate glass, and would be the preferred choice for use as the core of a silica-clad fibre.

2.2.3 Borosilicate Glasses

In contrast to phosphorus pentoxide and germania, it has been found that the addition of boric oxide, B_2O_3, to silica reduces the refractive index of the compound glass below that of silica[17], especially in highly-quenched samples. Thus Van Uitert et al[13] were able to demonstrate that borosilicate glass was a promising cladding material for silica-based optical fibres, even though the refractive index of bulk annealed samples was only marginally less than that of pure silica. Two volatile halides of boron, namely boron trichloride, BCl_3, and boron tribromide, BBr_3 are readily available, and both form boric oxide when oxidised at high temperature. Binary borosilicate glasses may be prepared by the HCVD technique according to the reaction equations:-

$$\begin{aligned} x\,SiCl_4 + xO_2 &\longrightarrow x SiO_2 \downarrow + 2xCl_2 \uparrow \\ 2yBCl_3 + \tfrac{3}{2}y\,O_2 &\longrightarrow yB_2O_3 \downarrow + 3yCl_2 \uparrow \\ \text{or}\quad 2yBBr_3 + \tfrac{3}{2}y\,O_2 &\longrightarrow yB_2O_3 \downarrow + 3yCl_2 \uparrow \end{aligned} \qquad (2.3)$$

to form the composite borosilicate glass $xSiO_2{:}yB_2O_3$ in which the molar fraction of B_2O_3 is $M = y/x+y$. Of the two halides, BCl_3 is highly volatile and boils at about 5°C; boron tribromide is therefore the preferred material for purification by distillation.

Vitreous B_2O_3 is composed of boroxyl groups (planar rings containing six members, alternately boron and oxygen atoms) linked together in a three dimensional network by boron-oxygen-boron bonds[16]. The boron atom is triangularly co-ordinated, each being linked to three oxygen atoms, and the network liquid is structurally very different to the tetrahedrally co-ordinated silica. The more open structure of the planar boroxyl groups may be the reason for the low viscosity of glassy B_2O_3 compared with SiO_2 or GeO_2. As with phosphorus pentoxide, the addition of boric oxide to silica produces a significant decrease in viscosity, which in turn lowers the sintering temperature of the glassy soot deposited in the HCVD process. The reduced viscosity does not represent a serious limitation to the maximum amount of boric oxide that can be incorporated into the borosilicate glass by HCVD, because, in practice, it is found that the expansion coefficient mismatch with silica predominates.

In contrast to the phosphosilicate and germanosilicate glass systems, the refractive index of borosilicate glass depends on both the composition and cooling rate. Measurements on annealed samples of glassy B_2O_3 gave a refractive index[17] of n_D= 1.4582, and would indicate a maximum index difference of -3×10^{-4} with respect to silica. However, Wemple[18] demonstrated that the refractive index of high-silica borosilicate glass was particularly sensitive to cooling rate, and obtained an index difference of -8.7×10^{-3} in a 25 m/o B_2O_3glass prepared by rapid quenching. Figure 2.4 shows the compositional dependence of refractive index for quenched borosilicate glass over the range M = 0 to M = 0.15. The results are presented for annealed samples (Van Uitert et al[13]) and rapidly quenched samples (French et al[19]). In the quenched samples, French obtained an index difference of -8×10^{-3} with respect to silica at a boric oxide content of 15 m/o; at this composition, a numerical aperture of 0.16 is possible in a borosilicate-clad, silica-core fibre.

The coefficient of thermal expansion of boric oxide is $\alpha_T = 160 \times 10^{-7}\ °C^{-1}$, somewhat higher than that of P_2O_5 or GeO_2, and sets the limit to the maximum B_2O_3 level in the glass; at M = 0.20, the thermal expansion mismatch can produce excessive tensile stress in the deposited layers. To attain a numerical aperture in excess of 0.16 using a borosilicate cladding, it is customary to employ a doped-silica core to extend the core/cladding index difference beyond the thermal-stress limit imposed by the silica-core, borosilicate-clad configuration.

2.3 Preparation of High-Purity Raw Materials

In a study of the optical absorption due to transition metal impurities in silica, Schultz[20] found that the absorption coefficients of elements such as vanadium, chromium, and nickel could exceed 2dB/km per part per billion (ppb) of impurity over the wavelength region of interest to optical communications. To achieve ultra-low loss in optical fibres made by HCVD, it is thus necessary to reduce the transition metal impurity levels below the ppb level.

The raw materials used in the HCVD process are principally $SiCl_4$, $POCl_3$, $GeCl_4$, BBr_3 and oxygen, although other gases such as nitrogen, argon and helium may be added to adjust the deposition conditions. Oxygen and the other gases can be made virtually free of particulate matter, which may contain transition metals, by filtering through ultrafine filters. As a strong hydroxyl ion absorption band is also present at 0.95 μm and 1.4 μm in silica based glasses, the water content of the gases must also be minimised by employing liquified sources or by passing the gases over drying agents such as activated alumina.

Silicon tetrachloride and the dopant halides are generally purified by simple distillation techniques. Figure 2.5 shows the vapour pressure versus temperature characteristics of the source materials and the most common transition metal compounds likely to be present in them. The vapour pressure/temperature characteristic is an Arrhenius type of exponential function given by[21]:-

$$P = Ae^{-Q/RT}$$

where
- P = Vapour pressure
- A = Vapour pressure constant
- Q = Latent heat of vapourisation
- R = Gas constant
- T = Temperature in °K

By plotting the curves on a log P versus 1/T scale, the vapour pressure curve is a straight line for each material. The striking feature of the figure is that the source materials have very similar vapour pressures, which at temperatures below 100°C are several orders of magnitude greater than the vapour pressures of the transition metal impurities. A simple low-temperature distillation process can therefore reduce the impurity levels by several orders of magnitude.

Thus, using this technique to purify reagent-grade $SiCl_4$, $POCl_3$ and BCl_3, the author was able to manufacture borosilicate-clad, phospho-silicate-core graded-index fibres with ultra-low loss over the 0.75 μm to 1.3 μm wavelength range.[23]

More recently, ultra-high purity chemicals have become commercially available[22] and in Table 2.1 the assays of two materials, $SiCl_4$ and $POCl_3$ are given. It can be seen that for both materials, the level of impurities has in most cases been reduced to below the limit of detection, which is still above the level dictated by the work of Schultz. In practice, however, a further stage of purification is obtained in the HCVD process where the reactant vapours are picked up from the liquid phase by bubbling high-purity carrier gas through the liquids which are held at about 20°C in glass Dreschel bottles. Obviously at this temperature the vapour pressure of the transition metal halides is very much lower than that of each reactant, and purification by more than an order of magnitude would not seem unlikely.

2.4 The HCVD System

Although low loss may be a pre-requisite for the use of optical fibres in telecommunications, from a system viewpoint additional parameters play an important part in defining the optical fibres' performance. Fundamental properties such as overall fibre diameter, core size, numerical aperture, refractive index profile, and the glass systems used to manufacture the fibres have a direct effect upon the fibres' operating characteristics. The control of these parameters in the HCVD process is therefore of comparable importance to the attainment of low impurity levels in the waveguide glasses, and requires accurately controlled deposition and collapsing processes.

2.4.1 Chemical Vapour Collection and Distribution

To control the composition and quantity of glass deposited in the HCVD process the reactant vapours must be collected and delivered to the silica deposition tube in controlled volumes. This is achieved by saturating a carrier gas with reactant vapour by bubbling the carrier through the liquid reactant; varying the flow rate of carrier gas thus varies the amount of reactant vapour transported to the deposition zone.

Figure 2.6 is a schematic diagram of a system for collecting and distributing controlled amounts of $SiCl_4$, $POCl_3$, $GeCl_4$ and BBr_3 vapours. Each liquid halide is held in a Dreschel bottle through which a controlled flow of carrier gas is passing. Vapours of the halides are collected, brought together in a manifold and mixed with additional oxygen before being piped to the deposition zone. The mass pick-up of each reactant is theoretically determined only by the vapour pressure of the reactant and the carrier gas flow rate. If the carrier gas is fully saturated by the reactant vapour then the volumetric flow 'S_I' of reactant 'I' is given by:-

$$S_I = \frac{P_{IT}}{Po - P_{IT}} \cdot V_{CI} \qquad (2.5)$$

where P_{IT} = vapour pressure of reactant I at temperature T

Po = atmospheric vapour pressure

V_{CI} = carrier gas flow rate through reactant I

The total reactant flow rate is given by $\sum_{I=1}^{4} S_I$ where the vapour pressure of each reactant is given by [21]:-

$SiCl_4$:

$$\log_{10} P = 7.9312 - 1656.6/T \qquad (2.6)$$

$POCl_3$:

$$\log_{10} P = 7.8953 - 1892.5/T \qquad (2.7)$$

$GeCl_4$:

$$\log_{10} P = 8.0072 - 1812.7/T \qquad (2.8)$$

BBr_3:

$$\log_{10} P = 7.9580 - 1833.5/T \qquad (2.9)$$

Oxygen is normally used as the carrier gas for the first three reactants but nitrogen is used for BBr_3 as there is evidence of oxidation of BBr_3 to B_2O_3, and of free bromine, when oxygen is present within the Dreschel bottle.

When depositing a binary silicate glass the refractive index will depend upon the relative concentrations of silicon tetrachloride and dopant-halide within the reaction zone. The ratio R of the required carrier flow rate through the dopant halide to that through the silicon tetrachloride is related to the molar fraction of dopant in the vapour phase by the equation

$$R = K \cdot \frac{M}{(1 - M)} \qquad (2.10)$$

where K is a constant depending on the vapour pressure of the reactants and the number of molecules of dopant halide necessary to yield one molecule of dopant. Assuming that the reactants are held at 20°C, the equations for the binary silicates can be written:-

Phosphosilicate glass:

$$R_{P_2O_5} = 17.8 \frac{M}{(1 - M)} \qquad (2.11)$$

Germanosilicate glass:

$$R_{GeO_2} = 3.48 \frac{M}{(1 - M)} \qquad (2.12)$$

Borosilicate glass:

$$R_{B_2O_3} = 9.38 \frac{M}{(1 - M)} \qquad (2.13)$$

Equations (2.11)→(2.13) assume complete saturation of the carrier gas streams. Early in the project it was realised that a variation of pick-up efficiency with carrier-gas flow rate, material, or liquid height in the bubbler could lead to large differences between the theoretical and actual values of S for each material.

An experimental study of the variation of pick-up efficiency with carrier-gas flow rate was undertaken using $POCl_3$ as the source[14]. The efficiency was indeed found to be sensitive to the carrier flow rate, the height of the $POCl_3$ in the Dreschel bottle and also the bubble-size of the carrier as it passed through the liquid. Increasing the surface area of the liquid/carrier interface by reducing the bubble size, and increasing the path-length of the carrier through the $POCl_3$ produced a significant improvement and pick-up efficiencies of $\eta = 0.90 \pm 0.05$ were reproducibly obtained over the normal range of carrier gas flow-rates. If the pick-up efficiency does not vary from bubbler to bubbler then the values of K in equations (2.11)→(2.13) do not need modification. The volumetric flow rate however will be reduced and equation (2.5) must be modified accordingly:-

$$S_I \text{ actual} = \eta \text{ pick-up} \times S_I \qquad (2.14)$$

Although the problem of pick-up efficiency could be overcome by employing an electronic mass flowmeter sited downstream of each Dreschel bottle in a feedback loop with the carrier-gas flow controller, this approach has not been investigated because the highly corrosive nature of the reactant would probably result in corrosion of the flowmeter and contamination of the vapour streams. Indeed, even if the correct volumes of reactants are delivered to the deposition zone, the gas-phase reaction is such that there is no guarantee that the deposited glass will have the same dopant content as the reactive gas stream. In fact, as will be described in Section 2.5.2 it is necessary to calibrate the HCVD process in terms of dopant level and refractive index difference and then to adjust the value of K in equations (2.11) to (2.13) so that the value of M used in the equations corresponds to the composition of the binary silicate glass and not to the composition of the gas-phase reactant stream.

2.4.2 Reactant Vapour Distribution System

Figure 2.7 is a detailed schematic of the reactant vapour distribution system developed during the course of this study. It represents the final design of a number of systems which have been constructed and modified after experimental evaluation. It was found that the reactants readily attacked any metallic component with which they were in contact, and so care was taken to eliminate metallic valves etc. from the vapour handling system. On the other hand non-metallic flow controllers made in PTFE were found to be inaccurate and gave insufficient control over the carrier gas streams. A dual approach was finally adopted in which a precision carrier gas distribution system was constructed using metallic components; this was connected to a chemical vapour handling system comprised of only glass and PTFE. This permits accurate control of the carrier gas streams and prevents contamination of the chemical vapour stream. Thus in figure 2.7 the line AA′ delineates the metallic/non-metallic interface.

High-purity carrier gases (oxygen and nitrogen) are supplied to the gas control equipment via driers and filters which remove hydrogen-containing species and particulate matter from the gases. The carrier gas flow rate through each bubbler is controlled by either a precision flow meter or an electronic mass flow controller. An additional flow of oxygen may be provided to vary deposition conditions and to provide an excess of carrier gas downstream of the bubblers.

The liquid reactants are held in silica Dreschel bottles having temperature-controlled water jackets to maintain the vapour pressure of each reactant at a constant value. Each bubbler has a large porous frit with many fine holes to give a blanket of small carrier-gas bubbles distributed over the entire cross-section of the container; this provides a large surface area for the carrier gas/reactant interface and ensures efficient pick-up of reactant vapour. The Dreschel bottles were constructed in silica to minimise the possibility of impurities leaching from the container walls. Each bubbler may be sealed using all PTFE valves, and a bypass line is provided for each carrier-gas stream. When the system is not in use a small carrier flow is passed through each line, via the bypass, to prevent backstreaming of reactant vapours into the gas control equipment.

The gas and vapour streams are brought together and mixed in a PTFE manifold before passing to the deposition tube. A 0.1 um line filter provides final filtration of the gas stream and prevents particles produced by wear of the PTFE rotary joint from entering the deposition tube.

Control of the dopant carrier-gas flow rates during deposition is achieved by applying preset voltage levels to the inputs of the electronic mass flow controllers (MFCs). The voltage levels may be obtained using analogue electronics to divide down a reference voltage, or by using digital techniques to store the flow rate values on magnetic tape, random access memory (RAM) or read-only memory (ROM). Each preset value may then be read from store and applied to an analogue to digital (A to D) converter, the output of which is fed to the MFC. Of these approaches the magnetic tape storage is the most elegant since it allows the computer to calculate and directly store the flow rates required to synthesise a specific refractive index profile.

2.4.3 Modified Glass-Working Lathe for HCVD

The original development work on the HCVD process was undertaken using the fibre drawing machine to translate the deposition tube vertically through a hot-zone provided by the fibre-drawing furnace[23]. As the silica tube was supported at one end only, severe elongation and distortion of the tube frequently occurred. A purpose-built machine, in which the tube was rigidly supported at both ends and the hot-zone was vertically translated, produced a significant improvement and is described in detailed in Reference 24. However, thermal expansion of the machine during deposition and collapse frequently led to misalignment between the chucks which gripped the silica tube, and to an asymmetric preform cross-section. To overcome these problems a horizontal glass-working lathe has been adapted for the HCVD process, and is shown in figure 2.8.

The lathe is a standard glass-working lathe having two driven spindles on a 54" bed (Heathway Model No. S3L). To adapt the machine to the HCVD process, the following modifications have been made:-

1. A motorised drive system has been fitted to the burner carriage to provide accurately controlled translation of the hot-zone produced by a surface-mix burner mounted on the carriage. A stepper motor system was selected to give a wide dynamic speed range; traversal rates of zero to 80 cm/min can be obtained. Adjustable microswitches mounted on the lathe bed are used to set the limits to which the carriage translates.

2. The silica tube is gripped between the rotating spindles by precision engineering chucks mounted on the spindles. The chucks tightly grip the tube, ensuring accurate alignment and preventing relative rotation between the two ends of the tube due to chuck slippage. Heat shields protect the chucks from excessive temperatures during processing.

3. The reaction rate of the chemicals inside the silica tube during deposition depends largely upon the temperature of the hot-zone. An optical pyrometer has therefore been fitted to the burner carriage to monitor the hot-zone temperature, and forms part of a feedback loop with a three-term controller and an electronic solenoid valve to control the flow of oxygen to the burner, as shown schematically in figure 2.9a. Natural gas is used as the fuel gas over the normal range of deposition temperatures (1500°C to 1800°C), but must be replaced by hydrogen to achieve the higher temperatures necessary for collapsing the tube. Figure 2.9b shows the variation of temperature along the deposition length of a silica tube at a burner traverse rate of 10 cm/min and at a hot-zone set-temperature of 1600°C. It can be seen that apart from the initial overshoot at the start of the traverse, the temperature is maintained to within $\pm$ 5°C over the cycle.

4. Extract systems have been fitted to remove chlorine from the output of the silica tube during deposition and collapse, and also to remove the silicon monoxide vapour liberated from the silica tube during the high-temperature collapse.

The system offers an inexpensive machine for the fabrication of preforms up to 1 metre in length, and does not suffer from thermal distortion problems encountered with earlier equipments. It has now been in regular operation for more than three years without needing major modification or maintenance.

2.5 Deposition of Doped Silica Glasses

Many experiments have been performed to characterise the important parameters affecting the deposition process and the deposited glass. If high-quality optical fibres are to be fabricated, it must be possible to control the refractive index and thickness of each glass layer for whichever glass system is being employed. A knowledge of the effects of reactant flow rate, dopant level and traverse speed upon refractive index and layer thickness is of utmost importance.

2.5.1 Control of Deposited Layer Thickness

The thickness of glass deposited during each hot-zone traverse will clearly depend upon reactant flow rate, traverse speed, tube dimensions and deposition temperature. The influence of these variables has been assessed for the phosphosilicate, germanosilicate and also the ternary phospho-germanosilicate glass systems. In figure 2.10a the deposited layer thickness is plotted as a function of carrier gas flow through $SiCl_4$ for a 10 m/o phosphosilicate glass deposited at constant traverse rate (10 cm/min) in a 15 mm diameter silica tube having a 1 mm wall thickness. A number of layers were deposited at different carrier flow rates and the tube was then sectioned for measurement of the layer thicknesses. Figure 2.10b shows a photomicrograph through the deposited layers which are easily distinguished under transmitted light illumination. Seven layers were deposited at carrier flow rates in the range 100 ml/min to 300 ml/min, and the process was then repeated a second time to give a total of 14 layers; in each series, two layers were deposited at the lower flow rates to improve the measurement accuracy.

The deposited layer thickness is seen to vary linearly with carrier gas flow rate over the flow range examined. At a carrier flow of 300 ml/min a deposition thickness of 32 μm/pass was obtained. Under these conditions only seven passes would be required to deposit sufficient material to form a preform with a 1:2.5 core/cladding ratio (e.g. 50 μm core, 125 μm OD fibre).

Similar experiments performed on tubes of different cross-sectional area show that, for constant carrier flow rates, the layer thickness increases with decreasing internal tube diameter; moreover the cross-sectional area of the layers was found to be independent of tube size. The HCVD process thus yields a constant volume of deposited material per unit time at a specified reactant flow rate. As the gas-phase reaction occurs homogeneously over the cross-section of the tube, this result might well be expected. It is thus possible to normalise the deposition rate in terms of volume of material deposited per unit time per unit volume of reactant vapours as shown in figure 2.11 for the above mentioned glass systems. To allow for the fact that the results were obtained using different bubbler temperatures (and hence reactant vapour pressures) the reactant flow rate is expressed directly in ml/min $SiCl_4$ vapour. The results were obtained from measurements on many preforms fabricated using a wide range of deposition conditions, in particular the reactant vapour pressure, dopant level, hot-zone traverse speed and silica tube size were varied from preform to preform. The striking feature of the results is that the deposition rate is a linear function of $SiCl_4$ flow-rate over the range of flows commonly encountered It is thus possible to manufacture preforms having pre-selected core/cladding diameter ratios by varying the reactant flow rate or traverse speed to give the required thickness of deposited material. For example, at the highest reactant flow rate (270 ml/min $SiCl_4$) layers of 36 μm thickness were deposited at a traverse speed of 17 cm/min. However, at such high deposition rates bubbles frequently form in the deposited layers due to gas entrapment and it would be preferable to deposit twice as many layers of 18 μm thickness at the same traverse speed (thereby requiring a $SiCl_4$ flow of 135 ml/min).

2.5.2 Control of Refractive Index

For each glass system the refractive index of the deposited glass will be a function of the glass composition and its thermal history (particularly for the borosilicates). To permit accurate profile synthesis, the HCVD process has been calibrated for each glass system in terms of the refractive index difference with respect to silica as a function of the molar composition of the gas phase reactants.

The refractive index data was derived by measurement of the numerical aperture of fibres drawn from preforms manufactured using known gas-phase reactant concentrations. It is felt that direct measurements on fibres are more desirable than measurements on bulk samples because the thermal history of bulk samples is not sufficiently representative of the state of stress within a fibre.

2.5.2.1 Phosphosilicate Glasses

Figure 2.12 shows the refractive index difference between the binary phosphosilicate glass and silica as a function of the molar content of P_2O_5 present in the gas phase. The circular points represent values obtained from the measurement of the numerical aperture of a number of step-index fibres fabricated using different gas-phase ratios of $POCl_3$ to $SiCl_4$ assuming that the glasses so-formed were the stoichiometric products of the gas-phase oxidation reaction. Experimental points identified by a cross were obtained from graded-index fibres by first measuring the NA of the fibre to give the maximum core index difference and then deconvolving the index difference as a function of core radius from refractive index profiles obtained by a near-field scanning technique[25]. The theoretical refractive index difference derived in section 2.2.1 is also plotted (solid line). The close coincidence of the experimental results and the theoretical predictions confirms the assumption of complete stoichiometric oxidation and shows that the composition of the deposited glass closely follows the ratio of the reactant chloride concentrations up to P_2O_5 levels of about 15 m/o. The discrepancy between the results at higher levels may in part be due to the out diffusion of P_2O_5 from the glass during the high temperature collapsing process, and also to a stress-optic reduction of the refractive index under the high tensile stresses present in highly-doped phosphosilicate-core fibres.

2.5.2.2 Germanosilicate Glasses

In contrast to the phosphosilicate glass system, it was found that the incorporation of GeO_2 into germanosilicate glass is non-stoichiometric. Although the index difference with respect to silica is a linear function of dopant level, the specific index difference (index difference per m/o GeO_2 in gas-phase) falls surprisingly below the theoretical prediction. Electron microprobe analysis (EPMA)[26,27] of preform samples revealed that the incorporation ratio of GeO_2 into glass in the HCVD process was less than half the stoichiometric gas-phase ratio, as shown in fig. 2.13. The GeO_2 content of the glass is seen to be a non-linear function of the gas-phase concentration. and there is considerable scatter between the results from preform to preform. The most likely explanation of this apparently random fluctuation is that the germania incorporation ratio is temperature dependent, the incorporation efficiency increasing with decreasing substrate temperature.

Thus at high GeO_2 doping levels the reduced viscosity of the deposited glass permits a lower deposition temperature, and the proportion of germania in the glass increases. Similarly, at low GeO_2 levels a higher deposition temperature must be employed (to ensure fusion of the deposited soot), and the germania incorporation efficiency drops accordingly. The scatter between results at constant gas-phase GeO_2 levels probably arises because the deposition temperature was not held constant from preform to preform. (The need for accurate temperature control of the deposition process is clearly evident). There is qualitative evidence to justify this theory in the fact that graded-index germania-doped preforms made under constant-temperature conditions exhibit smoothly varying concentration profiles which are only severely perturbed when the deposition temperature is changed. The practical implication of this effect is that even though the hot-zone temperature may be maintained at a constant value throughout a deposition, unless the set-temperature is the same from one deposition to another then random fluctuations in numerical aperture will occur from preform to preform.

Nevertheless, when the refractive index difference with respect to silica is plotted as a function of the actual germania content of the glass, as shown in figure 2.14, the experimental data agrees well with the theoretical prediction. The specific index difference is found to be $\Delta n = 15 \times 10^{-4}$ per mole percent GeO_2 in the glass.

If a linear relationship is fitted to the data of figure 2.13 (implying constant incorporation efficiency at constant temperature) it is possible to combine the data of figures 2.13 and 2.14 to conveniently give the gas-phase concentration of $GeCl_4$ necessary to achieve a specified refractive index in the glass, figure 2.15. For example, using this graph, it is found that to obtain a 0.24 NA in a silica-clad fibre, a gas-phase concentration of 25 m/o $GeCl_4$ is required, about twice the actual GeO_2 content of the resultant germanosilicate glass. The validity of this approach has been confirmed by EPMA analysis of a graded-index preform of accurately known fabrication conditions and core/cladding index difference. In figure 2.16 the plots of the radial variation of refractive index of a fibre (measured by near-field scanning) and the radial variation of GeO_2 content in the preform prior to drawing have been superimposed; also shown (as circular points) are the glass-phase GeO_2 contents expected from the vapour-phase reactant concentrations

The agreement between index difference, actual glass composition and predicted glass composition is excellent apart from the central core region where the GeO_2 content of the innermost deposition layer has been perturbed by outdiffusion of dopant during the preform collapsing operation. Nevertheless the close coincidence of the results demonstrates that the refractive index of the germanosilicate glass produced by HCVD can be accurately controlled by adjusting the $GeCl_4$ level in the gas-phase in accordance with figure 2.15.

2.5.2.3 Borosilicate Glasses

The refractive index behaviour of borosilicate glass produced by HCVD has been characterised by the measurement of numerical aperture and refractive index profile in borosilicate-clad, silica-core fibres.

The problems of depositing a silica-core were overcome by adopting a rod-in-tube technique whereby the borosilicate cladding was deposited on to a silica substrate tube into which a rod of 'synthetic' silica was subsequently introduced. The rod-in-tube preform was then drawn into fibre at a temperature sufficient to ensure complete closure of the annular clearance between rod and tube; in this manner fibres having a precise step-index profile were obtained. Graded-index fibres having a borosilicate cladding and a graded borosilicate core were also fabricated by conventional HCVD.

The variation of refractive index difference with relative concentration of B_2O_3 in the gas stream is shown in Fig. 2.17. Also included in the figure are the results obtained by French et al[19] who have studied the borosilicate system in great depth. As both sets of measurements were performed on samples prepared by fibre drawing, the borosilicate glass will be in a highly quenched state, and at each composition the refractive index of the glass should be near its minimum value. It can be seen that there is good general agreement between the results obtained at Southampton and those obtained by French. In each case the refractive index difference is seen to be a non-linear function of the gas-phase B_2O_3 content, the rate of change of index decreasing with increasing B_2O_3 level.

French found from EPMA measurements that the relative composition of B_2O_3 in the glass phase was only marginally below that of the gas-phase, and attributed the non-linear refractive index variation to a compositional sensitivity of the index depression caused by quenching. This may well be the explanation for the reduced index differences measured in the graded-index fibre VD143 compared with the values obtained from step-index fibres made at Southampton. To produce fibres with predetermined refractive index profiles using a borosilicate cladding it is thus necessary to use the empirically established relationship between index difference and gas-phase B_2O_3 level, and to ensure that the quench-rate does not vary from fibre to fibre.

2.6 Preform Collapse

It has been found that while the quality of the core glass is governed principally by the deposition process, the geometrical characteristics and dimensional uniformity of the final preform are strongly affected by the collapse process. Great care is thus required during this stage of preform manufacture.

To effect collapse of a composite silica/doped-silica tube prepared by HCVD, one end of the tube is heated above the softening point of silica using an oxyhydrogen flame (from the surface-mix burner previously used for the deposition with a natural gas/oxygen flame). The hot-zone, which is about 30 mm long, is then slowly traversed along the rotating silica tube, and the surface tension forces of the glass are sufficient to produce a reduction in diameter of the tube.

The degree of shrinkage will depend upon parameters such as the hot-zone temperature, traverse speed, silica-tube size, deposited glass composition and the pressure within the tube. All these parameters may be varied from preform to preform to meet requirements dictated by the fibre's eventual application. In general, however, a number of burner traverses are made to progressively collapse the composite tube into the preform; it has been found that preform circularity can be degraded by the large change in dimensions when collapsing the preform in only one burner pass.

A second problem commonly experienced when collapsing preforms having doped-silica cores is the outdiffusion of dopant from the innermost core layers due to the increased vapour pressure of the dopant relative to silica at the collapse temperature.

This effect is particularly common in phosphosilicate preforms where the high vapour pressure of the P_2O_5, and the low glass viscosity, give a high P_2O_5 diffusion coefficient. In addition, the low viscosity of the core glass creates an increased tendency for the tube to deform asymmetrically during collapse.

A number of techniques have been developed to enhance the control of the collapse process:-

1. The outdiffusion of dopant can be reduced by creating a dopant-rich atmosphere within the hot-zone during collapse[28]. In the initial stages of collapse this is achieved by passing dopant-halide vapours, with oxygen, through the tube. The dopant concentration must be adjusted to eliminate the dip without diffusing excess dopant into the glass. During the final stage of the collapse the tube is sealed and it is not possible to pass the dopant through the tube. However a dopant-rich atmosphere can still be maintained by depositing dopant soot ahead of the hot-zone prior to sealing the tube; as the hot-zone moves along the tube the dopant is continuously volatilised and condensed ahead of the zone.

2. The circularity of the preform can be maintained by applying a slight positive pressure to the inside of the tube during collapse. The pressure may be adjusted to balance the surface tension forces which cause tube shrinkage. Thus by exerting an outward radial force marginally less than the inward radial forces due to surface tension, it is possible to progressively reduce the tube diameter whilst still retaining circularity. In practice a positive pressure of 1 - 2 millibar is provided by a dynamic gas-bleeding system employing a variable flow valve and manometer to adjust and monitor the internal pressure of the tube.

3. The preform circularity can also be affected by any offset of the tube from the rotational axis of the lathe spindles. If the tube is offset it will move alternately into and away from the burner as the tube rotates, establishing a non-uniform temperature distribution around the preform which will in turn cause an asymmetric collapse. To overcome this problem a guide system has been developed which can be fitted to the lathe to re-align the tube with its rotational axis before initiating collapse. Not only does this assist the circularity of the preform, but also it maintains the straightness of the preform over the collapsed length.

4. A high-pressure air stream can be employed to rapidly quench the preform shortly after its closure into a solid rod thereby preventing distortion of the rod due to viscous flow whilst still at temperatures above the softening point.

It should be noted that the quality of the silica substrate tube can have a significant effect upon preform quality. In particular, variations of wall thickness around the tube ('siding') will cause eccentricity between the deposited glass and the outer surface of the preform, and generally also lead to ellipticity of the core due to asymmetric temperature and surface tension distributions. Also, the optical characteristics of the preform can be degraded by the presence of small bubbles within the silica tube which migrate radially to the interface between the substrate and the deposited glass during collapse. Care must therefore be paid to the selection of substrate tubes of high geometrical uniformity and low bubble content.

2.7 Manufacture and Characteristics of HCVD Preforms

The HCVD process has been applied to the manufacture of preforms for both multimode and monomode fibres, more than two hundred preforms having been fabricated during the course of this study. The development of the process has been on-going, and even now there are still areas for substantial improvement. However a number of preferred techniques have been evolved for the manufacture of high-quality preforms at high yield. In this section practical examples of manufacturing details for step-index, graded-index and monomode preforms are presented.

2.7.1 Step-Index Multimode-Fibre Preforms

The techniques for the manufacture of step-index preforms are essentially straightforward, requiring only the deposition of a core glass of constant composition within a cladding which may be deposited material or the silica substrate itself.

Having specified the numerical aperture required in the fibre, the core/cladding diameter ratio, and the glass systems to be used for core and cladding, it is necessary to determine the volume of material to be deposited (this is a function of the cross-sectional area of the substrate tube), the carrier gas flow rates to give the required index difference, and to control only the traverse speed and number of traverses to deposit the requisite volume of material.

The manufacturing technique and uniformity of refractive index across the core are largely governed by the choice of glass systems used in the preform. For example, figures 2.18 to 2.21 show the refractive index profiles and cross-sections of four step-index fibres having the following core and cladding configurations:-

Fibre	Preform	Core	Cladding	NA
VD175	A	P_2O_5/SiO_2	SiO_2	0.15
VD148	B	GeO_2/SiO_2	SiO_2	0.15
VD154	C	SiO_2	B_2O_3/SiO_2	0.13
VD173	D	$P_2O_5/GeO_2/SiO_2$	SiO_2	0.24

Preform A has a 15 m/o phosphosilicate core, deposited in 15 passes within a 15 mm OD, 12.5 mmID Heralux silica tube, and has a numerical aperture of 0.15. The refractive index profile is a good approximation to a step-index profile over much of the core, but the high volatility of P_2O_5 at the preform collapsing temperature has produced a large refractive index depression on the core axis. It was not possible to completely compensate the outdiffusion of P_2O_5 by creating a dopant-rich atmosphere during collapse. Even though internal pressurisation had been employed during collapse the low viscosity of the phosphosilicate glass at the collapsing temperature has also resulted in a significant degree of ellipticity within the core, as shown by the fibre cross-section, figure 2.18b.

Using germanosilicate glass as the core (preform B) only 5 m/o GeO_2 is required to give a 0.15 numerical aperture. The reduced doping level compared to the phosphosilicate core, and the increased viscosity of the germanosilicate glass has enabled a high degree of core circularity to be obtained, figure 2.19b. However, whilst the lower doping level and reduced volatility of GeO_2 has resulted in less outdiffusion of GeO_2 during collapse, the refractive index profile of the core consists of a series of 18 annular rings, each ring corresponding to one deposition layer. Clearly, the refractive index distribution within each layer is non-uniform, a consequence of the variation of GeO_2 incorporation efficiency along the length of the deposition hot-zone[29]. Furthermore, the mean index level of each layer increases with decreasing core radius giving a graded-index structure; this effect is thought to be due to the variation of GeO_2 incorporation efficiency with deposition temperature, a problem which was subsequently overcome by the use of a temperature-controlled hot-zone during deposition.

In the borosilicate-clad, silica-core fibre both the geometry and refractive index profile are as desired, figure 2.20. However, production of such a large silica core by HCVD is inefficient because the very high deposition temperature required to fuse the silica soot necessitates the deposition of many silica layers at low reactant flow rates; the high deposition temperature leads to severe tube distortion unless an internal pressurisation system is used to control the tube diameter[30]. As in the case of this preform, to achieve an acceptable core/cladding diameter ratio, a rod-in-tube approach is generally adopted, and a high-quality synthetic silica rod must be procured for the core.

The binary glass systems thus possess processing characteristics which make it difficult to obtain good geometry and an accurately-stepped refractive index profile in long lengths of fibre: The viscosity and refractive index properties of phosphosilicate glass invariably result in non-circularity and excessive dopant out-diffusion in fibres having a numerical aperture in excess of 0.12.

For the germanosilicate glass, the high viscosity dictates the need for a high deposition temperature with its attendant problems, namely tube shrinkage, a perturbed refractive index profile, and, often, bubble formation due to gas entrapment within the deposited glass. Whilst the borosilicate-clad, silica-core fibre provides the desired optical configuration, the rod-in-tube approach is viable only for the manufacture of short lengths of fibre for experimental purposes. Faced with these limitations, it was decided to investigate the ternary glass systems formed by the mixing of any two of the three binary systems.

Initial attempts to manufacture phospho-borosilicate glasses revealed that it was difficult to deliver the reactant vapours to the deposition tube, due to a room temperature reaction between $POCl_3$ and BBr_3 which produces a solid precipitate. Similar problems were not experienced when mixing $GeCl_4$ vapour with either $POCl_3$ or BBr_3 vapours. Germanoborosilicate glasses were found to have a lower fusion temperature than the germanosilicates and by a suitable choice of dopant levels it was possible to obtain either positive or negative refractive index differences with respect to pure silica. The opposite senses of the refractive index difference due to each dopant is a disadvantage of this system, since the total dopant level to achieve a specified refractive index in the glass must be higher than would normally be the case. Finally, investigation of the ternary phosphogermanosilicate system demonstrated that by a suitable choice of dopant levels it was possible to obtain a glass exhibiting most advantageous processing characteristics.

It follows from the discussion of the phosphosilicate and germanosilicate glasses in earlier sections that the addition of small amounts of P_2O_5 to germanosilicate glass will reduce the soot-fusion temperature in much the same way as for P_2O_5 in silica. The practical significance of this is twofold. Firstly, the ternary glass may be deposited at a temperature below that normally used for germanosilicate glass, and, secondly, the deposition rate can be increased without causing bubble formation due to gas entrapment within the deposited layers. The lower deposition temperature also reduces the concentration gradient within each layer, and thus improves the accuracy with which an ideal refractive index profile may be approximated.

Furthermore, if the phosphorous pentoxide doping level does not exceed 5 m/o, then the viscosity of the ternary glass remains sufficiently high to prevent severe ellipticity of the preform during the collapsing operation. Although dopant evaporation still occurs at the high temperature used for collapsing, the depletion zone is generally no greater than that obtained in a binary germanosilicate core; as will be shown in chapter 4, the dopant loss can be effectively compensated by creating a germania-rich atmosphere in the closure zone during collapse.

The ternary phosphogermanosilicate glasses thus possess processing characteristics which combine the advantageous properties of each of the binary systems. The ternary system was adopted as the 'standard' for use in the multimode fibres produced at Southampton, and led to distinct improvements in the quality and yield of the HCVD preforms. In figure 2.21 the refractive index profile and cross-section of a silica-clad, phosphogermanosilicate-core fibre is shown. The use of a low deposition temperature and an increased deposition rate has enabled the intended step-index profile to be well-approximated, and excellent core circularity has been obtained. In Table 2.2 the typical deposition conditions for the fabrication of a step-index preform are given along with the details of the processing time and dimensions of the final product. By employing a 20mm OD x 1.5mm wall-thickness substrate tube it has been possible to increase the deposition rate by a factor of three compared with earlier fibres made by HCVD[24]. The reduced tube shrinkage associated with the P_2O_5-GeO_2-SiO_2 system and the larger substrate tube has also enabled twice as many layers to be deposited in each preform. The volume of deposited glass has therefore increased by a factor of six, making it possible to draw 125 μm fibres in lengths in excess of 5km from preforms which can be fabricated in less than six hours.

The considerable benefits of the ternary system were subsequently recognised by a number of other laboratories; for example, workers at Corning Glass Works realised that the low sintering temperature of the phosphogermanosilicate glasses would permit the use of a substrate having a lower softening temperature, and successfully employed Vycor (96% silica, 4% boric oxide) tubing as a direct replacement for silica[31].

Even though the development work on the P_2O_5-GeO_2-SiO_2 system was undertaken in 1975 and 1976, to date no superior alternative has been reported, and, at most fibre manufacturing facilities, the ternary system is in general use for the manufacture of high-quality multimode fibres.

2.7.2 Graded-Index Multimode-Fibre Preforms

Gloge and Marcatili[32] have shown that by grading the core refractive index of multimode fibres according to a power-law profile, the group velocity differences between modes can effectively be equalised, increasing the fibre's bandwidth by up to three orders of magnitude over the step-index case. In a subsequent analysis which took account of the dispersive properties of the core and cladding glasses, Olshansky[33] found an optimum index profile given by:-

$$n(r) = n_1\left[1 - 2\Delta\left(\frac{r}{a}\right)^{\alpha}\right]^{1/2} \quad \text{for } r \leq a$$

$$n(r) = n_1\left[1 - 2\Delta\right]^{1/2} \quad \text{for } r > a \qquad (2.15)$$

$$\text{and } \alpha_{opt} = 2 - 2P - 12\Delta/5$$

where $n(r)$ = index at radial coordinate r

a = core radius

n_1 = refractive index at $r = 0$

Δ = relative index difference = $\dfrac{n_1^2 - n_2^2}{2n_1^2}$

n_2 = index at $r \geq a$ $\left(= n_1\left[1 - 2\Delta\right]^{1/2}\right)$

α_{opt} = power law exponent characterising profile,

and P is the profile dispersion parameter defined by

$$P = \frac{n_1}{N_1} \cdot \frac{\lambda}{\Delta} \cdot \frac{d\Delta}{d\lambda} \qquad (2.16)$$

and

$$N_1 = n_1 - \lambda \frac{dn_1}{d\lambda} \qquad (2.17)$$

Using step-index fibres as described in the previous section Dr. F.M.E. Sladen was able to determine the value of the profile dispersion parameter over an extended wavelength range for the binary glass systems[33]. It was found that in the case of germania and boron-doped glasses the value of α_{opt} varied considerably with wavelength, whilst for phosphorus-doped glasses α_{opt} remained almost constant at 1.9 over the 850 - 1300 nm spectral range. Furthermore, it was shown that high-bandwidth graded-index fibres could only be obtained in these glass systems if the refractive index profile of the fibre (and preform) closely approximated the profile given by equation 2.15.

2.7.2.1 Profile Synthesis

In the HCVD process, graded-index profiles are fabricated using a stepped series of deposition layers, the refractive index being controlled from layer to layer to give the best approximation to the desired profile. The greater the number of layers the better is the fit to the power-law profile. However, the restraints of deposition times, speeds, and flow-rate control dictate a finite upper limit to the number of layers which can be deposited. Although preforms having up to 120 core layers have been manufactured using HCVD, we have found that about 40 layers are sufficient to give a good approximation to the desired profile whilst allowing the use of high deposition rates for a reasonable yield.

A computer program has been developed to model the deposition process and to calculate the composition of each deposition layer to obtain a specified α-value in the preform. Having specified the numerical aperture and α-value required in the fibre, the program allows the choice of glass systems and then employs the data of figures 2.12, 2.15 and 2.17 to calculate the layer by layer compositions for the deposition process.

The program takes account of the coordinate transformation which occurs in the preform collapse, and outputs plots of the stepped approximation to the α-profile in the preform, and also the refractive index variation with deposition layer number.

These plots are shown in figure 2.22 for two approximations to an $\alpha = 2$ graded index profile, namely a 20 layer deposition and a 40-layer deposition. The 40-layer approximation is clearly a better fit to the required profile, although it can be seen that in both cases the profile is perturbed near to the core centre. Although increasing the number of layers would improve the accuracy of the approximation, it is felt that, since the grading at the core extremities has the greatest effect upon fibre bandwidth, a 40 layer deposition provides an acceptable solution.

In Table 2.3 the computer print-out of the relative carrier gas flow rates R_I (equations 2.11 to 2.13) is given for the above profile having a numerical aperture of 0.25, a borosilicate cladding and a graded phospho-germanosilicate core. The numerical aperture due to the borosilicate cladding is 0.13, and a sufficient cladding thickness is provided by depositing 12 layers of constant composition cladding glass before grading out the B_2O_3 in the first core layer The P_2O_5 is graded into the core over only two layers and then held constant throughout the remainder of the deposition; in this way the lower sintering temperature offered by the use of P_2O_5 can be utilised throughout the major part of the deposition. The GeO_2 is added to the core glass when the P_2O_5 level has reached its maximum. The maximum gas-phase GeO_2 content is 30m/o with respect to silica, giving a germania concentration of 10.5m/o in the deposited glass.

2.7.2.2 Fabrication and Properties

Table 2.4 gives the deposition conditions for the fabrication of a typical preform having the profile described in the previous section. A 20 mm OD x 17 mm ID Heralux WG silica tube of 75 cm length was used for the deposition; a 35 mm OD by 25 cm length of low-quality silica tubing was fused to the WG tube to provide a low-impedance exhaust for the undeposited soot transported out of the deposition zone. The tube was given a thorough cleaning procedure and etched for about 15 minutes in a 25% aqueous solution of hydrofluoric acid to provide a clean substrate for the deposition. The tube was rinsed in de-ionised water and dried using high-purity acetone and nitrogen before being connected to the HCVD system.

By traversing the hot-zone at about 1750°C along the tube, micro-cracks and flaws on the inner surface were removed by fire-polishing, providing a pristine surface for the deposited glass. The borosilicate cladding and graded-index core were deposited over a 50 cm length of the WG tube, the 55 layers requiring a total deposition time of about $4\frac{1}{2}$ hours. The hot-zone temperature was maintained constant throughout the core deposition to ensure that the GeO_2 incorporation efficiency did not fluctuate from layer to layer. At the 300 ml/min $SiCl_4$ - carrier flow rate and hot-zone traverse speed of 10 cm/minute a deposition layer thickness of 13μm/pass was expected.

Preform collapse was accomplished in four low-speed passes taking about 1 hour 20 minutes in all. Since the hot-zone position varies somewhat with traverse speed, the temperature control loop was not used during the collapse, and the fuel-gas flows to the burner were set manually to predetermined values. During the first three collapse traverses $GeCl_4$ and oxygen were passed through the silica tube to reduce the GeO_2 dopant loss due to outdiffusion. The tube was then sealed and internal pressurisation was employed to maintain the preform's circularity during the preform closure pass. Approximately 45 cm of useful preform was obtained.

A cross-section of the partially-drawn preform is shown in figure 2.23a, and a plot of the preform's diameter along its length is given in figure 2.23b. The geometry of the preform is very good, having a core to cladding diameter ratio of 0.47, and a core ellipticity of less than 3%; this slight ellipticity will be further reduced in the fibre drawing operation. The borosilicate cladding layer can be clearly distinguished as the dark annular ring surrounding the core, in which the individual deposition layers can be resolved near the core centre.

The dark spot at the core centre indicates that the GeO_2 loss during collapse has not been completely compensated, and that an index depression has consequently resulted. The preform diameter of 12.4 mm gives a core diameter in the preform of 5.8 mm; the mean thickness of the deposited layers in thus 12.5 μm/pass, in good agreement with the predicted value. The preform diameter is seen to be almost constant along 45 cm of its length, with a 1.5 mm diameter variation over the first 10 cm. This initial taper corresponds to the region where steady-state deposition conditions are being established at the start of each deposition pass. If the preform were to be drawn into 125 μm diameter fibre approximately 4 km of fibre could be obtained from the uniform section of the preform. If longer lengths of fibre are required in single sections, the yield may be improved by increasing the volume of deposited glass and sleeving the preform in a second silica tube before drawing.

The structural characteristics of the graded-index fibres have been investigated using a scanning electron microscope (SEM). When transverse sections of fibre are etched in dilute hydrofluoric acid the etch-rate is found to be strongly dependent upon the composition of the glass. Thus in an HCVD fibre each core layer etches at a different rate, and it is possible to resolve individual layers on a high resolution microscope. Figure 2.24 shows SEM photomicrographs of an etched fibre sample at increasing magnification. Of particular note are the preservation of the distinct step and layer structure and the compositional fluctuations within each core layer. The index depression at the core centre is evident as a raised tapered pip. The borosilicate cladding, which is of uniform composition, etches more quickly than the phospho-germanosilicate glass, and is revealed as the broad annular ring surrounding the core. Perhaps the most striking aspect of the photomicrographs is the fact that the radial symmetry of the deposited layers has been retained during the collapse and fibre drawing operation to give a circular core having near-perfect symmetry: this is not the case in fibres produced by the OVPO process where severe distortion of the innermost core layers is found in etched samples[35].

Finally, a recent development by Mr. Issei Sasaki at Southampton has enabled the accurate determination of the refractive index distribution within the preform[36]. Figure 2.25 shows the refractive index profile measured in a standard graded-index preform, and the expected refractive index profile calculated from the deposition conditions. As in the transverse cross-section of a similar preform (fig 2.23) the core layers near the core axis can be clearly resolved. The germania depletion has been well compensated during the collapse and reasonable agreement is obtained between the actual and predicted profiles.

As described in section 2.7.1, the refractive index perturbations across each layer may be reduced by increasing the P_2O_5 level within the core. This has been confirmed in the graded-index preforms by profile measurements on preforms with differing P_2O_5 doping levels. Hence in figure 2.26 the profile of a preform in which the P_2O_5 level was increased to 2 m/o is seen to be much smoother than the profile in the previous figure, where the P_2O_5 level was only 1 m/o. From the significant improvement in profile it is suggested that in future preforms the P_2O_5 content could be marginally increased to 2 m/o without detriment to the circularity of the preforms due to the higher doping levels.

2.7.3 Monomode-Fibre Preforms

The techniques for producing preforms for single-mode fibres have a number of distinct differences from the multimode case. Firstly, in the monomode fibre a considerable portion of the guided power travels in the cladding. In order to avoid excessive absorption losses, the cladding material must be of comparable purity to the core, and a low-loss cladding must be deposited prior to the core. Kapron and Lukowski[37] have presented design data for the required cladding thickness and have shown that a cladding: core diameter ratio of 4:1 should suffice to contain the guided energy within a low-loss material. Kawachi et al[38] have considered the diffusion of hydroxyl ions from the silica tube into the deposited cladding and suggest a barrier cladding: core diameter ratio of 5:1, an area ratio of 24:1. In contrast to the multimode case it is necessary to deposit far more cladding glass than core glass, and the deposition of the cladding layers will occupy the major portion of the deposition process.

Secondly, for true single-mode operation the parameters characterised by the core diameter and refractive index difference in the fibre must normally satisfy the condition $V \leqslant 2.405$ where the normalised frequency, V, is defined by[39]:-

$$V = \frac{2\pi a}{\lambda} \cdot \left(n_1^2 - n_2^2\right)^{1/2} \qquad (2.18)$$

where a = core radius

λ = wavelength of operation

n_1, n_2 = core and cladding refractive indices.

The choice of core size and index difference are thus governed by the constraints imposed by equation (2.18); increasing the core diameter requires a reduction of the index difference to maintain the V-value constant at the operating wavelength. The choice of core size and index difference is dictated by the trade-off between high-index-difference, small-core fibres which have good microbending performance and large-core, low-index-difference fibres in which jointing tolerances are somewhat eased[40]. In practice an index difference of $\Delta \sim 0.3\%$ (NA = 0.12) provides good mode confinement at V = 1.6 and above[14]. The doping levels are therefore very much lower than those in multimode fibres where typically $\Delta = 1.3\%$ (NA = 0.24).

2.7.3.1 Preform Manufacture

Two distinct approaches may be adopted for the manufacture of monomode-fibre preforms by HCVD. In the first approach, advantage is taken from the fact that the core size of the monomode fibre is very much less than that of the typical multimode fibre: by the deposition of a single core layer in a partially-collapsed silica tube it is possible to obtain a preform in which the core: overall diameter ratio is as required in the resultant fibre. Because the silica tube must be partially collapsed before the core is deposited, it is possible to deposit a reasonable thickness of low-loss silica cladding during the partial-collapse[14]. The drawback of this approach is that the preform is generally smaller than the multimode preforms, and consequently less fibre can be drawn from each preform.

In the second approach a significant volume of cladding and core glasses are deposited within a standard silica substrate tube, and the preform is collapsed in the normal manner. The core: preform diameter ratio is generally much greater than that required in the fibre and so to achieve the correct core: reference surface diameter ratio the preform is sleeved in silica tubes before drawing. The advantages of this approach are that better control of the geometry and refractive index profile of the preform is possible, and that much longer lengths of fibre can be drawn from each preform.

Both approaches have been pursued in this programme, and the first approach has been described in detail elsewhere[14]. Although it offered an excellent solution to the need for low-loss monomode fibres for experimental purposes, it is no longer used in fibre manufacture and will not be dealt with here. The preform-sleeving approach has been used to manufacture fibres having silica, phosphosilicate, or germanosilicate cores generally in a borosilicate cladding[41].

Indeed, the deposition of the cladding layers presents more difficulties than the core deposition. To maximise the spectral window over which low-losses can be obtained, silica is the first-choice cladding material[42]. However, the deposition of large volumes of silica is extremely difficult without feedback control of the substrate tube diameter using internal pressurisation[30]. Borosilicate glass has therefore been utilised as the cladding, and wherever possible the B_2O_3 doping level has been kept to a minimum value which allows deposition of the glass without excessive deformation of the substrate tube.

Typical deposition conditions for the manufacture of a borosilicate-clad, germanosilicate-core monomode preform are given in Table 2.5. The deposition proceeds as follows: A 14 mm diameter Heraeus WG silica tube having a wall thickness of 1.5 mm is cleaned, etched and fire polished in the usual manner. Nineteen cladding layers of borosilicate glass containing 3 m/o B_2O_3 are deposited at a higher deposition rate ($SiCl_4$ - carrier flow of 300 ml/min). A single layer of germanosilicate glass is then deposited at 1650°C to form the core of the preform. The composite tube is then collapsed to form a preform of 8.05 mm diameter, 40 cm in length. A noteworthy feature of the deposition is the use of a 14 mm diameter silica tube rather than a 20 mm tube as used for multimode preforms; the small tube enables a rapid preform collapse with less out-diffusion of dopant from the core and reduced hydroxyl diffusion from the silica substrate into the low-loss cladding.

A transverse cross-section of the preform, BSG1, viewed under transmitted light is shown in figure 2.27a. The core and cladding layers can be clearly distinguished inside the silica supporting structure, and it can be seen that the circularity and concentricity of the preform are excellent. The diameter over the borosilicate cladding in the preform was 4.0 mm whilst the core diameter was 0.9 mm, giving a cladding core diameter ratio of 4.4:1. By the use of the high deposition rate CVD it was possible to produce the preform in less than $2\frac{1}{2}$ hours from initial fire polish to final preform collapse.

Before the preform is drawn into fibre it is necessary to determine the core diameter and refractive index difference in the preform, in order that the correct drawdown ratio may be calculated for the monomode operation of the fibre at the specified wavelength. The core diameter may be most easily determined by measurements on transverse photomicrographs of the preform such as is shown in figure 2.27a. Alternatively, if the core-cladding interface is diffuse, the core may be clearly resolved by etching the end of the preform in dilute hydrofluoric acid. Figure 2.27b shows the transverse cross-section of the core and cladding of preform BSG1 illuminated under reflected light after etching for 10 minutes in 25% hydrofluoric acid. The core/cladding interface is now clearly distinguished as is each of the nineteen cladding layers. The outdiffusion of dopant from the core during collapse is identified by the 'pip' at the core centre where the reduced dopant level has resulted in a lower etch rate.

A number of techniques may be employed to establish the core to cladding index difference. One technique involves the laborious polishing of a thin slice of preform which is subsequently examined by interference microscopy[43]. An alternative, and very simple, technique is to draw a short section of rod from one end of the preform, to prepare its ends by cleaving and to measure directly the numerical aperture of the rod from its far-field radiation pattern. Because the rod is a highly multimode structure it can also be evaluated using techniques normally reserved for multimode fibres; for example, the refractive index profile in the preform can be evaluated using the near field scanning technique. Figure 2.28 shows the refractive index profile measured in a short section of partially drawn preform BSG2.

The rod was approximately 2 mm in diameter, the core diameter was 192 μm and the numerical aperture measured in the rod was 0.12; at the measurement wavelength of 0.55 μm the V-value was 131 and the rod was thus highly multimode. The solid curve in the figure denotes the refractive index profile obtained by applying leaky-mode correction factors to the near-field distribution (broken line). The preform has a nearly stepped refractive index profile with an axial dip due to GeO_2 loss during collapse; the relative index difference between the depleted region and the edge of the core is some 66% of the total index difference, and the depleted zone occupies 40% of the total core diameter. Gambling et al[44] have studied the effects of an index depression on the core axis in monomode fibres and have shown that a reduction in mode confinement is produced. However in practical terms they conclude that for an index distribution of the form shown in figure 2.28, the propagation characteristics are almost identical with those of a step-index fibre. Of course the dopant depletion may be eliminated by using a pure silica core in a borosilicate or fluorosilicate cladding, or it may be compensated by creating a dopant-rich atmosphere in the closure-zone during collapse.

It must also be mentioned in passing that whilst the above techniques for preform evaluation are both quick and simple, they only provide data pertaining to the end(s) of the preform. A further improvement in the characterisation of the preforms may be obtained by the use of the preform scanning technique[36], which not only yields more accurate information on core size and index difference, but also enables non-destructive measurements to be performed along the length of the preform. Unfortunately at the completion of this particular stage of the PhD project the preform scanning system was in its early stages of development and so it is not possible to present experimental results here; an excellent indication of the technique's capabilities are given in Reference 30.

Because the doping levels are generally much lower in single-mode preforms than in multimode preforms, phosphosilicate preforms having near-perfect core circularity can be reproducibly manufactured. The use of P_2O_5 rather than GeO_2 as the core dopant enables lower losses to be attained in the short wavelength region (600nm to 850nm) where the Rayleigh scattering of the phosphosilicate glass is comparable with that of silica. It is also possible, by a suitable choice of core and cladding dopants, to balance the stress levels within the deposited glasses such that no stress discontinuity occurs at the core/cladding interface. This approach was found to be particularly effective in the manufacture of monomode fibres exhibiting very low birefringence[45], the characteristics of which are described in Chapter 4.

2.8 References to Chapter 2

1. Jones M.W. and Kao, K.C. "Spectrophotometric studies of ultra low loss optical glasses: part 2: double beam method"; Journal of Physics E, Series 2, Vol 2, No. 4, pp 331-335.

2. Kapron, F.P., Keck, D. B., and Maurer, R.D.: "Radiation losses in glass optical waveguides" Applied Physics Letters, 17, 10 pp 423-425.

3. French, W.G., Pearson, D., Tasker, G.W., and MacChesney, J.B.: Low-loss fused-silica optical waveguide with borosilicate cladding', App. Phys. Letter. 23 (1973) pp 338-339.

4. Black P.W., Irven J., Byron, K., Few, I.S., and Worthington R.: 'Measurements on waveguide properties of GeO_2 - SiO_2 - cored optical fibres', Electron. Lett. 10 (1974), pp 239-240.

5. French, W.G., MacChesney, J.B., O'Connor, P.B., and Tasker, G.W.: Optical waveguides with very low losses', B.S.T.J. 53 (1974) pp 951-954.

6. Payne, D.N., and Gambling, W.A.: 'New silica-based low-loss optical fibre', Electron Lett 10 (1974), pp 289-290.

7. Wood, D.L., MacChesney, J.B., and Luongo, J.P.: 'Investigation of the reactions of $SiCl_4$ and O_2 at elevated temperatures by infra-red spectroscopy', J. Mat. Sci. 13 (1978), pp 1761 - 1768.

8. Standley, R.D., and Holden, W.S.: 'Experimental results on a single-material optical fibre', BSTJ 53(1974), pp 779 - 783.

9. Hammond, C.R., and Payne, D.N.: 'Single-material fibres', Annual Report of Research Activities, Department of Electronics, University of Southampton, 1974-75, p 112.

10. Gambling, W.A., Payne, D.N., Hammond, C.R., and Norman S.R. 'Optical communication through fibres: Annual Report 1974-1975', Department of Electronics, University of Southampton.

11. Abe, K.: 'Fluorine doped silica for optical waveguides', Proc. Second European Conference on Optical Communications, Paris 1976, Paper II.4.

12. Cormia, R.L., McKenzie, J.D. and Turnbull, D.: 'Viscous flow and melt allotropy of phosphorus pentoxide', J. App. Phys. 34 (1963), p 2245-2248.

13. Van Uitert, L.G., Pinnow, D.A., Williams, J.C., Rich T.C., Jaeger, R.E., and Grodkiewizc. W.H.: 'Borosilicate glasses for optical fibre waveguides', Mat. Res. Bull. 8 (1973), pp 469-476.

14. Norman, S.R.: 'The fabrication and properties of optical fibre waveguides', Minithesis, Department of Electronics, University of Southampton, 1977.

15. Grabmaier, J., Schneider. H., Lebetzki, E., and Douklias, N.: 'Preparation of low-loss fused-silica optical fibres by modified chemical vapour deposition technique', Siemens Forsch. - u Entwickl. - Ber, 5(1976), pp 171-175.

16. Doremus R.H.: 'Glass science', John Wiley & Sons, 1973.

17. Kato, D.: 'Fused-silica-core glass fibre as a low-loss optical waveguide, App. Phys. Lett, 22 (1973), pp 3-4.

18. Wemple, S.H., Pinnow, D.A., Rich, T.C., Jaeger, R.E., and Van Uitert, L.G.: 'Binary SiO_2-B_2O_3 glass systems: refractive index behaviour and energy gap considerations', J. App. Phys. 44 (1973), pp 5432-5437.

19. French, W.G., Tasker, G.W., and Simpson, J.R.: 'Graded index fibre waveguides with borosilicate composition: fabrication techniques', App. Opt. 15(1976), pp 1803-1807.

20. Schultz, P.C.: 'Optical absorption of the transition elements in vitreous silica', J. Amer. Ceram. Soc., 57 (1974), pp 309-313.

21. American Physics Handbook.

22. E. Merck & Co., Darmstadt, W. Germany: 'Materials for optical fibres, sample assay'.

23. Payne, D.N. and Gambling, W.A.: 'A borosilicate-cladded, phosphosilicate-core optical fibre', Opt. Commun. 13(1975) pp 422-25.

24. Gambling, W.A., Payne, D.N., Hammond, C.R., and Norman S.R.: 'Optical fibres based on phosphosilicate glass', Proc. IEE, 123(1976) pp 570-576.

25. Sladen F.M.E., Payne, D.N., and Adams, M.J.: 'Determination of optical fibre refractive index profiles by a near-field scanning technique', App. Phys. Lett., 28(1976), pp 255-258.

26. Hammond, C.R., and Norman, S.R.: 'Silica-based binary glass systems - refractive index behaviour and composition in optical fibres', J. Opt. Quant. Electron., 9(1977) pp 399-409.

27. Wilson, C.M., 'Electron microprobe analysis of optical fibres', Department of Ceramics, Glasses and Polymers, University of Sheffield.

28. Akamatsu, T., Okamura, K., and Ueda, Y.: 'Fabrication of graded-index fibres without an index dip by chemical vapour deposition method', App. Phys. Lett., 31(1977), pp 515-517.

29. 'Distribution of GeO_2 in fused-silica fibre made by CVD method', Furukawa Electric Co. Report, October 1976.

30. Okada, M., Kawachi, M., and Kawana, A.: 'Improved chemical vapour deposition method for long-length optical fibre', Electron. Lett 14(1978), pp 89-90.

31. Sommer, R.G., Deluca, R.D., and Burke, G.E.: 'New glass system for low-loss optical waveguides', Electron. Lett., 12(1976), pp 408-409.

32. Cloge, D., and Marcatili, E.A.J.: 'Multimode theory of graded-core fibres', B.S.T.J., 52(1973), pp 1563-1578.

33. Olshanksky, R., and Keck, D.B.: 'Pulse broadening in graded-index optical fibres', App. Opt. 15(1976), pp 483-491.

34. Sladen F.M.E., Payne, D.N., and Adams, M.J.: 'Profile dispersion measurements for optical fibres over the wavelength range 350 nm to 1900 nm', Fourth European Conference on Optical Communications, Genoa 1978, Conference Proceedings pp 48-57.

35. Sladen, F.M.E., 'Fibres for optical communications', Ph.D. Thesis, University of Southampton, 1978.

36. Sasaki, I., Payne, D.N., Mansfield, R.J., and Adams, M.J.: 'Variation of refractive index profiles in single-mode fibre preforms measured using an improved high-resolution spatial-filtering technique', Sixth European Conference on Optical Communications, York 1979, Conference Proceedings pp

37. Kapron, F.P., and Lukowski, T.I.: 'Monomode fibre design: power containment', App. Opt. 16(1977) pp 1465-1466.

38. Kawachi, M., Horiguchi, M., Kawana, A., and Miyashita, T.: 'OH ion distribution profiles in rod preforms of high-silica optical waveguide', Electron Lett., 13(1977), pp 247-248.

39. Gloge, D.: 'Weakly guiding fibres', App. Opt., 10(1971), pp 2252-2258.

40. Gambling, W.A., Matsumura, H., and Cowley, A.G.: 'Jointing loss in single-mode fibres', Electron. Lett., 14(1978), pp 54-55.

41. Norman S.R.: 'Fabrication and evaluation of single-mode fibres', Phys. Chem. Glasses, 21(1980), pp 53-57.

42. Izawa, T., Shibata, N., and Takeda, A.: 'Optical attenuation in pure and doped fused silica in the IR wavelength region; App. Phys. Lett., 31(1977), pp 33-35.

43. Kawana, A., Miyashita, T., Nakahara, M., Kawachi, 17., and Hasaka, T.: 'Fabrication of low-loss single-mode fibres', Electron. Lett., 13(1977), pp 442-443.

44. Gambling, W.A., Matsumura, H., and Ragdale, C.M.: 'Wave propagation in a single-mode fibre with a dip in the refractive index', Opt. Quant. Electron. 10(1978), pp 301-309.

45. Norman, S.R., Payne, D.N., Adams, M.J., and Smith A.M.: 'Fabrication of single-mode fibres exhibiting extremely low polarisation birefringence', Electron Lett., 15(1979), pp 309-311.

	MATERIAL	
IMPURITY	SILICON TETRACHLORIDE	PHOSPHOROUS OXYCHLORIDE
Copper (Cu)	< 1	< 5
Nickel (Ni)	< 1	< 5
Cobalt (Co)	< 1	< 5
Iron (Fe)	< 5	< 20
Manganese (Mn)	< 1	< 5
Chromium (Cr)	< 1	< 5
Vanadium (V)	< 2	< 10

The impurity levels are in parts per billion (gravimetric)

The materials and assays were supplied by
E. Merck GmbH, Frankfurt.

Table 2.1: Impurity assays of two commercially available chemicals for use in the HCVD process.

Starting Tube: 20mm O.D., 1.5mm wall thickness
Heraeus WG silica, 75cm length.

Tube Preparation: Soap cleaned, water rinsed, acid etched, water rinsed, and dried.

Fire Polish: 4 passes at 10 cm/min, hot-zone temperature = 1750°C.

Deposition:

1) Cladding: 10 layers at 12 cm/min
Deposition hot-zone temperature = 1650°C.

$SiCl_4$ carrier (O_2)	=	300 ml/min
BBr_3 carrier (N_2)	=	300 ml/min
Additional oxygen	=	600 ml/min

2) Core: 40 layers at 12 cm/min
Deposition hot-zone temperature = 1600°C.

$SiCl_4$ carrier (O_2)	=	300 ml/min
$GeCl_4$ carrier (O_2)	=	500 ml/min
$POCl_3$ carrier (O_2)	=	100 ml/min
Additional oxygen	=	600 ml/min

Deposition length 60cm
Total deposition time $\sim 4\frac{1}{2}$ hours (including fire polish)

Collapse: 5 passes at 5 cm/min. Hot-zone temperature 1900°C
Collapse duration $\sim$ 1 hour.

Preform Characteristics: Approx 55cm long by 12.5mm diameter
Numerical aperture = 0.25

Table 2.2 Deposition conditions for the manufacture of a step-index preform having a borosilicate cladding and a phosphogermanosilicate core.

Table 2.3 : Reactant carrier-gas flowrates for the manufacture of a graded-index preform of 0.25 NA and alpha = 2.0

PROFILE SYNTHESIS; CARRIER-GAS FLOWRATES
ALPHA VALUE = 2.00
NUMERICAL APERTURE OF FIBRE = 0.25
REACTANT LIQUID TEMPERATURE = 20 C
SiCl4 CARRIER-GAS FLOWRATE = 300 ml/min

CARRIER-GAS DATA FOLLOWS:-

	CARRIER-GAS FLOWRATES IN ml/min			
LAYER	SiCl4	BBr3	POCl3	GeCl4
0	300	292	0	0
1	300	257	0	0
2	300	222	0	0
3	300	189	0	0
4	300	161	0	0
5	300	137	0	0
6	300	111	0	0
7	300	86	0	0
8	300	65	0	0
9	300	44	0	0
10	300	19	0	0
11	300	0	10	0
12	300	0	54	2
13	300	0	54	13
14	300	0	54	23
15	300	0	54	34
16	300	0	54	45
17	300	0	54	57
18	300	0	54	68
19	300	0	54	80
20	300	0	54	92
21	300	0	54	104
22	300	0	54	117
23	300	0	54	130
24	300	0	54	143
25	300	0	54	157
26	300	0	54	170
27	300	0	54	185
28	300	0	54	199
29	300	0	54	214
30	300	0	54	229
31	300	0	54	244
32	300	0	54	260
33	300	0	54	276
34	300	0	54	293
35	300	0	54	310
36	300	0	54	328
37	300	0	54	346
38	300	0	54	364
39	300	0	54	383
40	300	0	54	403

Typical deposition conditions are given in Table 2.4

Starting Tube: 20mm O.D., 1.5mm wall thickness
Heraeus WG silica, 75cm length.

Tube Preparation: Soap cleaned, water rinsed, acid etched, water rinsed, and dried.

Fire Polish: 4 passes at 10 cm/min, hot-zone temperature = 1750°C.

Deposition:

1) Cladding: 12 layers at 12 cm/min

$SiCl_4$ carrier (O_2)	=	300 ml/min
BBr_3 carrier (N_2)	=	300 ml/min
Additional oxygen	=	600 ml/min
Deposition temperature		1650°C

2) Core: 40 layers at 12 cm/min
Reactant flow rates as given in Table 2.3
Deposition temperature ~ 1650°C.

Deposition length 60cm
Deposition period ~ 4½ hours

Collapse: 5 passes at 2.5 to 5 cm/min
Collapse temperature ~ 1900°C
Dopant compensation: $GeCl_4$ carrier = 8 ml/min
Additional oxygen = 100 ml/min
Collapse period ~ 1½ hours

Preform Characteristics: Length : 55cm
Diameter = 12.4mm (mean)
Numerical aperture = 0.23

Table 2.4 Deposition conditions for the manufacture of a graded-index preform having a borosilicate cladding and a phosphogermanosilicate core.

Starting Tube: 14mm O.D., 1.5mm wall thickness
Heraeus WG silica.

Tube Preparation: Soap cleaned, rinsed, HF etch, water rinse, acetone rinse and dried.

Fire Polish: 2 passes at 10 cm/min, hot-zone temperature = 1750°C.

Deposition:

1) Cladding: 19 layers at 12 cm/min
Deposition hot-zone temperature = 1650°C.

$SiCl_4$ carrier (O_2)	=	300 ml/min
BBr_3 carrier (N_2)	=	95 ml/min
Additional oxygen	=	600 ml/min

2) Core: 1 layer at 12 cm/min
Deposition temperature = 1650°C.

$SiCl_4$ carrier (O_2)	=	300 ml/min
$GeCl_4$ carrier (O_2)	=	100 ml/min
Additional oxygen	=	600 ml/min

(Liquid halides at 25°C)

Collapse: 3 passes at 5 cm/min. Hot-zone temperature = 1850°C

Preform Dimensions: 8.05mm dia x 40cm long

Table 2.5 Deposition conditions for the manufacture of a borosilicate-clad, germanosilicate-core monomode preform.

A) DEPOSITION OF DOPED-SILICA GLASSES

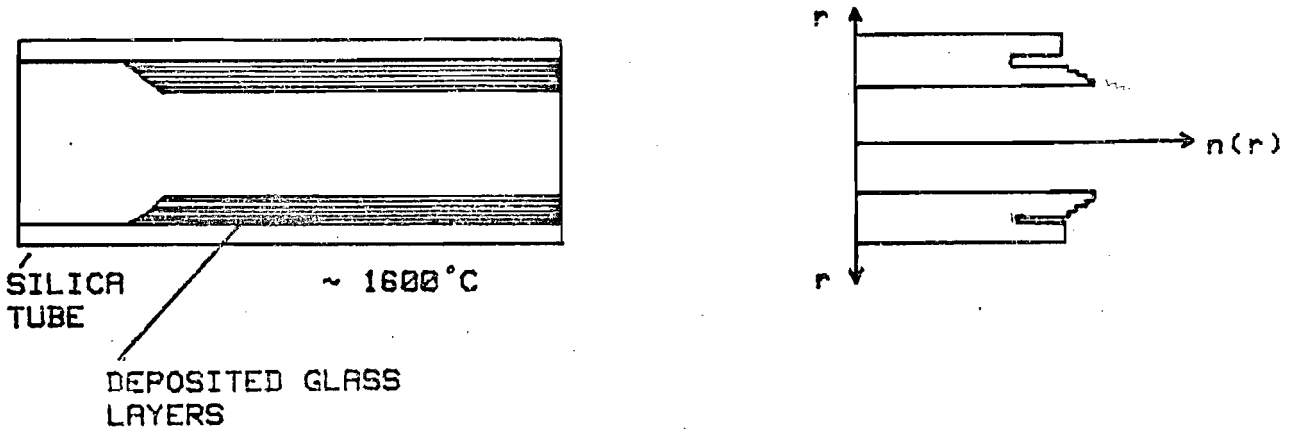

B) COLLAPSE OF COMPOSITE SILICA/DOPED-SILICA TUBE INTO PREFORM ROD

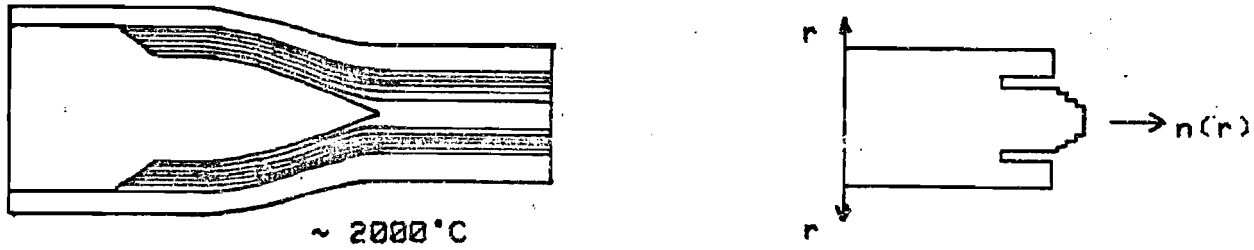

C) DRAWING OF PREFORM INTO FIBRE

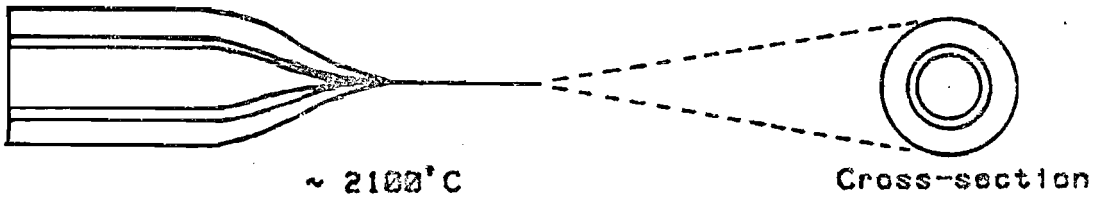

SCHEMATIC ILLUSTRATION OF THE APPLICATION OF THE MCVD PROCESS TO THE MANUFACTURE OF OPTICAL FIBRES.

FIGURE 2.1

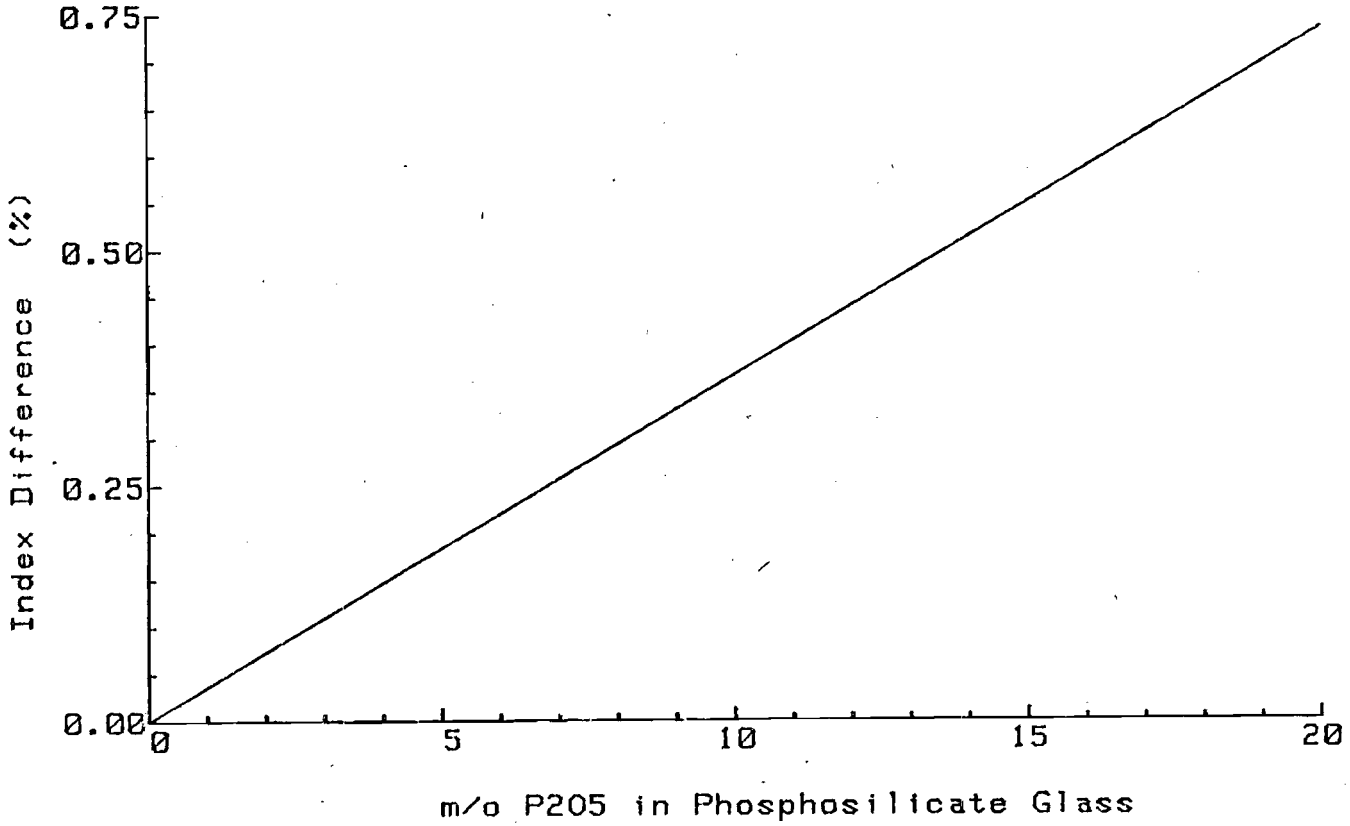

PHOSPHOSILICATE GLASS : PREDICTED REFRACTIVE INDEX DIFFERENCE RELATIVE TO SILICA AS A FUNCTION OF P_2O_5 CONTENT

FIGURE 2.2

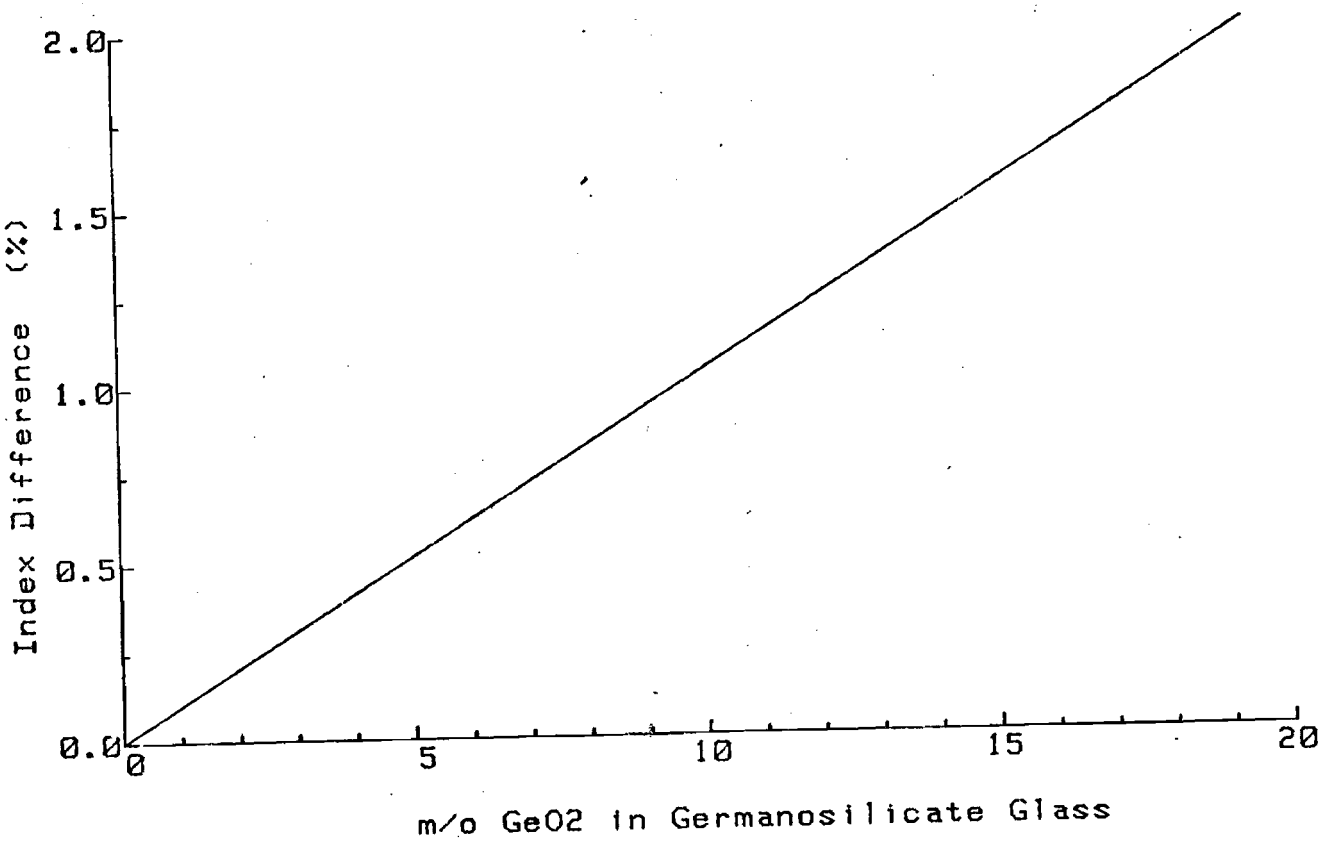

GERMANOSILICATE GLASS : PREDICTED REFRACTIVE INDEX DIFFERENCE RELATIVE TO SILICA AS A FUNCTION OF GeO_2 CONTENT

FIGURE 2.3

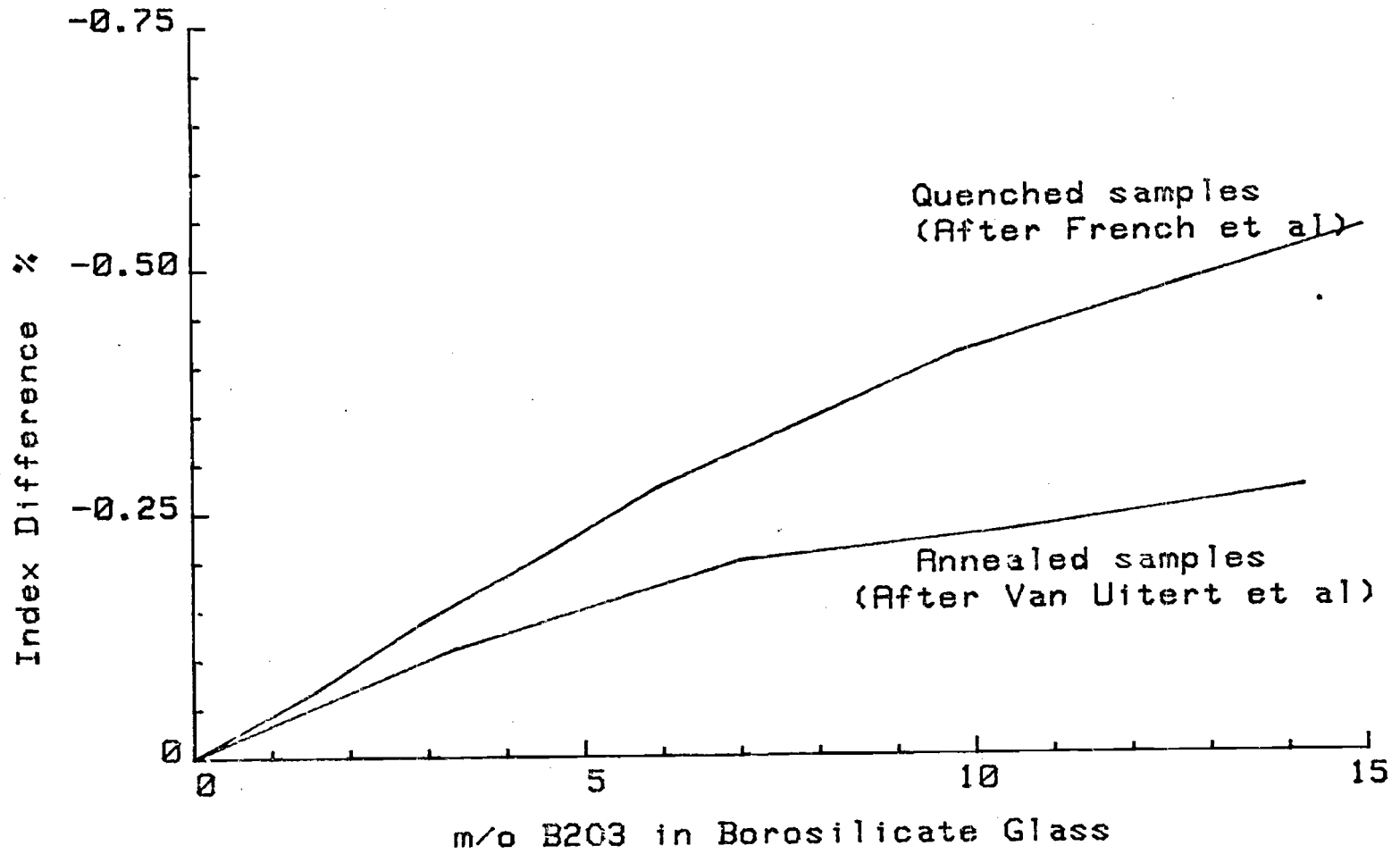

BOROSILICATE GLASS : REFRACTIVE INDEX DIFFERENCE RELATIVE TO SILICA AS A FUNCTION OF B_2O_3 CONTENT. The results are shown for annealed and quenched samples ; the index difference is seen to be dependent on the cooling rate.

FIGURE 2.4

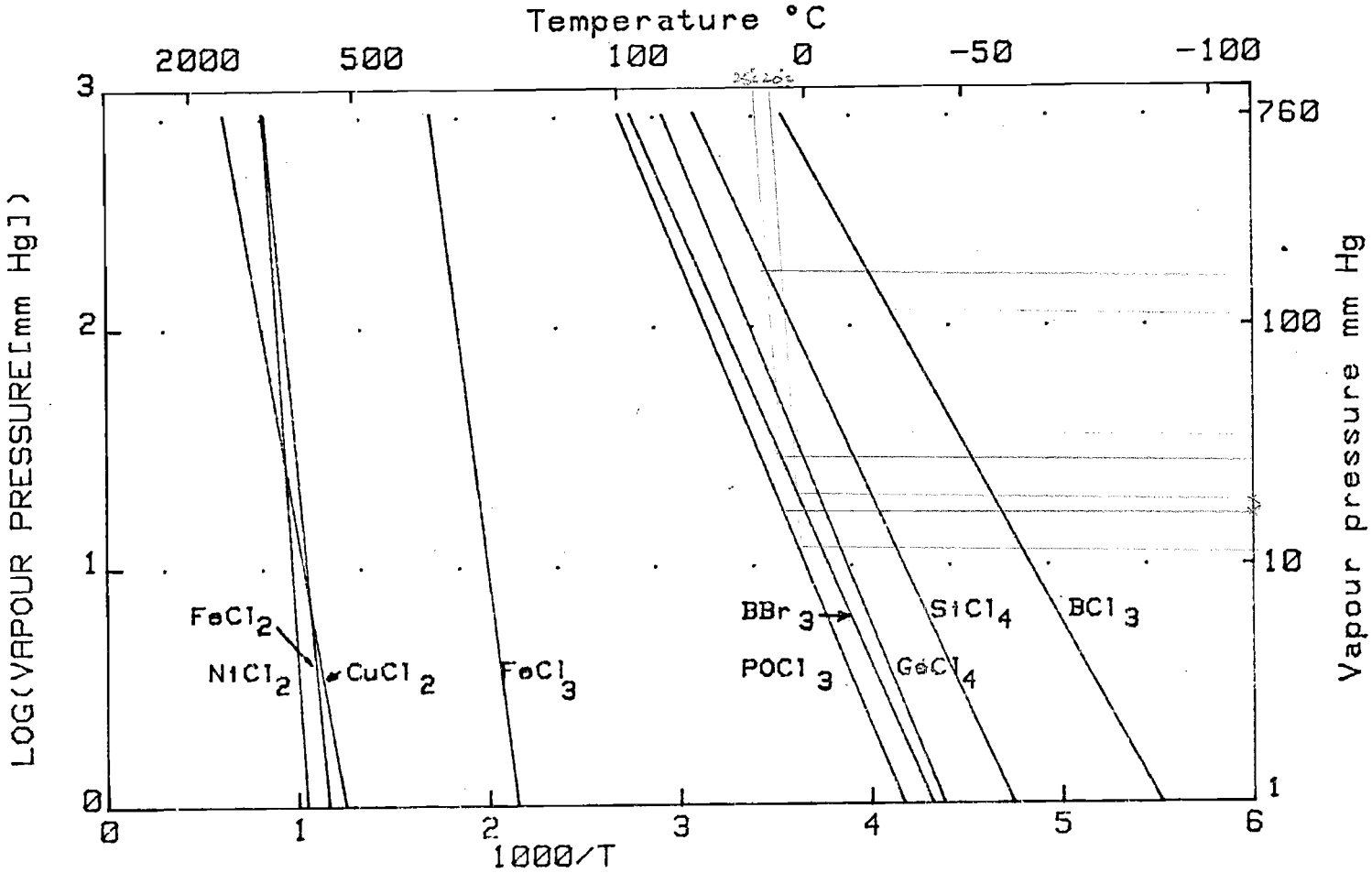

VAPOUR PRESSURE OF HCVD REACTANTS AND COMMON TRANSITION METAL IMPURITIES AS A FUNCTION OF TEMPERATURE

FIGURE 2.5

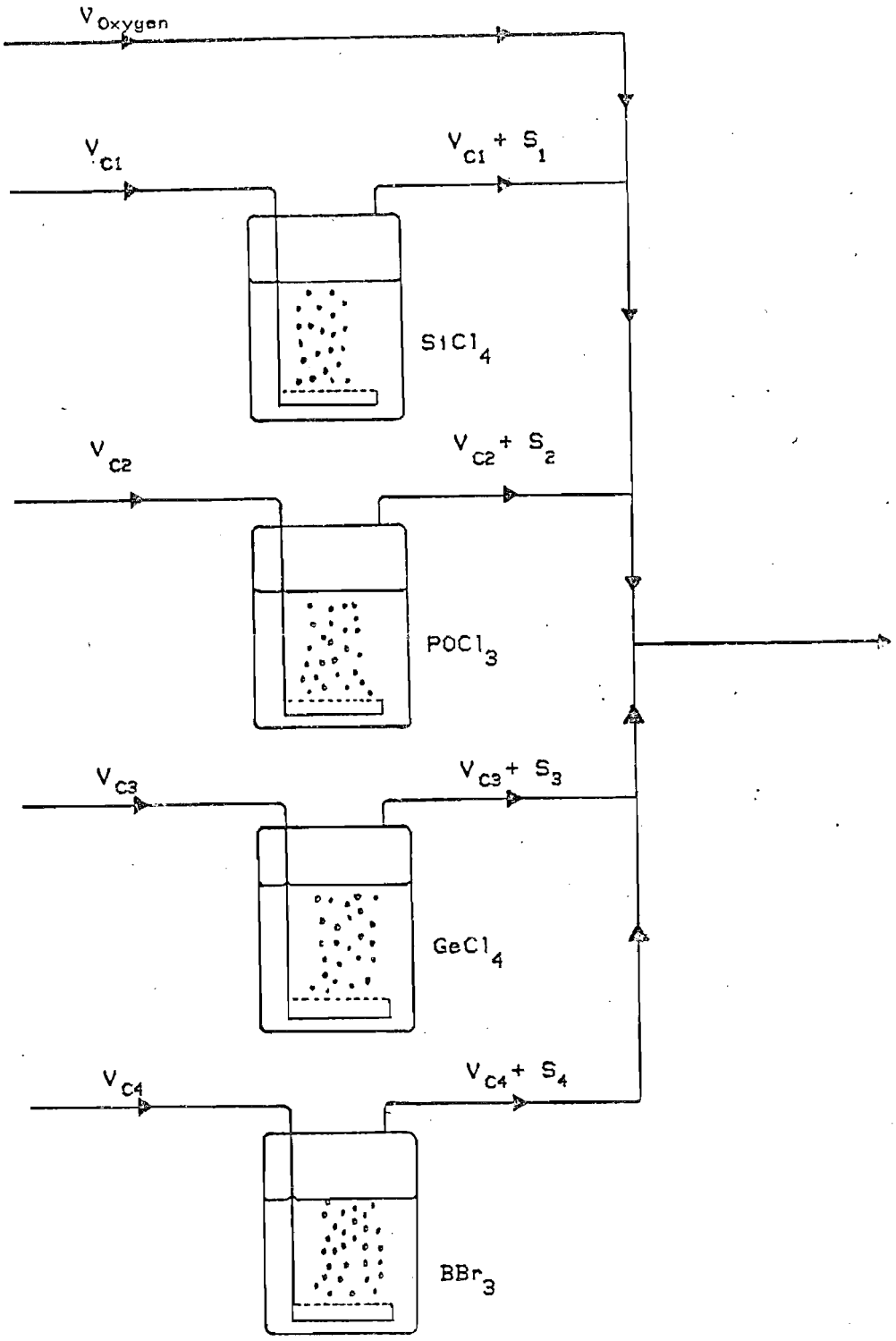

By varying the carrier-gas flowrate V_{CI} the reactant vapour flowrate S_I is controlled according to the equation:-

$$S_I = V_{CI} \cdot \frac{P_{IT}}{Po - P_{IT}}$$

where P_{IT} = vapour pressure of reactant I at temperature T
Po = atmospheric vapour pressure

SCHEMATIC ILLUSTRATION OF A SYSTEM FOR COLLECTING AND DISTRIBUTING CONTROLLED VOLUMES OF HCVD-REACTANT VAPOURS.

FIGURE 2.6

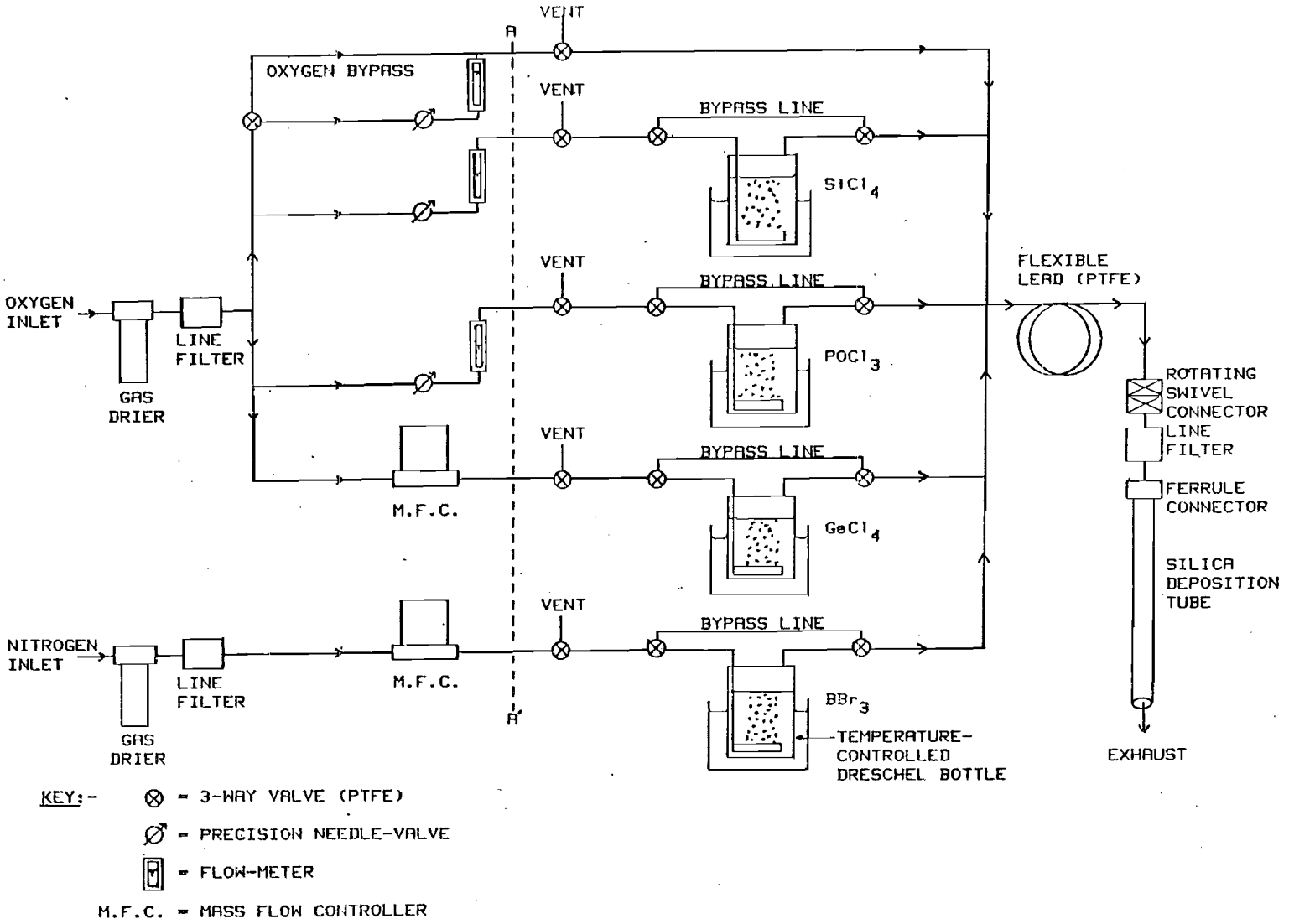

SCHEMATIC ILLUSTRATION OF REACTANT VAPOUR DISTRIBUTION SYSTEM FOR THE PREPARATION OF SILICA-BASED GLASSES BY HCVD

FIGURE 2.7

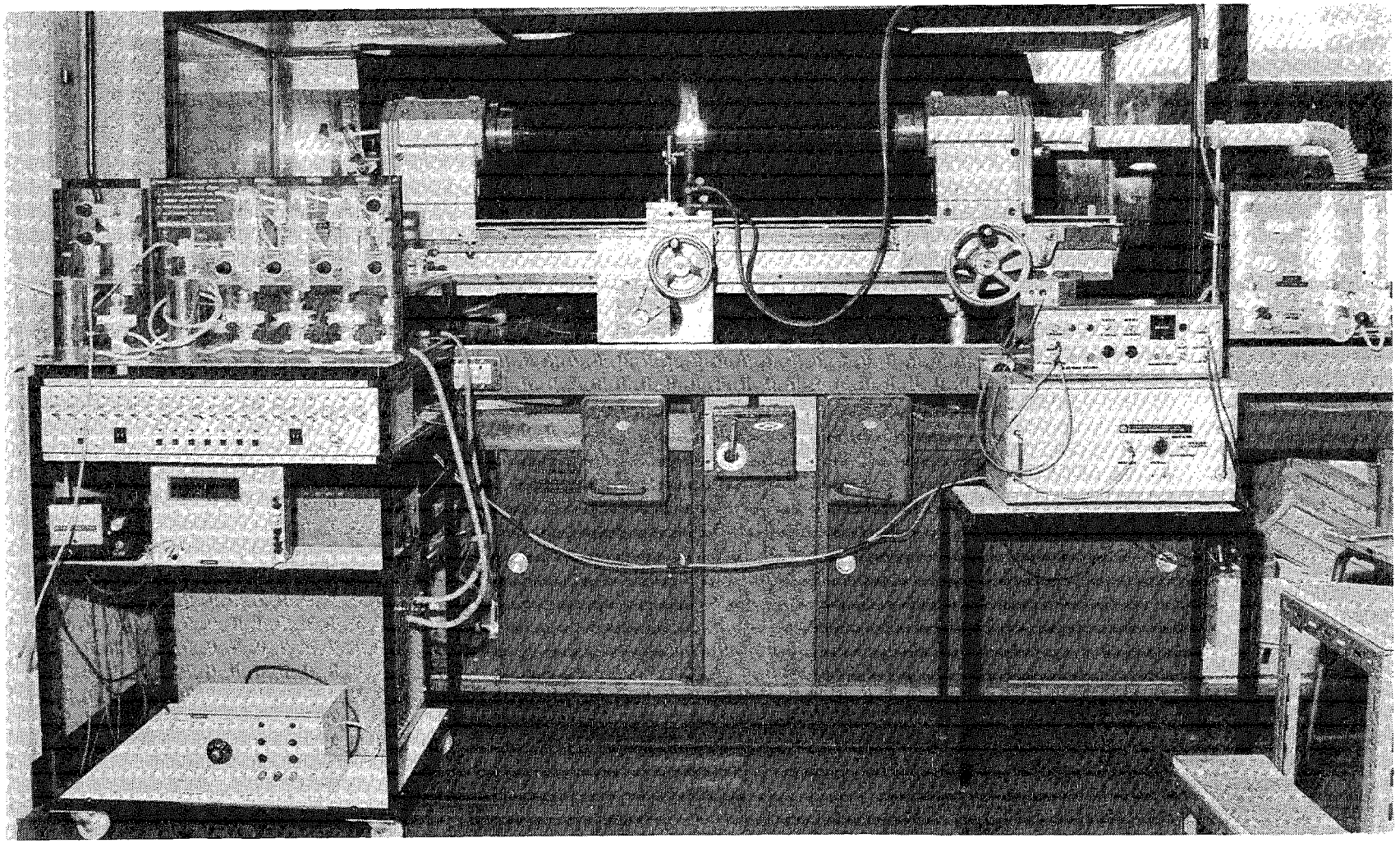

LATHE-BASED SYSTEM FOR THE MANUFACTURE OF OPTICAL FIBRE PREFORMS BY HCVD.

The reactant vapour distribution system is shown in the left foreground.

FIGURE 2.8

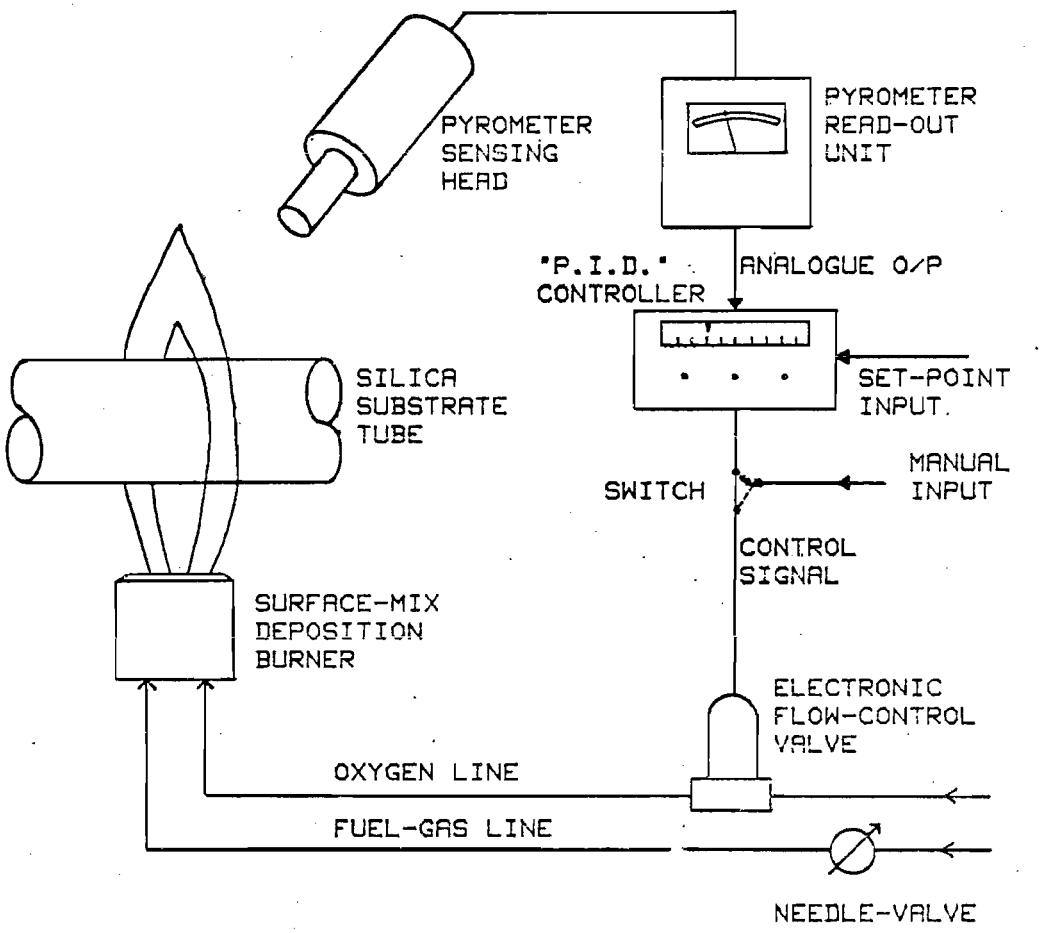

a) Schematic illustration of pyrometric feedback system for the control of HCVD deposition hot-zone temperature

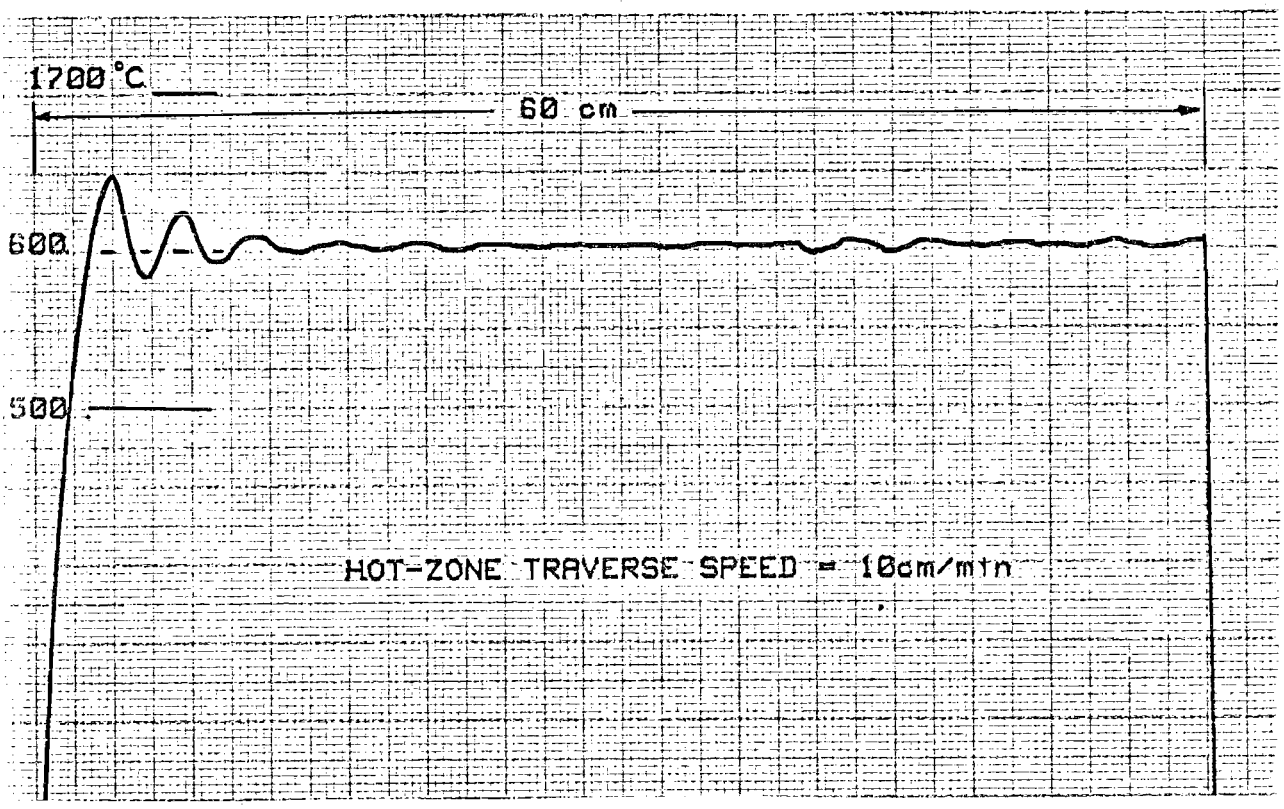

b) Variation of temperature along the deposition length of a silica substrate tube . Temperature control was obtained by means of the system shown in (a) above.

FIGURE 2.9

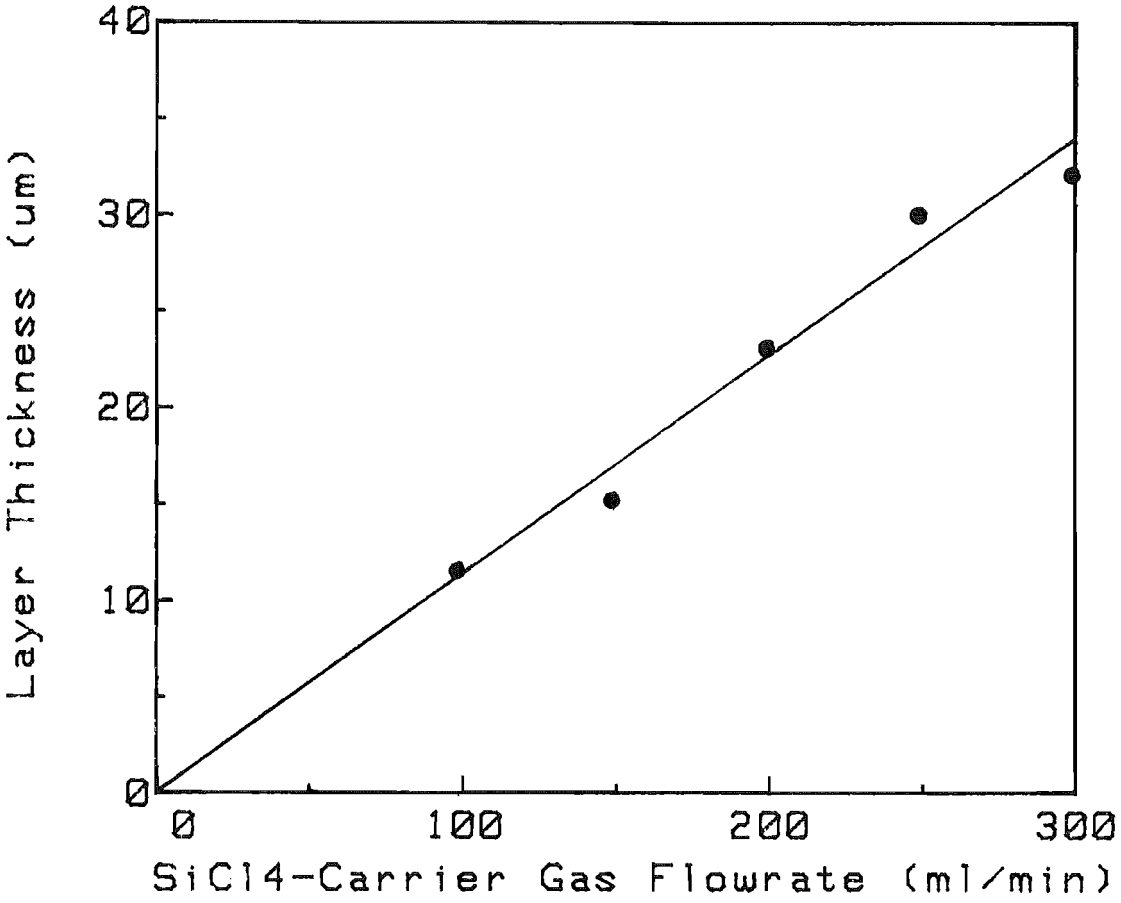

a) Deposited layer thickness as a function of carrier-gas flowrate

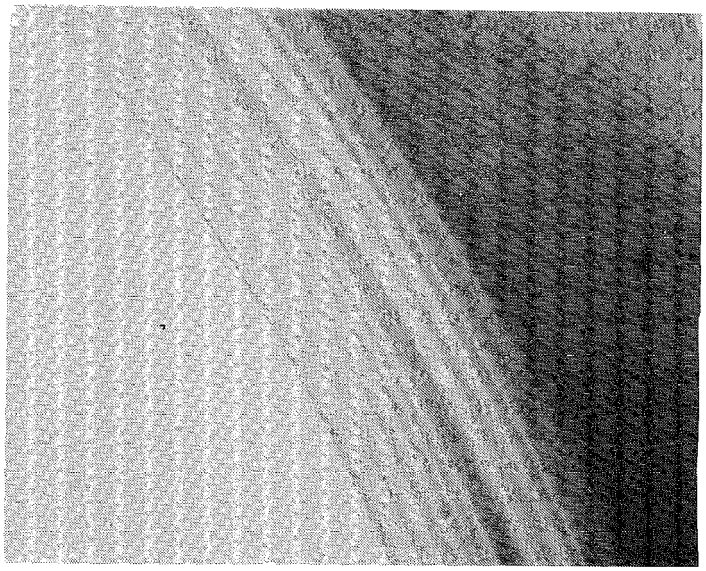

b) Section through 10m/o phosphosilicate glass deposited at different carrier-gas flowrates. The individual deposition layers can be clearly resolved; as shown in the graph above, the layer thickness varied linearly with carrier flowrate.

FIGURE 2.10

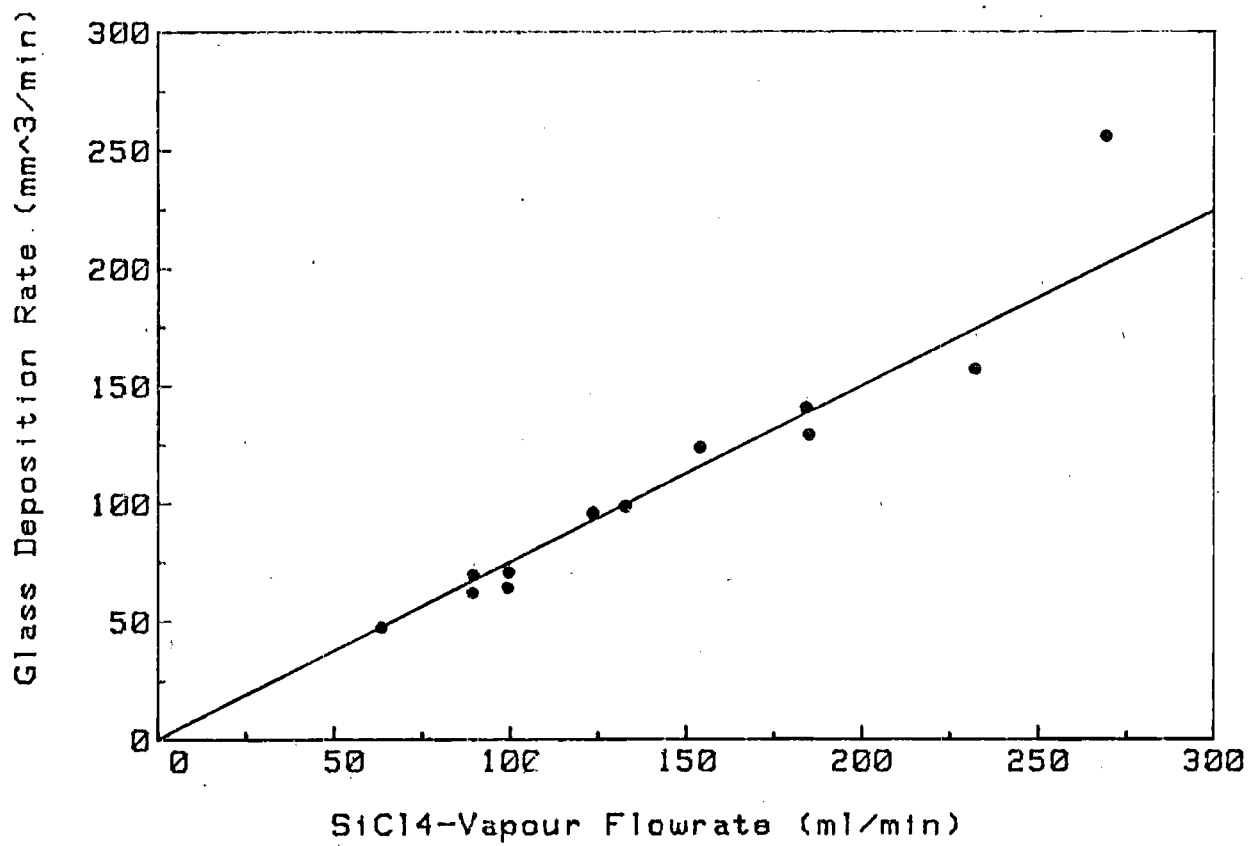

HVCD PROCESS : Glass deposition rate as a function of $SiCl_4$ reactant vapour flowrate.

FIGURE 2.11

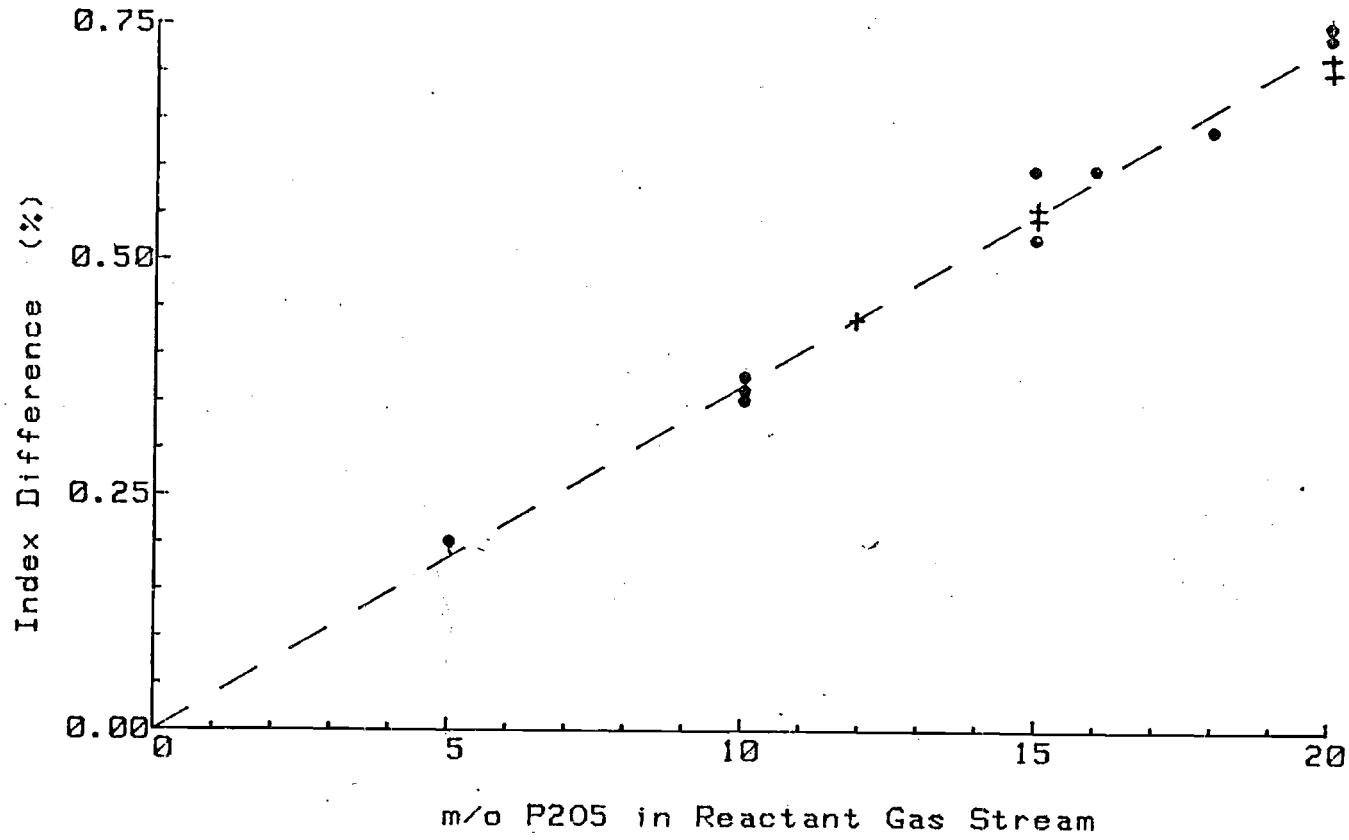

PHOSPHOSILICATE GLASSES PRODUCED BY HCVD : Measured refractive index difference relative to silica as a function of P_2O_5 content of reactant gas stream.

FIGURE 2.12

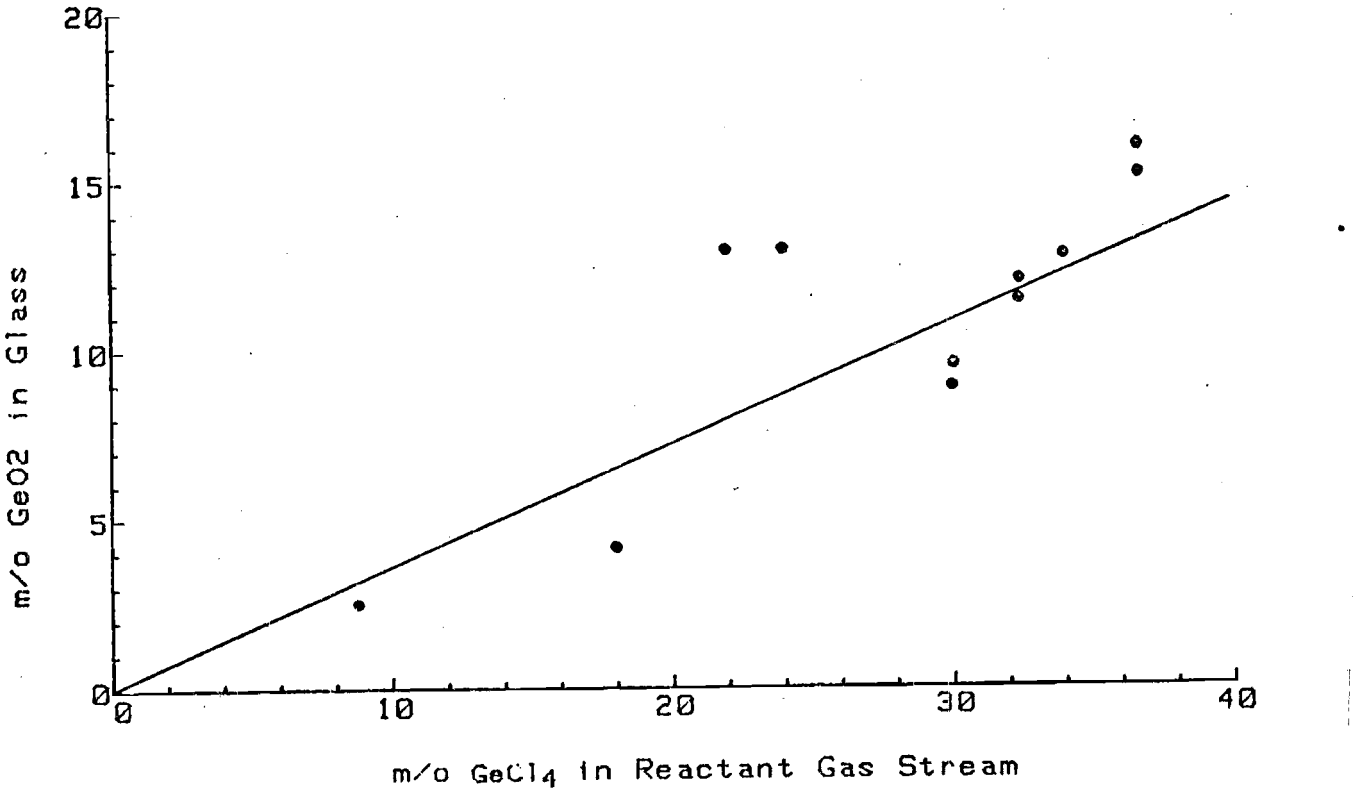

GERMANOSILICATE GLASSES PRODUCED BY HCVD : Composition of deposited glass as a function of $GeCl_4$ concentration in reactant vapour stream . The GeO_2 content of the glass was determined by Electron Microprobe Analysis .

FIGURE 2.13

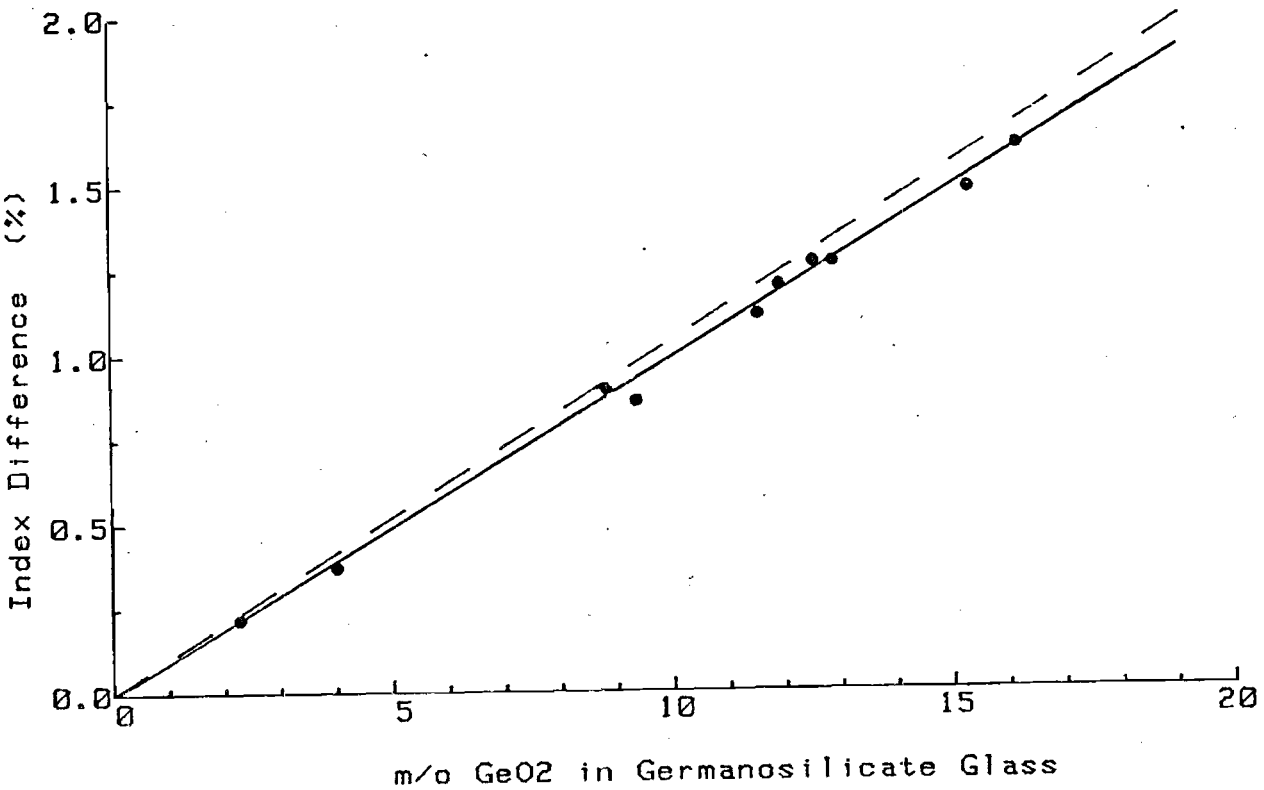

GERMANOSILICATE GLASSES PRODUCED BY HCVD : Refractive index difference relative to silica as a function of the actual GeO_2 content of the deposited glass. The data points were obtained by measurement of the numerical aperture in fibres of known composition. The broken line shows the index difference predicted by assuming that the refractive index varies linearly with GeO_2 content.

FIGURE 2.14

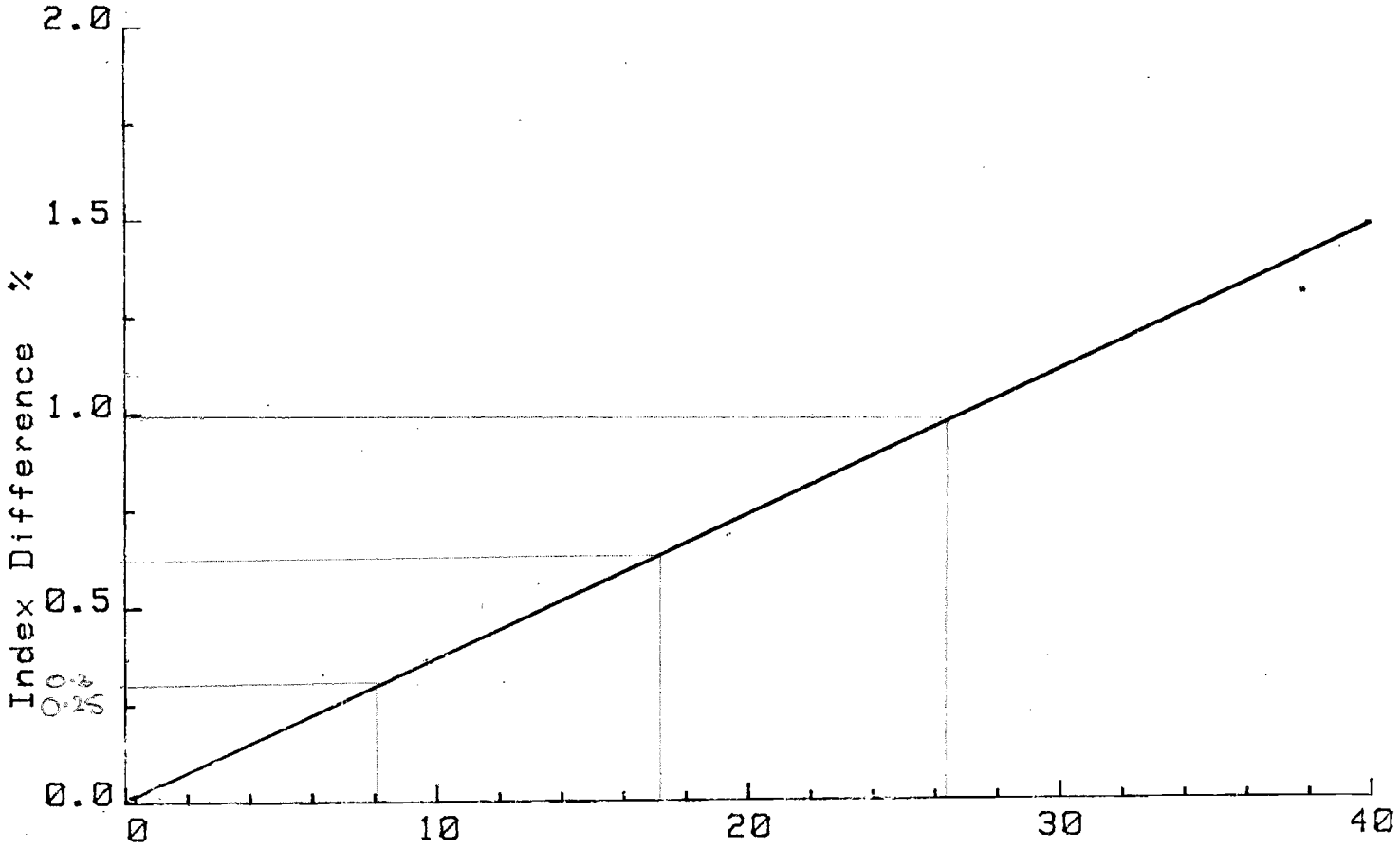

GERMANOSILICATE GLASSES PRODUCED BY HCVD : Refractive index difference relative to silica as a function of gas-phase concentration of $GeCl_4$. The results were computed from figures 2.13 & 2.14 assuming constant GeO_2 incorporation efficiency.

FIGURE 2.15

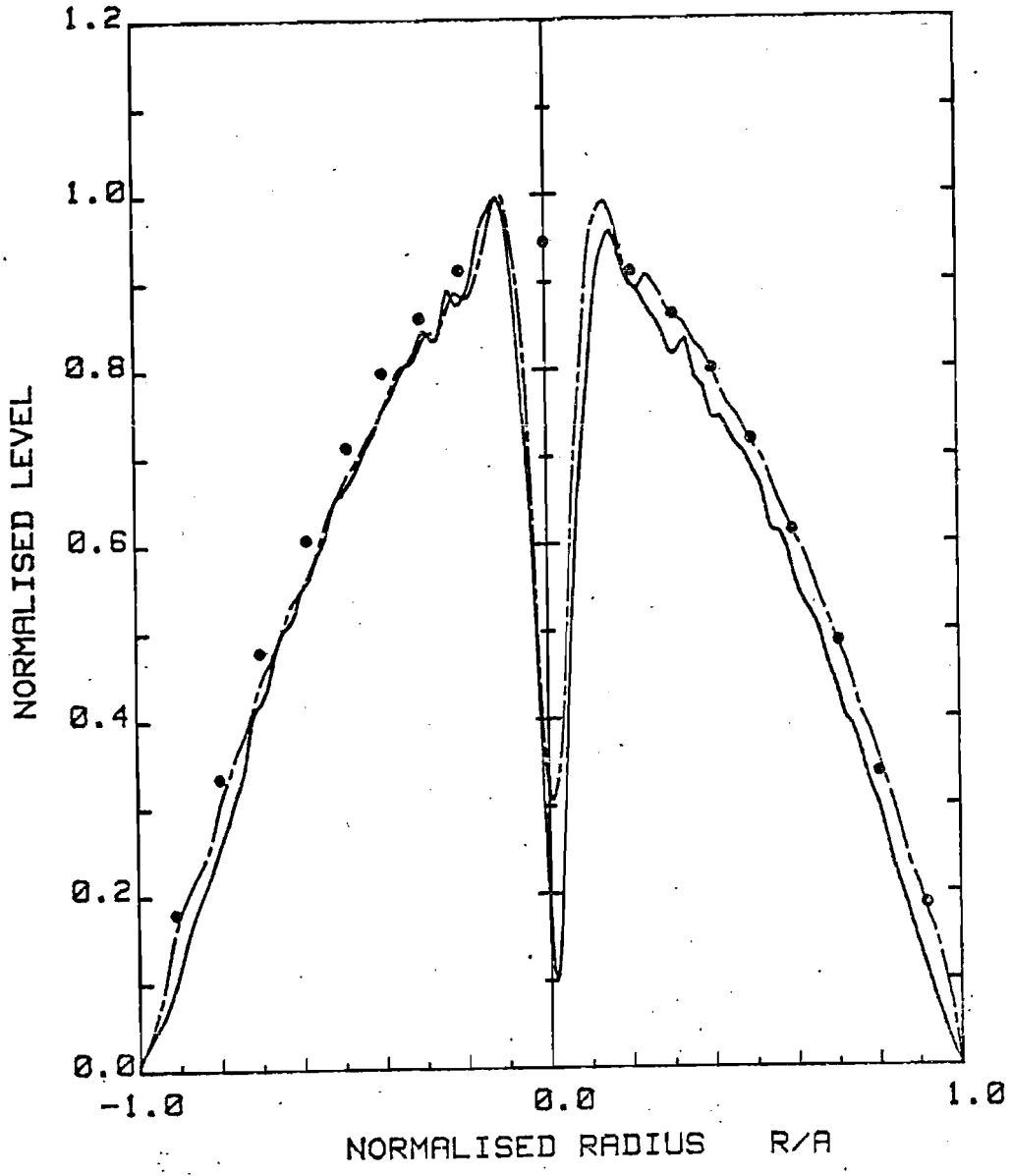

NORMALISED REFRACTIVE INDEX PROFILE (SOLID LINE) AND DOPANT CONCENTRATION PROFILE (BROKEN LINE) IN GRADED-INDEX GERMANO-SILICATE CORE OF FIBRE VD161. The circular points represent the glass-phase germania concentration profile expected from the vapour-phase reactant concentrations.

FIGURE 2.16

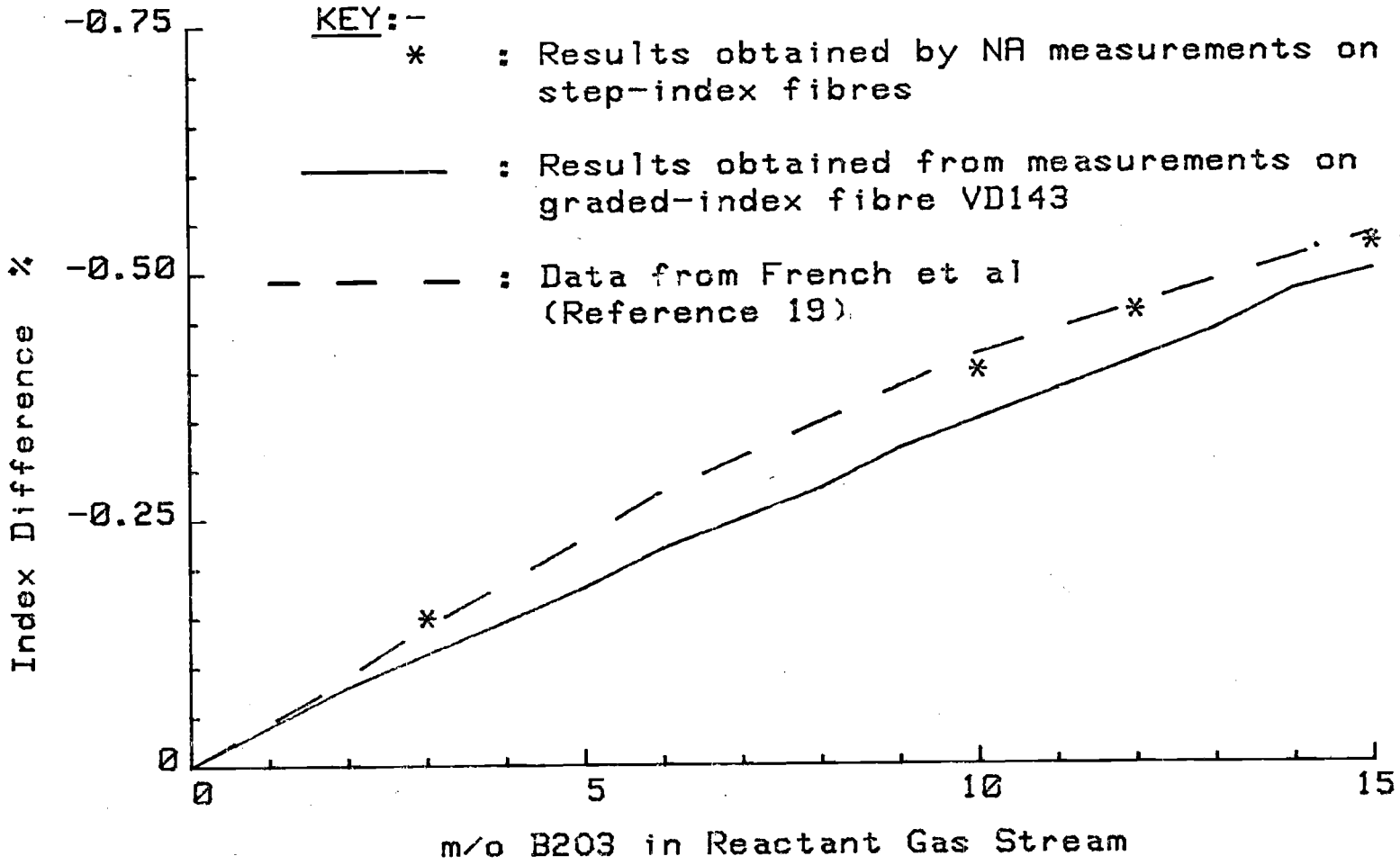

BOROSILICATE GLASSES PRODUCED BY HCVD : Measured refractive index relative to silica as a function of B_2O_3 content of reactant gas stream.

FIGURE 2.17

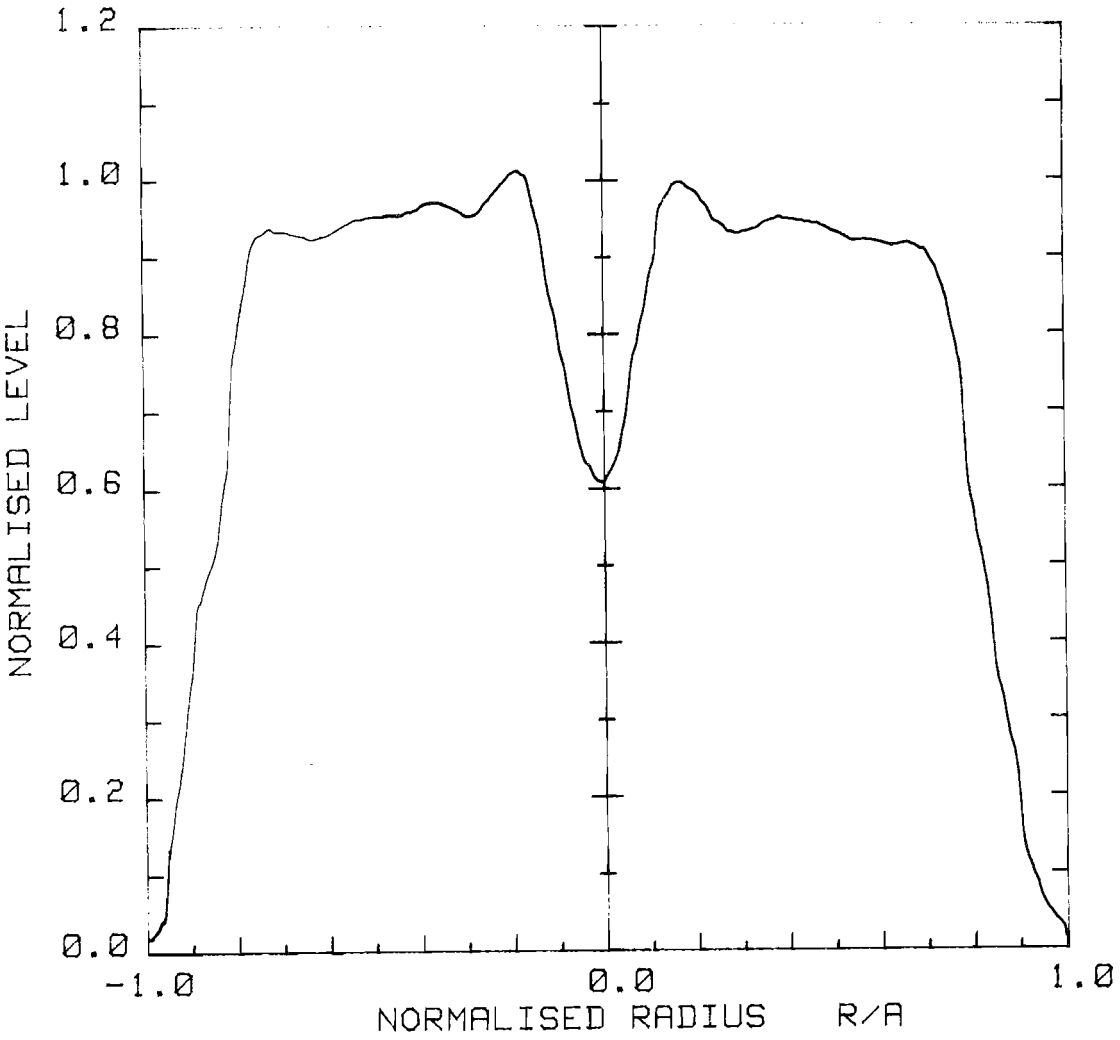

a) Refractive Index Profile

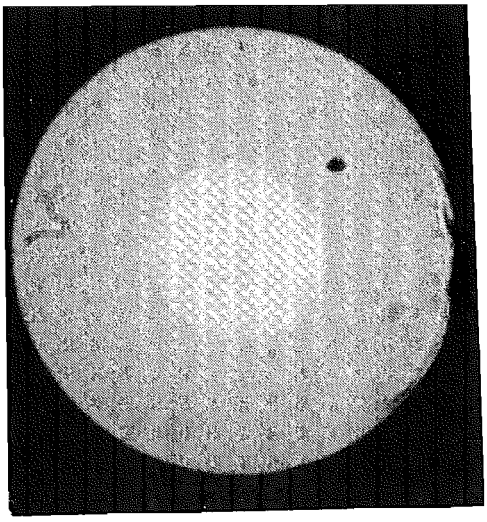

b) Transverse Cross-section

REFRACTIVE INDEX PROFILE AND CROSS-SECTION OF STEP-INDEX FIBRE WITH PHOSPHOSILICATE CORE.

FIGURE 2.18

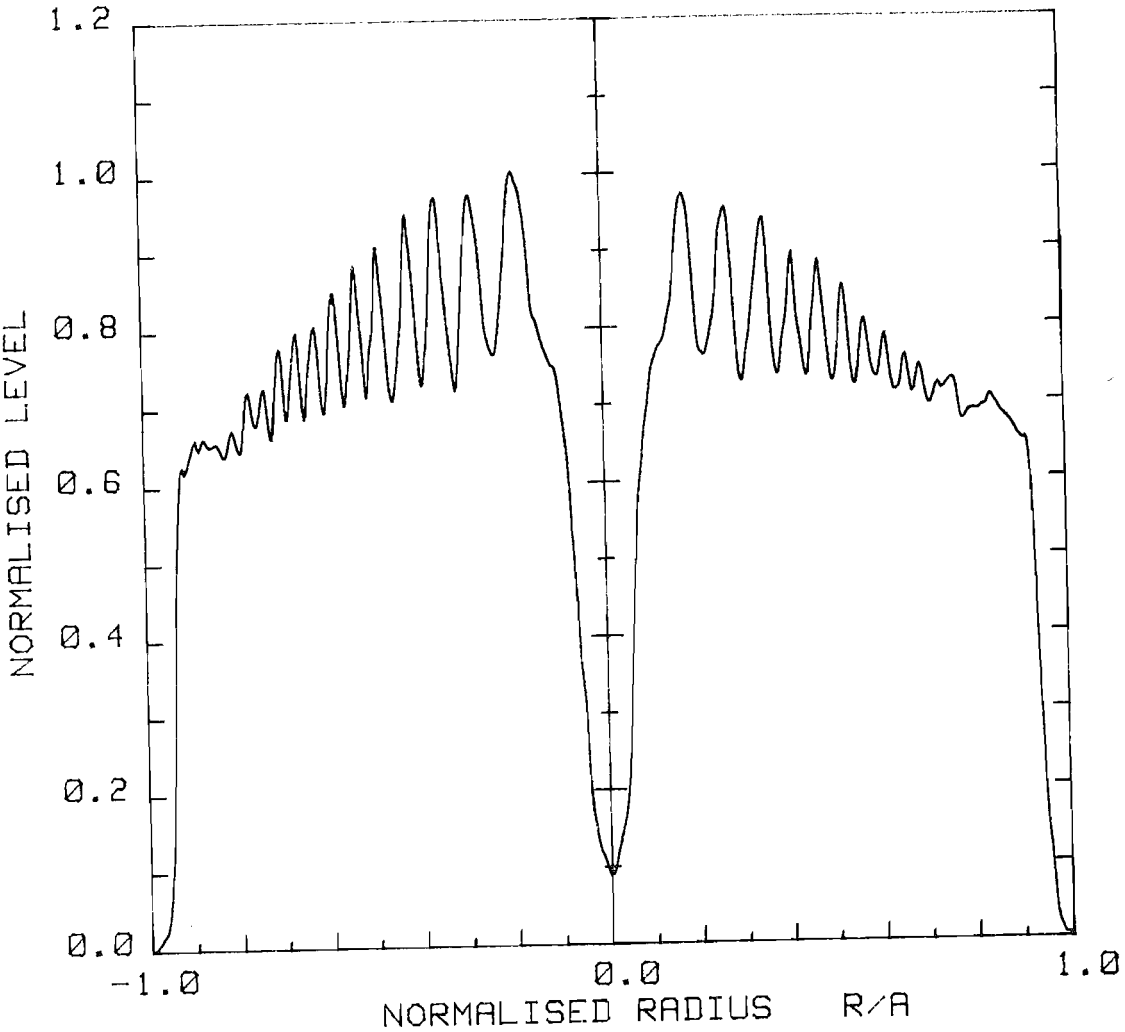

a) Refractive Index Profile

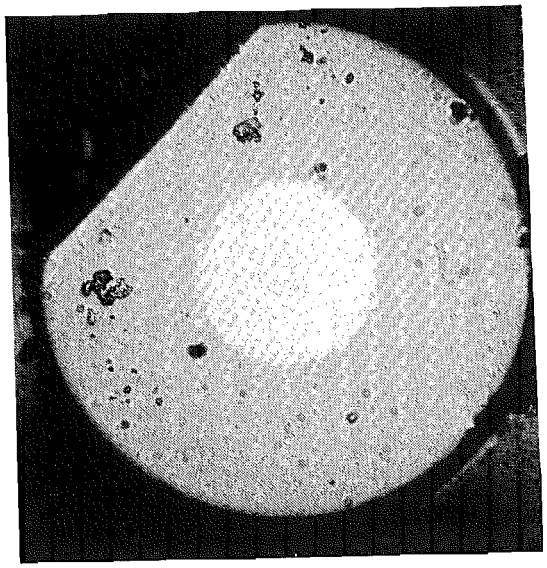

b) Transverse Cross-section

REFRACTIVE INDEX PROFILE AND CROSS-SECTION OF STEP-INDEX FIBRE WITH GERMANOSILICATE CORE.

FIGURE 2.19

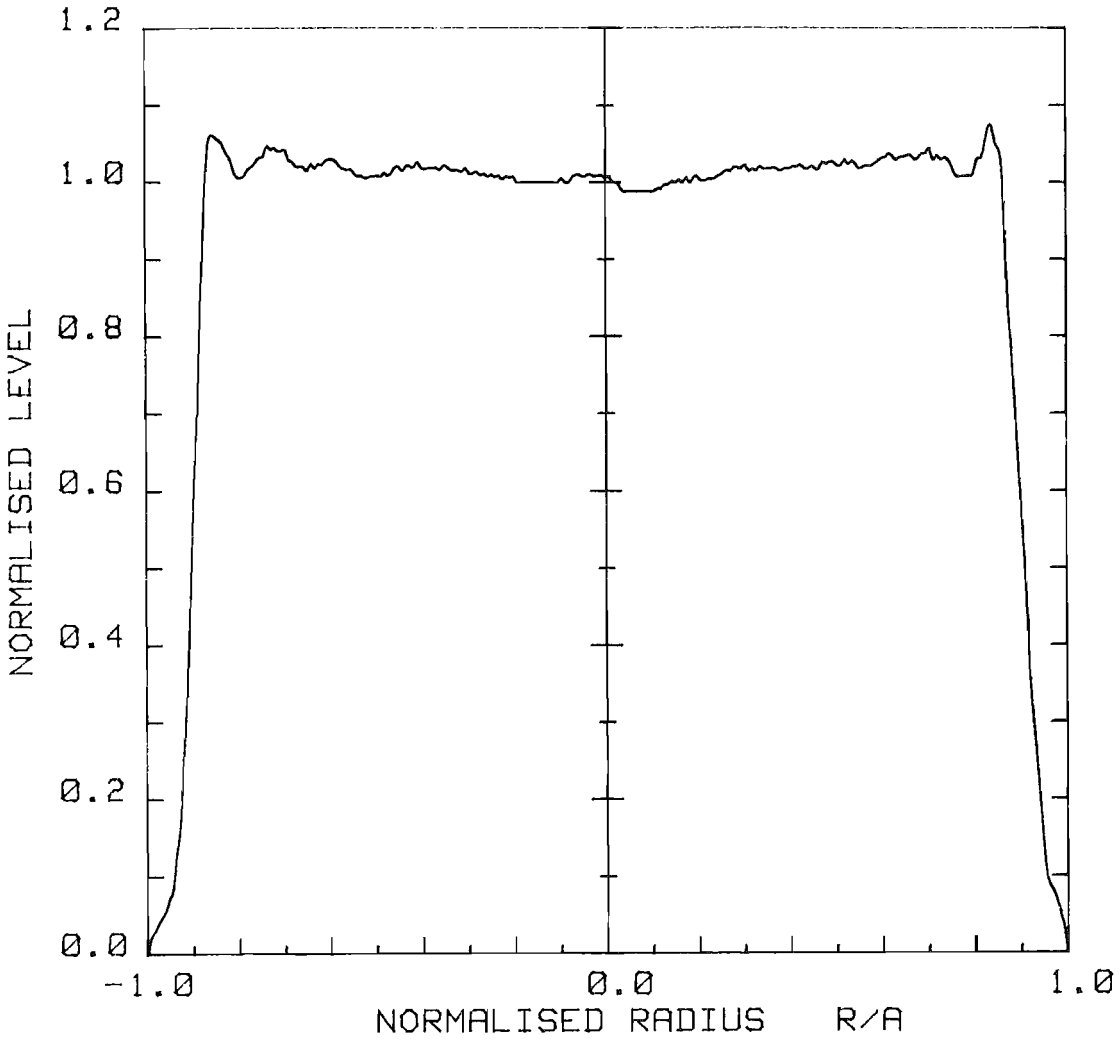

a) Refractive Index Profile

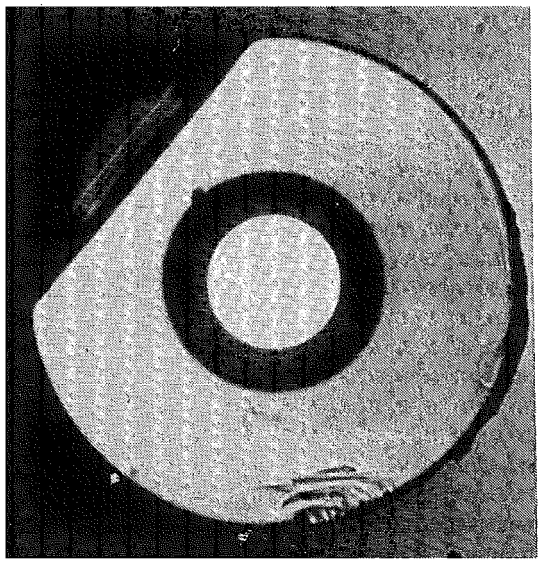

b) Transverse Cross-section

REFRACTIVE INDEX PROFILE AND CROSS-SECTION OF BOROSILICATE-CLAD, SILICA-CORE STEP-INDEX FIBRE.

FIGURE 2.20

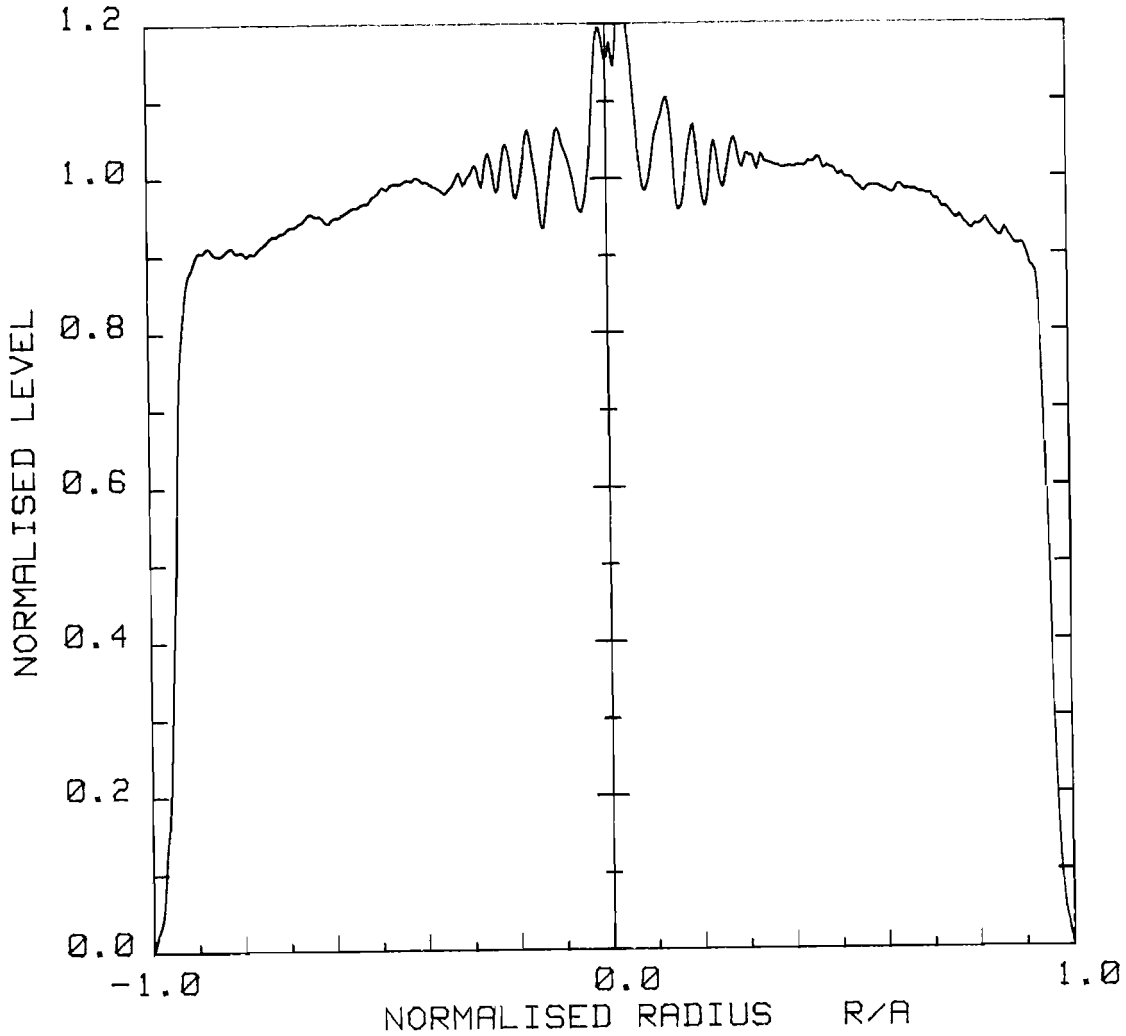

a) Refractive Index Profile

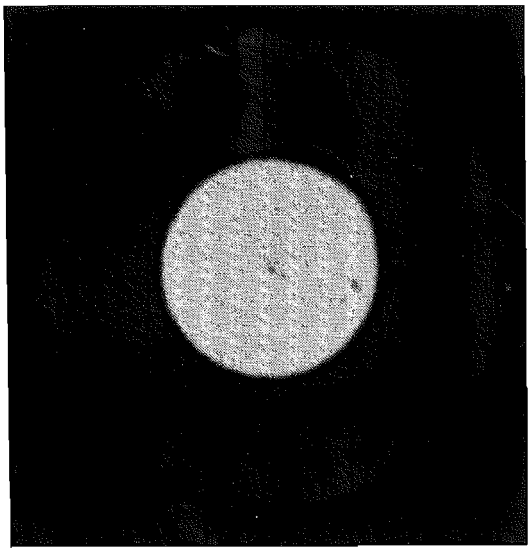

b) Transverse Cross-section

REFRACTIVE INDEX PROFILE AND CROSS-SECTION OF STEP-INDEX FIBRE WITH PHOSPHO-GERMANOSILICATE CORE.

FIGURE 2.21

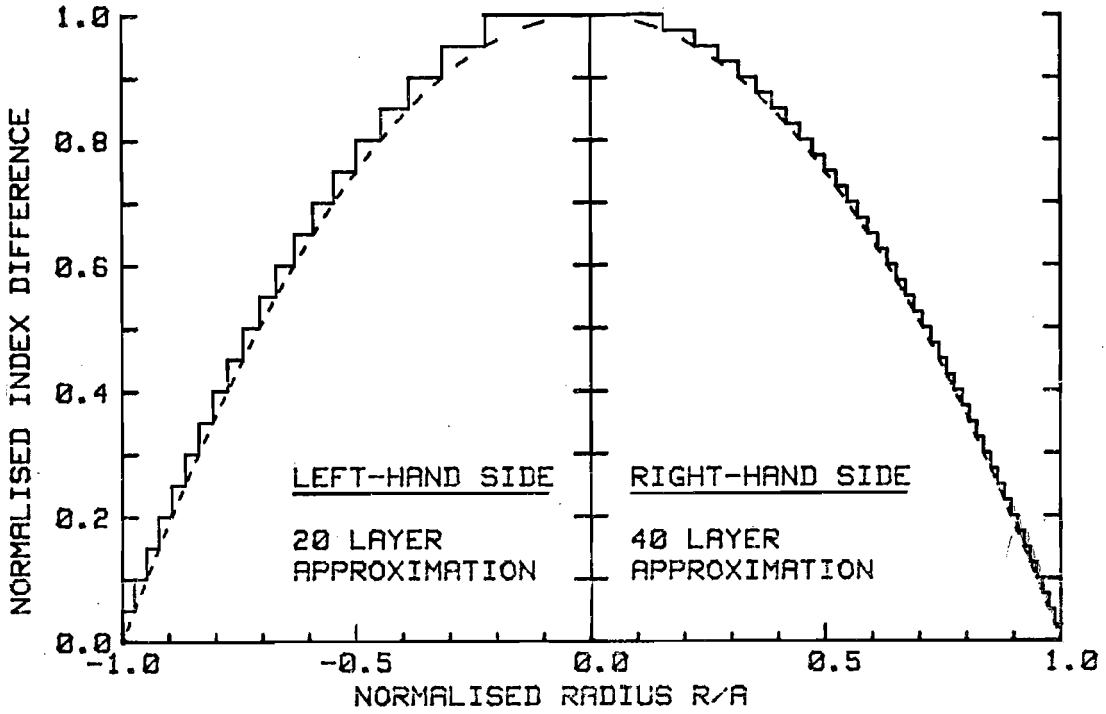

A. 40-LAYER AND 20-LAYER STEPPED APPROXIMATIONS TO AN "ALPHA-PROFILE" OF EXPONENT 2.0

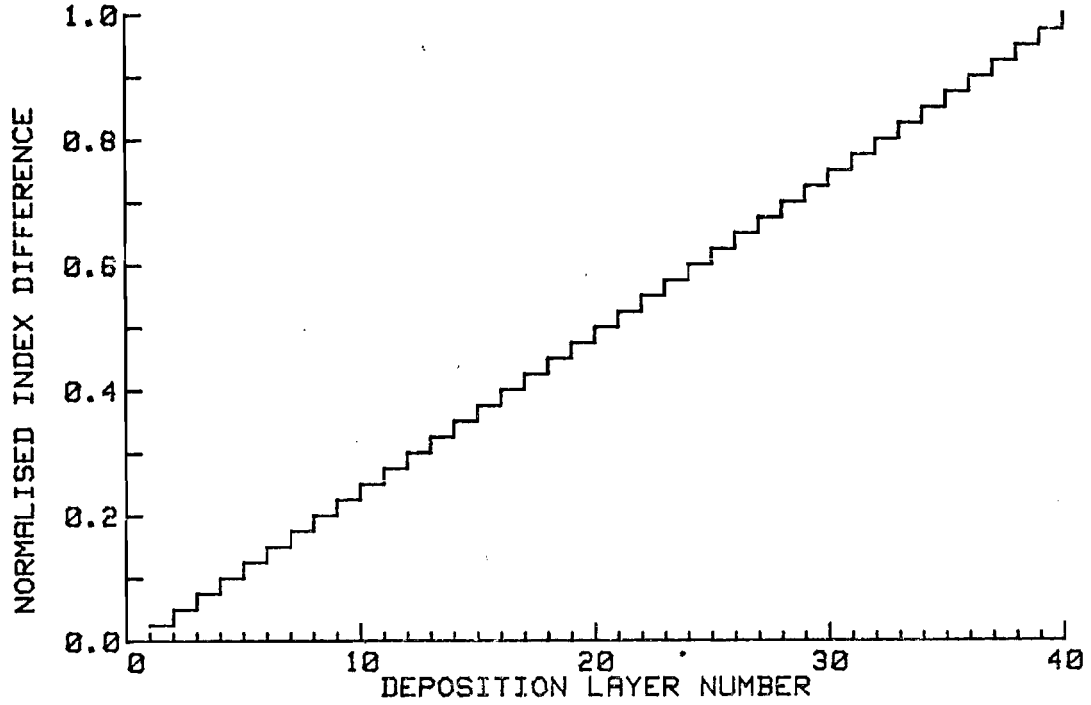

B. VARIATION OF REFRACTIVE INDEX DIFFERENCE WITH DEPOSITION LAYER NUMBER FOR THE 40-LAYER APPROXIMATION SHOWN ABOVE.

SYNTHESIS OF A GRADED-INDEX PROFILE USING A STEPPED APPROXIMATION

FIGURE 2.22

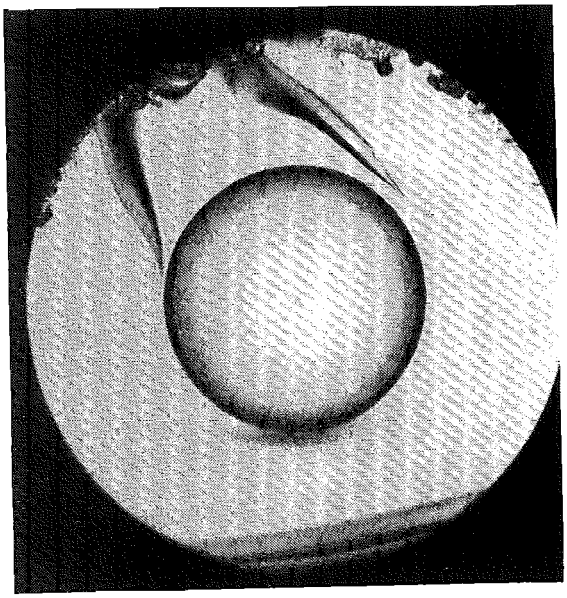

a) Transverse cross-section of "standard" preform having a graded-index P_2O_5-GeO_2-SiO_2 core in a borosilicate cladding.

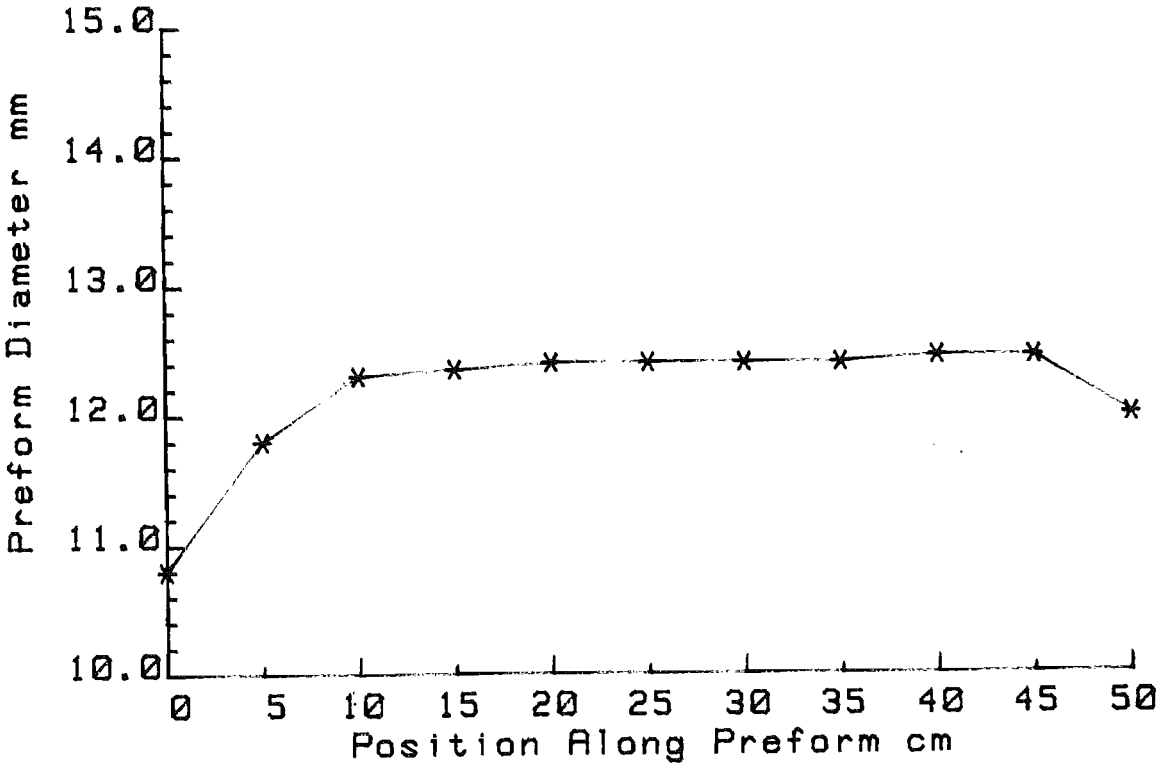

b) Preform diameter as a function of position along the length of the preform shown in (a) above.

FIGURE 2.23

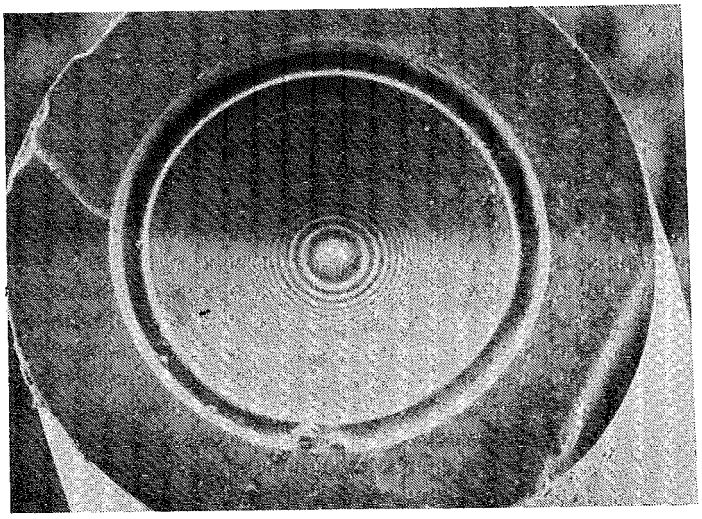

a) S.E.M. photomicrograph of etched P_2O_5-GeO_2-SiO_2 cored, B_2O_3-SiO_2 clad fibre. The core and cladding have etched more rapidly than the silica support structure, and can be clearly resolved. The circular symmetry of the fibre is near-perfect. Magnification = x700

Etchant : 25% HF acid

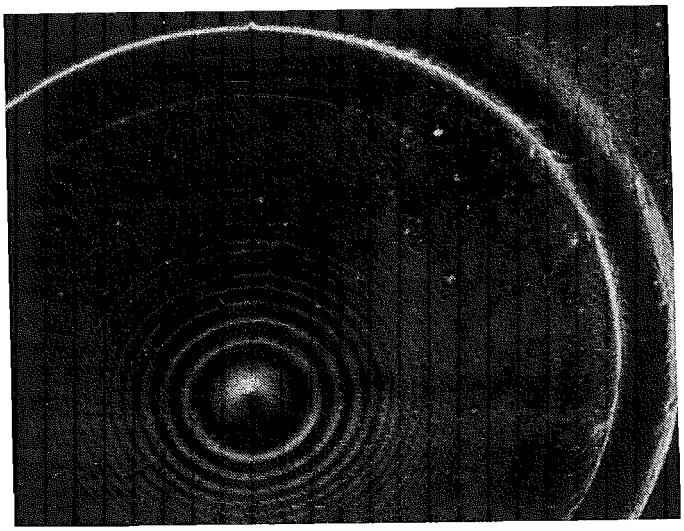

b) Detail of the core layers and core/cladding interface in the etched fibre sample shown above (figure 2.24a). The core layers can be individually distinguished, as can the central "pip" resulting from dopant evaporation during preform collapse. S.E.M. Magnification = x1400

FIGURE 2.24

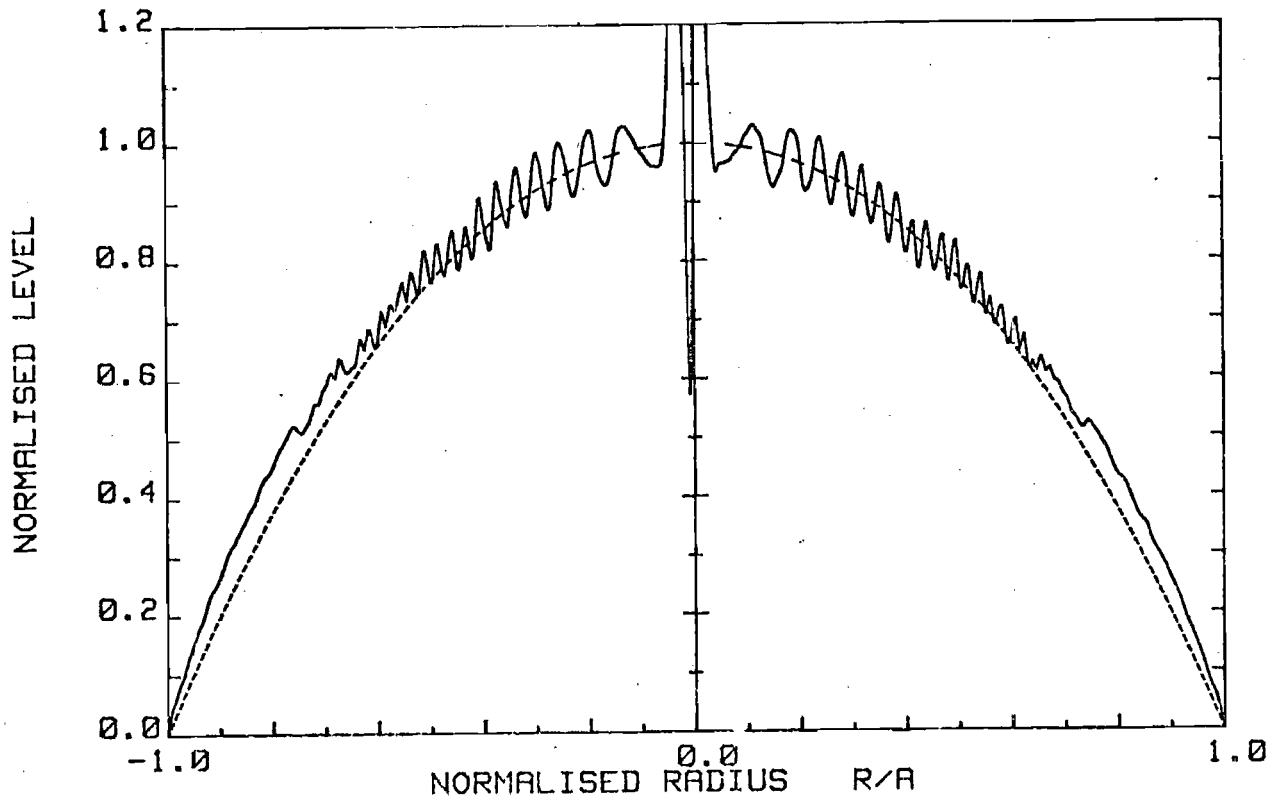

REFRACTIVE INDEX PROFILE ACROSS THE CORE OF A P_2O_5-GeO_2-SiO_2 GRADED-INDEX PREFORM (SOLID LINE) AND INTENDED "ALPHA-PROFILE" (BROKEN LINE).

Core diameter in preform = 5.0 mm. Maximum index difference = 1.2% relative to SiO_2

FIGURE 2.25

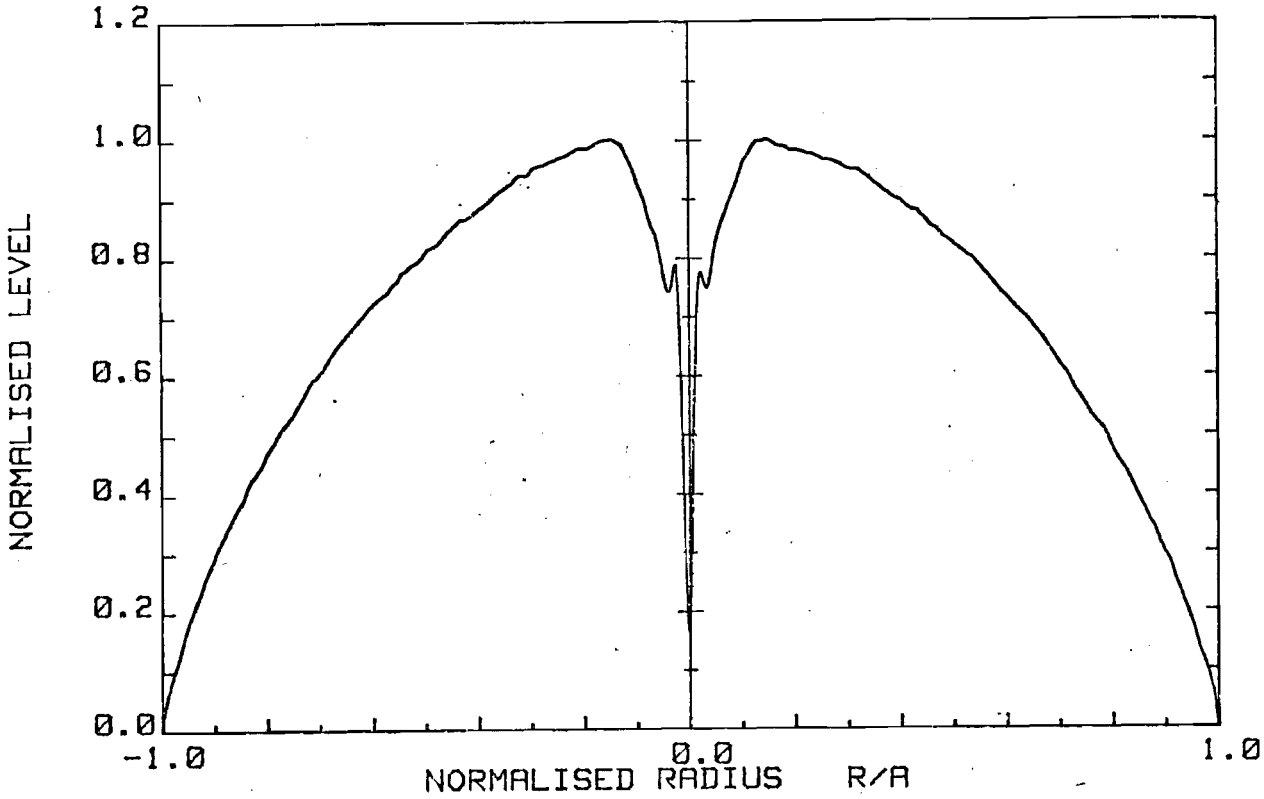

REFRACTIVE INDEX PROFILE ACROSS THE CORE OF A P_2O_5-GeO_2-SiO_2 GRADED-INDEX PREFORM IN WHICH THE P_2O_5 LEVEL HAD BEEN INCREASED TO 2 m/o .

FIGURE 2.26

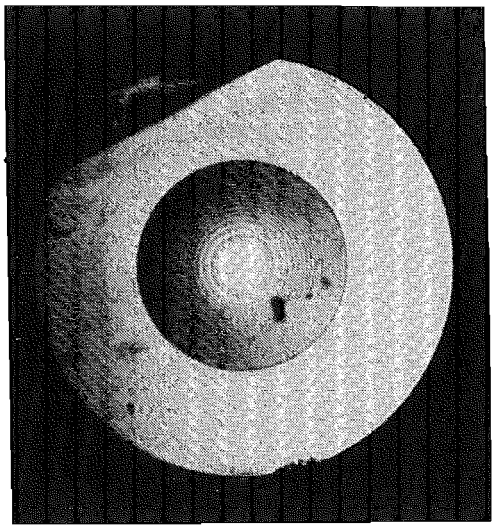

a) Transverse cross-section of monomode-fibre preform having a germanosilicate core in a borosilicate cladding. Core diameter = 0.9mm
Clad diameter = 4.0mm
Preform diameter = 8.05mm

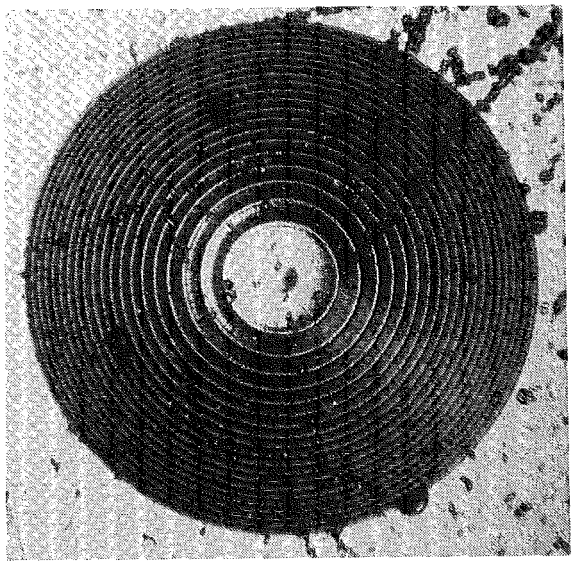

b) Core and cladding region of above preform after etching in 25% HF acid for 10 minutes. The photograph was obtained using an optical microscope with the sample under reflected light illumination. Each deposited layer can be resolved, as can the central "pip" due to dopant out-diffusion during preform collapse. Magn. = ×16

FIGURE 2.27

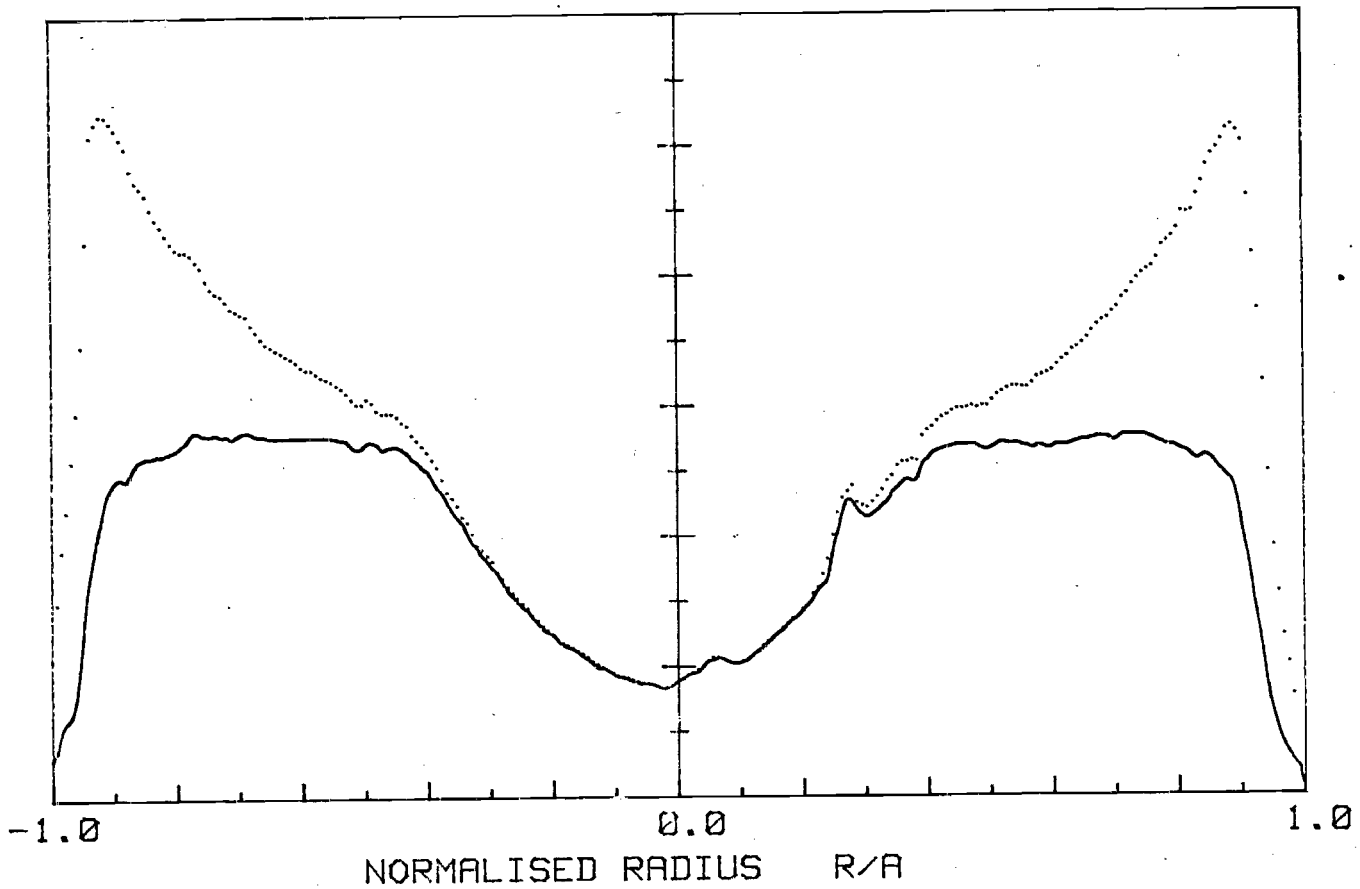

Near-field intensity distribution (dotted line) and deduced refractive index profile (solid line) of monomode-fibre preform GSB2 . The out-diffusion of dopant during preform collapse has produced a refractive index depression near the core centre. Measurement wavelength = 550nm. Sample length = 7.2cm. Core radius = 96um. NA = 0.12 .

FIGURE 2.28

CHAPTER 3 : THE DRAWING OF FIBRES FROM HCVD PREFORMS

The drawing of HCVD preforms into fibre is carried out on a purpose-built machine designed by Dr. D.N. Payne and constructed within the Electronics Department Workshops.[1] The machine was originally constructed for the drawing of soft-glass fibres, and has been used extensively since 1968 for the manufacture of 'rod-in-tube' fibres, fibre-tubes for liquid-core fibres and, more recently, silica-based fibres. In principle, the drawing of fibre from rods or preforms is a straightforward operation requiring a machine comprised of only three sub-units, namely a linear drive system, a stable heat source, and a winding drum or tractor system. The preform is mounted on the linear drive system and is fed vertically downwards into a hot-zone where the temperature of the glass is raised to a point at which a fibre filament may be drawn under tension from the tip of the preform onto a winding drum. By adopting a strategy of precision in the construction and control of the drawing machine, Dr. Payne established a system which has remained essentially unchanged over a period during which the attenuation of fibres has been reduced from typically 1000 dB/km to less than 1 dB/km. When drawing glasses having a low softening temperature, a platinum-wound resistance-heated furnace is employed as the heat source, while for high-silica glasses a resistance-heated furnace having a graphite element has been developed.[2]

At an early stage in the drawing of silica fibres it was realised that the temperature stability and uniformity of the furnace hot-zone would have a marked influence upon the diameter stability of the fibre. In addition to the routine drawing of fibres for experimental purposes, attention has therefore been devoted to the measurement of fibre diameter on-line with fibre drawing and to the reduction of the diameter variations by improvement of furnace stability. As will be seen in later sections, this aspect of the study was of great benefit, and led to the identification and elimination of a number of sources of fibre diameter variation, which had previously limited the minimum loss of the HCVD fibres. As a direct consequence of this work, it has been possible to reduce the losses of the graded-index fibres to a level approaching the fundamental limit.

3.1 Fibre Drawing Machine

The layout of the fibre drawing machine is shown schematically in figure 3.1, and is comprised of the following sub-systems:-

3.1.1 Preform Feeding & Fibre Winding Systems

These two sub-systems constitute the major structural part of the machine. The preform feeding system is mounted on two vertical, precision-steel bars which run the full height of the machine and are used as mounts for other sub-systems. The preform is gripped in a gimballed chuck which is mounted on a cross-head sliding on one of the bars. A precision leadscrew is coupled to the cross-head via a split-nut and is driven via a gearbox and reduction pulleys by a DC motor with tachometer. The use of a DC motor/tachometer combination in conjunction with a thyristor speed control unit enables a speed stability of better than 0.1% to be obtained. The threaded section of the leadscrew is greater than 1.25 metres in length, thus permitting a substantial length of preform to be accommodated.

The fibre winding system is floor-mounted and has a precision-machined and balanced metal winding drum of about 40 cm diameter and 50 cm width. To produce a uniform layer of fibre across the drum, the drum is mounted on roller bearings on a traversing table which translates as the fibre is wound. The pitch of winding is controlled by a leadscrew coupled through pulleys to the winding drum itself. The winding pitch may be adjusted by varying the ratio of the pulleys coupling the drum and leadscrew; typically 1.5 km of fibre can be wound in a single layer. The drum is driven by a DC motor and tachometer unit connected in a feedback loop with a thyristor controller. Speed stability of better than 0.1% is achieved over the normal range of winding speeds. Although originally capable of winding speeds of 0 to 10 metres/second, the pulling speeds for silica fibres generally fall well below the upper limit, and a reduction gearbox has recently beer added to bring the rotational speed of the DC motor into its optimal control range at normal fibre-drawing speeds.

Fibre is guided onto the winding drum by a grooved shoe, machined out of graphite (for its low friction and high temperature resistance). Fibre length is measured by an impulse counter which detects the rotational movement of the drum.

3.1.2 Graphite Resistance-Heated Furnace

Conventional oxyhydrogen-flame furnaces are unsuitable for precision fibre-drawing purposes because of their lack of controllability. After considering alternatives such as R.F. induction furnaces etc., graphite resistance heating was chosen because it offered several advantages. Firstly, it is the simplest and most readily controlled form of heating; accurate control of heating power is readily obtained using a standard SCR controller. Secondly, by adjusting the local resistance of the heating element it is possible to tailor the size and temperature profile of the hot-zone. A third, and important advantage is that graphite is inexpensive and can be machined using standard workshop machinery. Finally, graphite has excellent physical properties, high thermal shock resistance, high emissivity and high strength at elevated temperatures. Its one great disadvantage is that it readily oxidises when in contact with oxygen at high temperature; however, by flooding the furnace chamber with an inert atmosphere of argon it is possible to exclude air from the hot element.

A schematic representation of a vertical cross-section through the original furnace is shown in Figure 3.2. A detailed description of the furnace has been given elsewhere[2] and will not be included here. Noteworthy features of the design are the heating element, which has a short hot-zone formed by a 'meandering' resistive path, the protective furnace lining tube, the adjustable iris diaphragms at the top and bottom of the furnace, and the gas-flow arrangements within the centre of the furnace which ensure a flow of clean argon over the fibre and preform.

Measurement of the hot-zone temperature is achieved using an optical pyrometer which monitors the radiated optical power from a 1 mm x 1 mm surface on the meandering hot-zone. The output from the pyrometer is fed to a 'three-term' thyristor controller which compares the actual and set-point temperatures and controls the current to the heating element accordingly. A step-down transformer is used to reduce the output voltage from the controller to a value compatible with the very low resistance of the heating elements (about 0.1 ohms). The transformer is sited as close as possible to the furnace to minimise the resistive losses in the power leads.

3.1.3 Fibre Diameter Measuring System

A recent and most important addition to the fibre-drawing machine is the equipment for measuring the diameter of the fibre on-line with drawing. The equipment consists of a commercial diameter monitor (Anritsu Model SLB 501C) mounted on X-Y translation stages beneath the fibre-drawing furnace. The diameter monitor employs a scanning laser beam to determine not only fibre diameter, but also the X and Y co-ordinates of the fibre within the measurement zone. Because a 'tuning-fork' vibrating mirror is used to scan the laser beam across the fibre at 500 Hz, a 1 milli-second sampling period is obtained and very high frequency diameter fluctuations can thus be detected. The equipment is capable of measuring diameters in the range 10 to 999.9 μm with a resolution of 0.1 μm. A display unit shows fibre diameter, deviation from set-point, and fibre position in an X-Y plane, and has analogue signal outputs for recording and control purposes.

The diameter measuring unit is mounted on the X-Y translation stages to allow the 'tracking' of a fibre should its position change during the drawing process.

3.1.4 Primary Coating System

Equipment for the application of a protective primary coating to the fibre in-line with drawing has also been fitted to the machine and is dealt with elsewhere. It is worthwhile noting, however, that the system is essentially a 'passive ' item of equipment which can be swung out of the fibre-drawing line when not in use.

3.2 Fibre Drawing Conditions

3.2.1 Multimode Fibres

Multimode fibres are usually drawn to be 125 μm in diameter as this will be the internationally agreed standard. The drawing speed is typically 25 metres/minute although speeds as high as 100 metres/minute have been employed. Drawing temperatures in the range 1980°C to 2250°C have been employed, but, at the normal range of drawing speeds, a drawing temperature of about 2150°C provides an acceptable balance of drawing tension and drawing speed. Unless the preform is to be sleeved in another silica tube to increase the fibre-diameter:core-diameter ratio, the drawing conditions are directly calculated from a knowledge of the preform's overall diameter. Having specified the nominal drawing speed and the required fibre diameter, the preform feeding speed is calculated from the simple continuity equation:-

$$S_f . A_f = S_p . A_p \qquad (3.1)$$

where S_f = fibre drawing speed (mm/s)
A_f = fibre cross-sectional area (mm^2)
S_p = preform feeding speed (mm/s)
A_p = preform cross-sectional area (mm^2)

For a typical graded-index multimode preform based on a 20 mm OD x 1.5 mm wall thickness silica substrate, and possessing a 2:1 overall-diameter:core-diameter ratio, the preform diameter is of the order of 12.5 mm and S_p is then 0.04 mm/s.

Fibre drawing is commenced under manual control of drawing speed, and is switched to automatic control when the drawing conditions have stabilised. From a 45 cm length of preform, greater than 4 km of useful fibre can generally be obtained.

By depositing a larger core in the preform and sleeving the preform prior to drawing, up to 6 km of fibre has been obtained from one preform. If the preform is sleeved, account of the cross-sectional area of the sleeving tube must be made in the calculation of S_p from equation 3.1. For very much longer lengths of fibre to be obtained it is felt that the use of a larger substrate tube and higher deposition rates would be preferable to the preform sleeving approach.

3.2.2 Monomode-Fibres

Monomode-fibre preforms are generally sleeved before drawing to provide the necessary core to reference surface diameter ratio in the resultant fibre. Having established the core size and index difference in the preform, as described in Chapter 2, the draw-down ratio of the preform is determined by the V-value required in the fibre at its operational wavelength. Hence, if a_p is the core radius in the preform, and a_f the core radius in the fibre, then the draw-down ratio is given by:-

$$R = \frac{a_p}{a_f} = a_p \cdot \frac{V \cdot \lambda}{2\pi \sqrt{2n\Delta n}} \qquad (3.2)$$

where V = V-value of fibre at operating wavelength

$\sqrt{2n\Delta n}$ = numerical aperture of preform (assumed to be the same in the fibre.)

If r_f and r_p are the outer radii of fibre and preform respectively then the cross-sectional area of sleeving to give the specified core to reference surface diameter ratio in the fibre is given by:-

$$A \text{ sleeve} = \pi \left[\left(\frac{r_f}{a_f} \right)^2 \cdot a_p^2 - r_p^2 \right] \qquad (3.3)$$

Silica sleeving tubes are then selected to give the correct cross-sectional area, and they are carefully cleaned before being concentrically sleeved around the preform. The preform is then drawn in the same manner as the multimode fibres, although the furnace temperature may be set at a higher value to ensure the complete fusion of the sleeving tubes and preform in the draw-down zone.

For a preform having a 1 mm core diameter, an 8 mm overall diameter, and a numerical aperture of 0.12 to be drawn into monomode fibre having V = 2.4 at 1.3 μm, the core diameter in the fibre will be 8.3 μm, the draw-down ratio will be 121, and sleeving tubes of 128 mm^2 cross-sectional area will be required to provide an overall fibre diameter of 125 μm. Approximately 6.5 km of fibre could then be drawn from a 45 cm length of preform.

3.3 Investigation of Fibre Drawing Conditions & Diameter Stability

Previous experience with the drawing of soft-glass fibres had shown that the fibre drawing process was particularly stable and that long lengths of fibre could be drawn with diameter variations of less than $\pm$ 2 μm in 150 μm over a 1 kilometre length[1]. Fibre diameter control was effected simply by electronically interlocking the preform feed and fibre drawing drive systems such that a change in fibre winding speed was accompanied by a proportional change in preform feeding speed to maintain the diameter of the fibre constant at a pre-determined value. As this technique was successful with soft-glass fibres it was assumed that it would be so with silica fibres drawn from the graphite furnace, and many lengths of fibre were manufactured in this way[3].

However, with the acquisition of the scanning laser diameter measuring system it became clear that this was not always the case, and severe diameter disturbances were frequently experienced when drawing fibre from HCVD preforms. Systematic study of the fibre-drawing conditions revealed a number of diameter noise sources which were previously unknown, and led to modifications to the fibre-drawing furnace and also to the HCVD process itself.

3.3.1 Influence of Preform Surface Conditions Upon Fibre Diameter

When drawing multimode fibres from HCVD preforms it was found that, apart from the transients in fibre diameter which are experienced at the start of the draw (when steady state conditions are being established), severe fluctuations were also present throughout the drawing process. These variations were apparently random and could not be related to changes in pulling speed, preform feed speed or hot-zone temperature, which were all maintained constant throughout the pull. A typical diameter versus length plot for a 1.5 km section of graded-index multimode fibre, VD240, drawn under steady-state conditions with 'open-loop' diameter control is shown in figure 3.3. The fibre was drawn to be 125 μm overall diameter from a uniform preform having a 12.5 mm overall diameter; the section of fibre shown in the figure thus corresponds to a section of preform about 15 cm in length. It can be seen that there is a high-frequency diameter fluctuation of approximately $\pm$ 1 μm on which a number of low-frequency, major perturbations of diameter are superimposed. For example, at Point A on the figure, the fibre diameter falls to 115 μm, increases to 220 μm before decreasing to 117 μm and then returning to its steady-state value. The occurrence of such large diameter changes under apparently steady-state drawing conditions raised doubts about the homogeneity of the HCVD preform along its length.

To establish that the diameter fluctuations were not caused by instabilities in the drawing machine, a length of fibre was drawn under similar conditions from a high-quality synthetic silica rod; the diameter plot along its length is given in figure 3.4. No significant deviations from the set-point diameter were present along the entire 3 km length. As with the HCVD fibre, there was a high-frequency diameter oscillation of about $\pm$ 1 μm around the 125 μm set-point.

The diameter perturbations in VD240 were evidently due to the preform quality, and a number of other preforms were closely examined before drawing. In almost every case, small carbonaceous particles were found embedded in the preform surface; the particles were known to have originated from sooty deposits built up on the front-face of the deposition burner, which at that time was using an oxypropane flame for deposition. During the deposition process some of this soot would be carried from the burner by the flame and embedded in the surface of the silica deposition tube. Furthermore at the preform collapse stage the deposits migrated into the silica itself and could not easily be removed from the preform without etching. It was concluded that the deposits, being carbonaceous, would not draw-down in the same manner as a glass, and would therefore tend to 'hold-back' in the drawing zone until they reached a critical point at which they must pass out of the drawing zone, giving a large diameter increase.

The theory was confirmed in a controlled experiment in which a synthetic silica rod was subjected to a flame treatment over half its length by a sooty, oxypropane flame. The whole rod was then fire-polished using an oxyhydrogen flame, and was subsequently examined for the presence of sooty deposits beneath the surface of the glass. Many deposits were found along the first section and their position was noted before the rod was drawn into fibre. The diameter versus length plot is shown in figure 3.5, and it can be seen that many diameter perturbations occurred in the section of fibre drawn from the oxypropane flame-treated section, and that none occurred in

the fibre drawn from the 'control' section. The position of the diameter perturbations along the length of the fibre correlated exactly with the position of the deposits on the preform. The form of the fluctuations is consistent with the theory that the deposits do not draw-down, and it is interesting to note that a reduction in fibre diameter occurs before and after the large increase in diameter.

The use of propane as the fuel gas during deposition was immediately discontinued and a natural gas supply was installed as a replacement. Natural gas is principally composed of methane and hydrogen, and thus gives a much cleaner flame which is more suitable for use in the deposition process. The improvement in preform quality was significant, and the severe fibre diameter fluctuations due to surface contamination were eliminated. Figure 3.6 shows the diameter versus length plot along a 1 km section of a 4 km length of fibre, VD244, drawn from a preform made using an oxy-natural-gas deposition flame. The diameter is now much more stable with less then 1μm drift in mean diameter over this section; the high-frequency diameter noise of about $\pm$ 1μm still exists. Over the full 4 km length the mean diameter remained constant at 125μm for the first 3.4 km and then began to fall smoothly over the remaining length, reaching a minimum of 121μm at the 4 km point; this tapering effect is due to the taper in preform diameter at the start-of-deposition end, and can be avoided by the use of the diameter monitor in a feedback loop to control the fibre diameter by varying the drawing speed (see Section 3.2.3).

3.3.2 Influence of Furnace Conditions Upon Fibre Diameter Noise

Having eliminated the source of major diameter variations during drawing, attention switched to the reduction of the high-frequency diameter noise, which can lead to mode coupling and increased attenuation in multimode fibres. It was found that the diameter noise was particularly sensitive to the gas-flow conditions within the graphite resistance-heated furnace.

Although the furnace element temperature was normally controlled to within $\pm$ 0.1 deg. C of the set-point[2], fluctuations in the flow of argon through the furnace were found to produce significant changes in the magnitude of the high-frequency noise. Increasing the total flow rate of argon through the furnace generally led to increased diameter variations, whilst altering the ratio of gas introduced at the top of the furnace to that introduced at the bottom also had a marked effect: Whilst reducing the flow rate of argon would obviously have a beneficial effect upon diameter stability, due regard had to be given to the possible reduction of furnace lifetime by the ingress of atmospheric oxygen. Furthermore, Kaiser[4] had shown that the flow of inert gas over the fibre and preform provided a clean environment for fibre-forming, thereby preventing contamination of the fibre by dust within the furnace atmosphere.

In the furnace developed at Southampton[2], argon is fed into the furnace chamber through two ports, and leaves the furnace through either of the iris diaphragms at the top and bottom of the chamber, or through the outlet port which is sourced from the region of the furnace hot-zone, see figure 3.2. In practice, the upper iris is closed around the preform and the major portion of the gas is exhausted to the atmosphere via the lower iris and the outlet vent. It would not seem unreasonable to assume that a reduction of argon into the upper part of the furnace would lead to a reduction of the gas turbulence within the hot-zone and a reduction in diameter noise. In fact the opposite was found, and after further investigation it was established that the gas flow within the upper half of the furnace was being affected by airflow from a fan which, by blowing across the top of the furnace, was intended to cool the upper iris and its housing. At low argon flows the pressure within the upper part of the furnace was insufficient to prevent air entering the furnace through the narrow clearances around the power terminals, and the fibre diameter was thus modulated by the fan. By simply dis-connecting the fan, a reduction in diameter noise by a factor of two was achieved as shown in fig. 3.7(a) and (b); however, without the air cooling the upper iris and its housing rapidly overheated.

The furnace top was therefore redesigned with a view to improving the water cooling of the iris diaphragm and to providing gas-tight seals around the terminals. At the same time Dr. Payne modified the element design to provide a more robust element which would have a longer lifetime than the rather intricate elements of the original design. The use of the new components was a complete success and obviated the need for additional forced-air cooling of the furnace top-plate. Reduction of the argon flow through the furnace was possible and a substantial improvement in fibre diameter noise was obtained as shown in figure 3.7(c). Further work on the characterisation of the noise power spectrum has been undertaken by Mr. M.R. Hadley[5], who has been able to identify the resonances within the furnace and to adjust the gas flows to a near-optimal value, thereby achieving the remarkable r.m.s. noise figure of $\pm$ 0.16 μm over a kilometre length of fibre.

3.3.3 Reduction of Long-Term Diameter Variations

By incorporating the Anritsu diameter measuring system in a feedback loop with the winding drum's speed controller, it has been possible to obtain automatic control of fibre diameter in-line with fibre drawing. The Anritsu unit provides an analogue signal output which is proportional to the deviation of the actual fibre diameter from the set fibre diameter. This analogue signal is applied to a signal-conditioning three-term controller which in turn provides the set-speed reference signal for the fibre winding drum. Deviations of the fibre diameter about its set-point are thus accompanied by a change in drawing speed which brings the fibre diameter back to its desired value. Although this system was intended to control long-term diameter deviations due to preform taper it has been found that diameter variations having a spatial frequency as high as 0.5 m^{-1} can be controlled[5].

A further degree of improvement in fibre diameter deviations has thus been obtained, and very long lengths of fibre have been drawn with accurately controlled diameter. For example, in figure 3.8, the diameter versus length characteristics of a 5 km length of graded-index multimode fibre, VD281, are shown. The high-frequency noise is less than $\pm$ 0.5 μm over the entire length, there are no severe disturbances due to surface contamination of the preform, and the long-term drift in diameter due to preform taper has been eliminated. Compared with the results presented in figure 3.3, it is seen that a significant improvement of fibre quality has been obtained, and, as will be shown in Chapter 4, this has been accompanied by a reduction in the wavelength-independent waveguide losses present in the multimode HCVD fibres. These improvements to the fibre-drawing equipment and preform manufacturing processes have thus led to an improvement in the quality of the fibres, and, perhaps more importantly, have established the viability of the fibre-drawing machine for use in an industrial manufacturing environment. There is little doubt that the technology would not have been attractive to industry if the fibre diameter noise had not been reduced to its current level.

3.4 References to Chapter 3

1. Gambling, W.A., and Payne, D.N.: 'The preparation of glass- and liquid-core optical fibres', Opto-electronics, 5(1973), pp 297 - 307.

2. Payne, D.N., and Gambling, W.A.: 'A resistance-heated high-temperature furnace for drawing silica-based fibres for optical communications', Bull. Am. Ceram. Soc., 55 (1976), pp 195 - 197.

3. Gambling, W.A., Payne, D.N., Hammond, C.R., and Norman, S.R.: 'Optical fibres based on phosphosilicate glass', ProcIEE, 123 (1976), pp 570 - 576.

4. Kaiser, P.: 'Contamination of furnace-drawn silica fibres', App. Opt., 16 (1977), pp 701 - 704.

5. Hadley, M.R., Payne, D.N., and Mansfield, R.J.; 'Identificacion of sources of diameter fluctuations in smooth optical fibres by analysis of their spatial power spectrum', Proc. Sixth European Conference on Optical Communications, York 1980, pp 53 - 56.

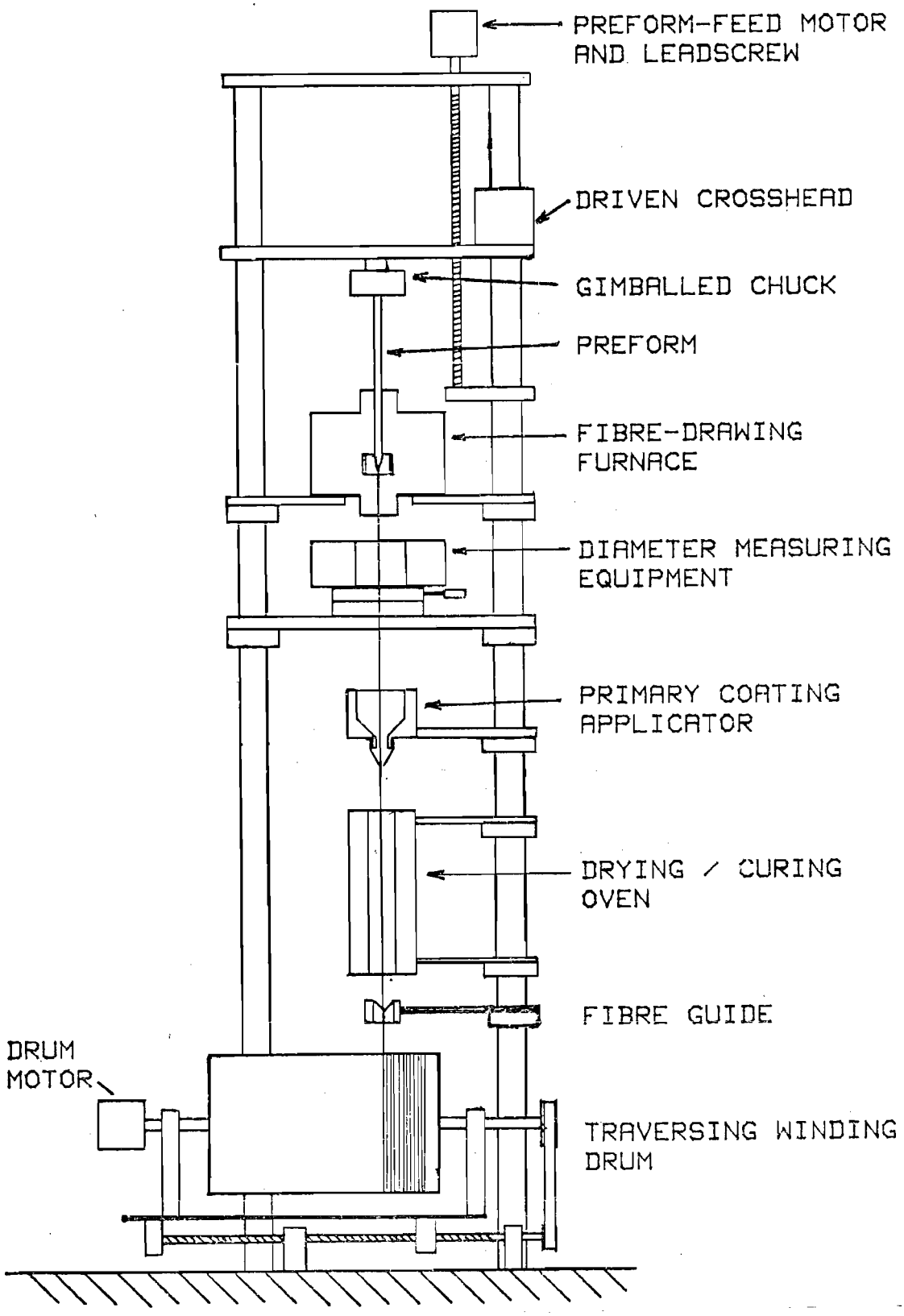

SCHEMATIC ILLUSTRATION OF FIBRE DRAWING MACHINE

FIGURE 3.1

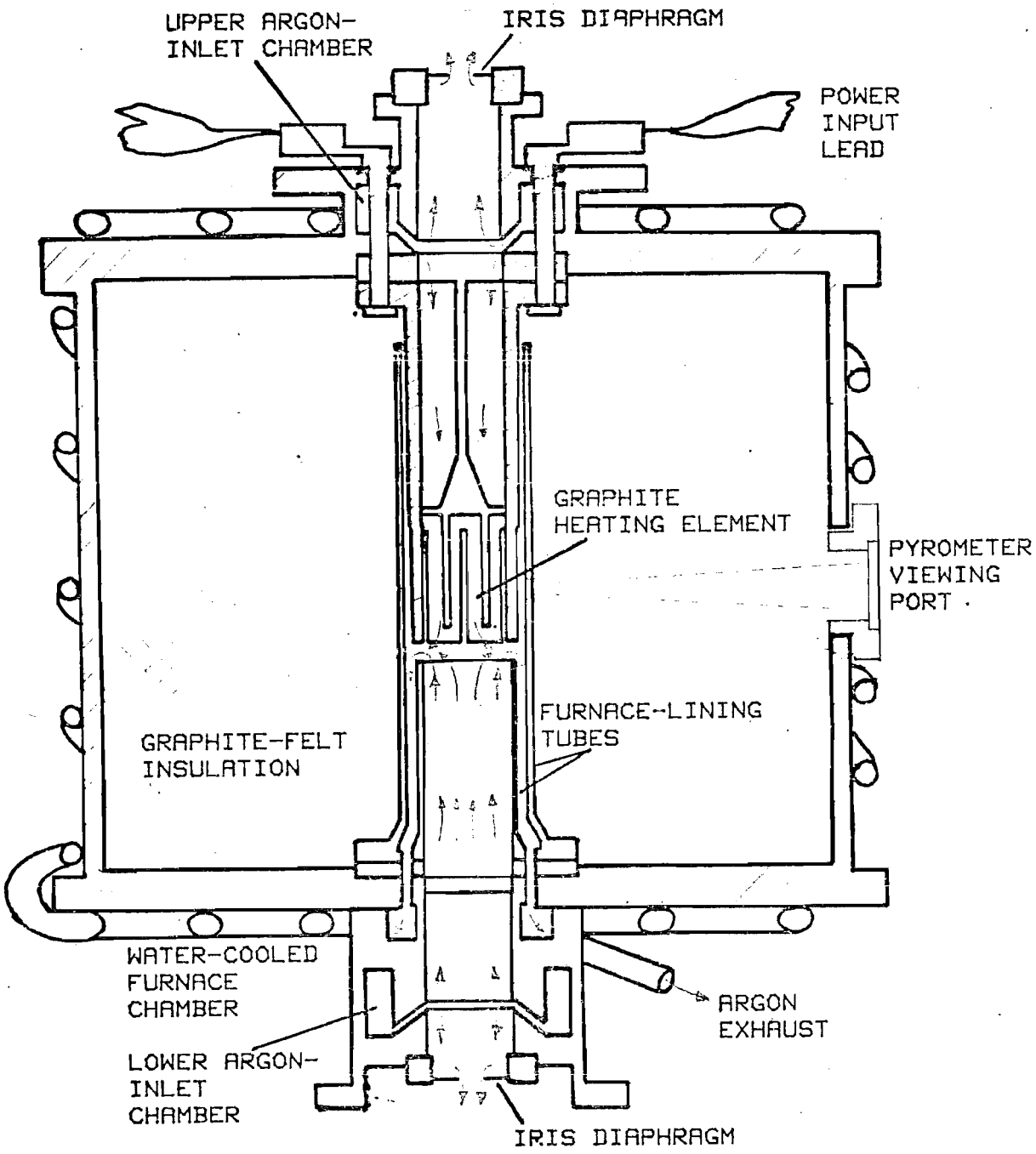

NOTE: ARROWS DELINEATE THE ARGON FLOW PATHS

SCHEMATIC REPRESENTATION OF A VERTICAL CROSS-SECTION THROUGH THE GRAPHITE RESISTANCE-HEATED FURNACE FOR DRAWING OF SILICA-BASED FIBRES

FIGURE 3.2

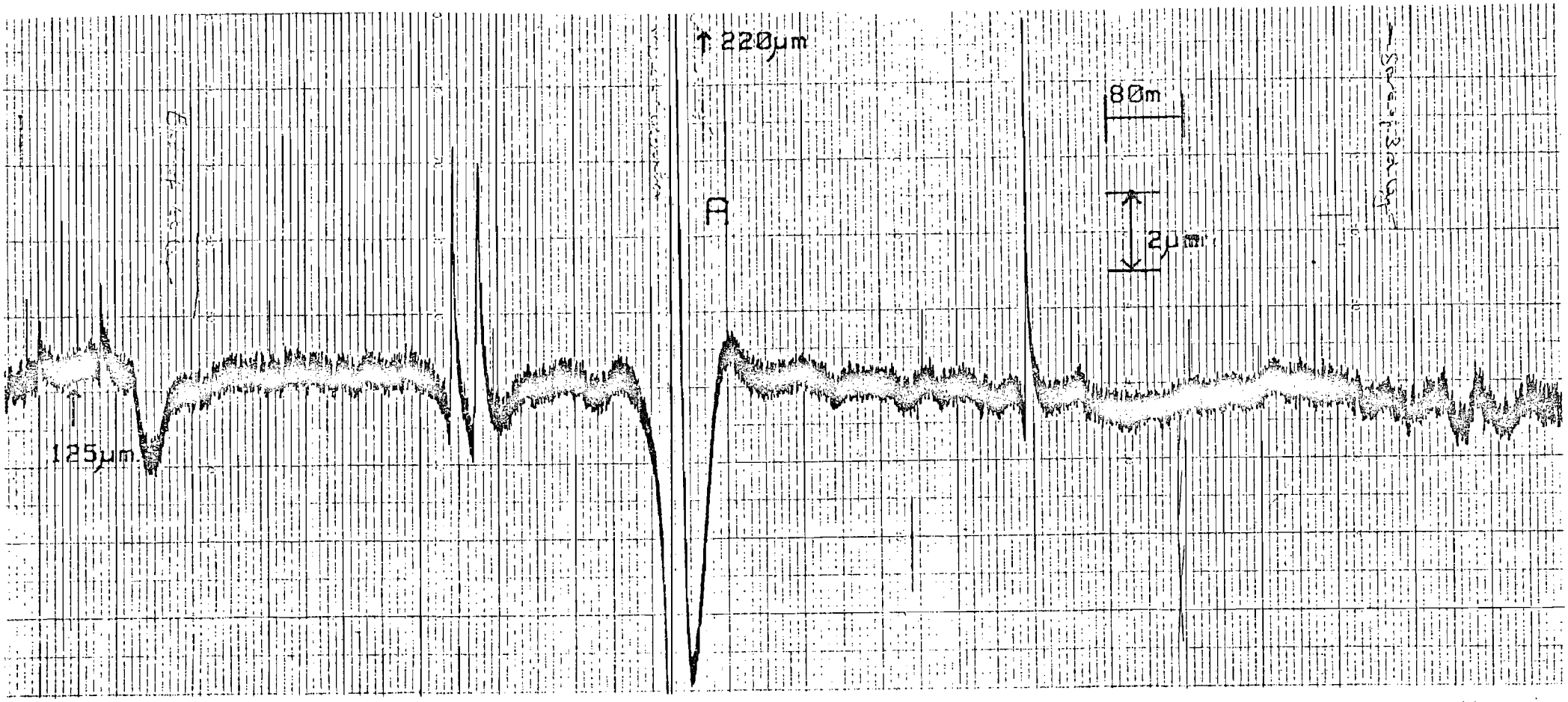

Diameter variations in fibre VD240. Nominal fibre diameter= 125μm.

The fibre was drawn at constant speed and constant furnace temperature.

FIGURE 3.3

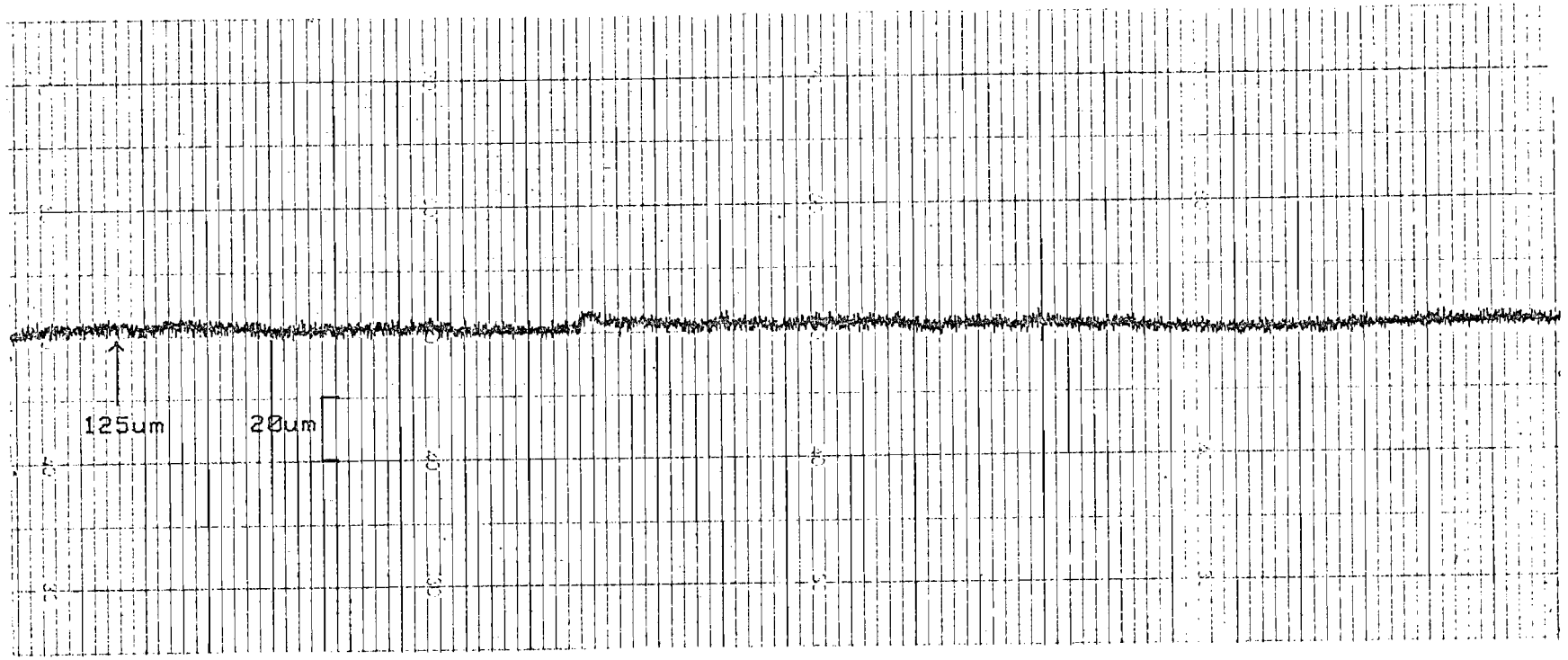

Nominal fibre diameter = 125um

DIAMETER VARIATIONS ALONG A LENGTH OF FIBRE DRAWN FROM SYNTHETIC SILICA ROD. The figure shows the diameter fluctuations along a 1km section of the 3km length. The fibre was drawn under "open-loop" control of fibre-diameter; the drawing-temperature, drawing-speed, and feed-speed were held constant. No severe diameter perturbations were observed over the entire length.

FIGURE 3.4

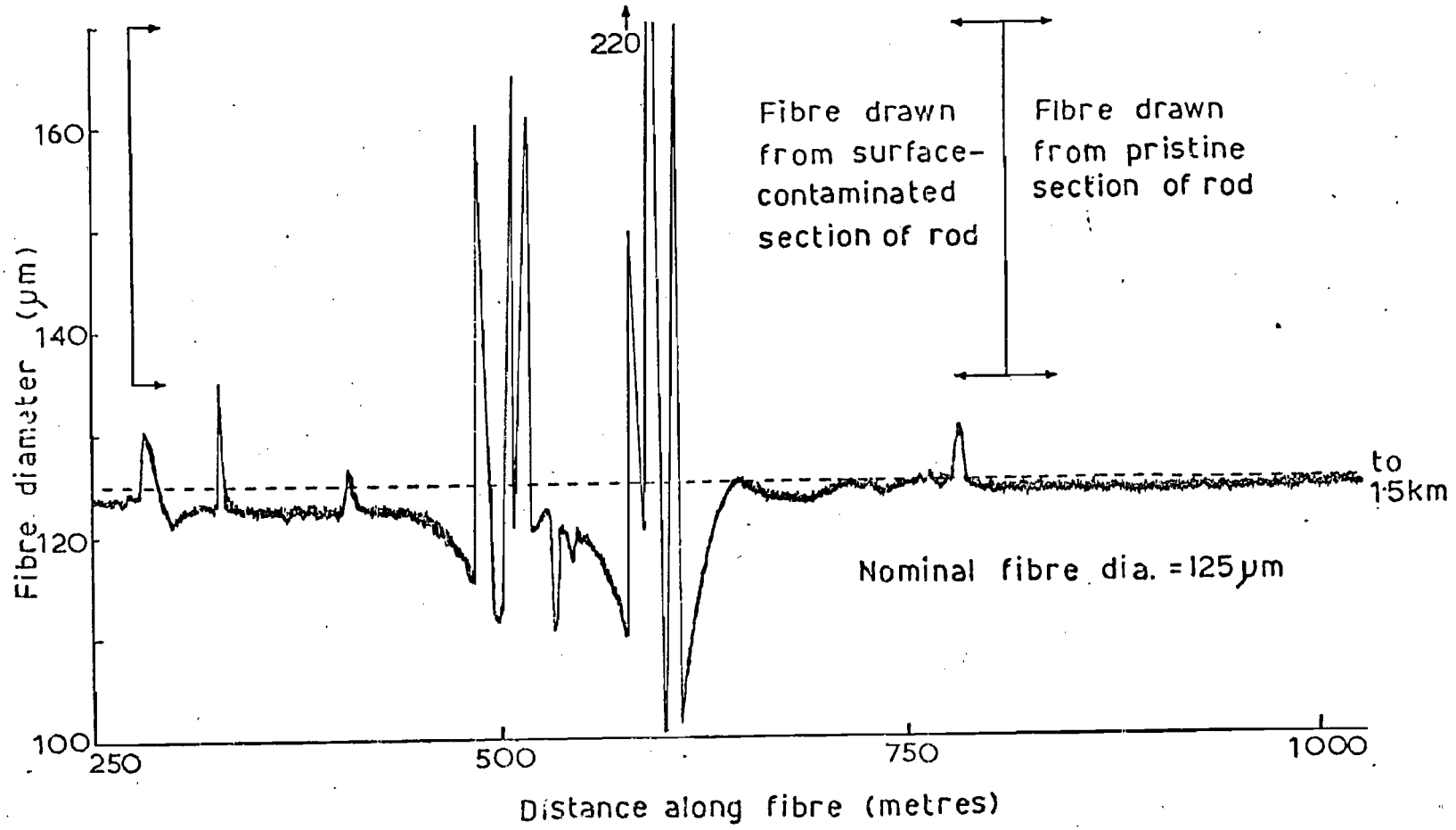

INFLUENCE OF PREFORM SURFACE CONTAMINATION UPON THE DIAMETER VARIATIONS IN A LENGTH OF SILICA FIBRE. The fibre was drawn from a synthetic silica rod which had been flame-treated along a section of its length by a sooty oxypropane flame. The severe perturbations of the fibre diameter occurred at points where carbonaceous deposits were present on the surface of the silica rod.

FIGURE 3.5

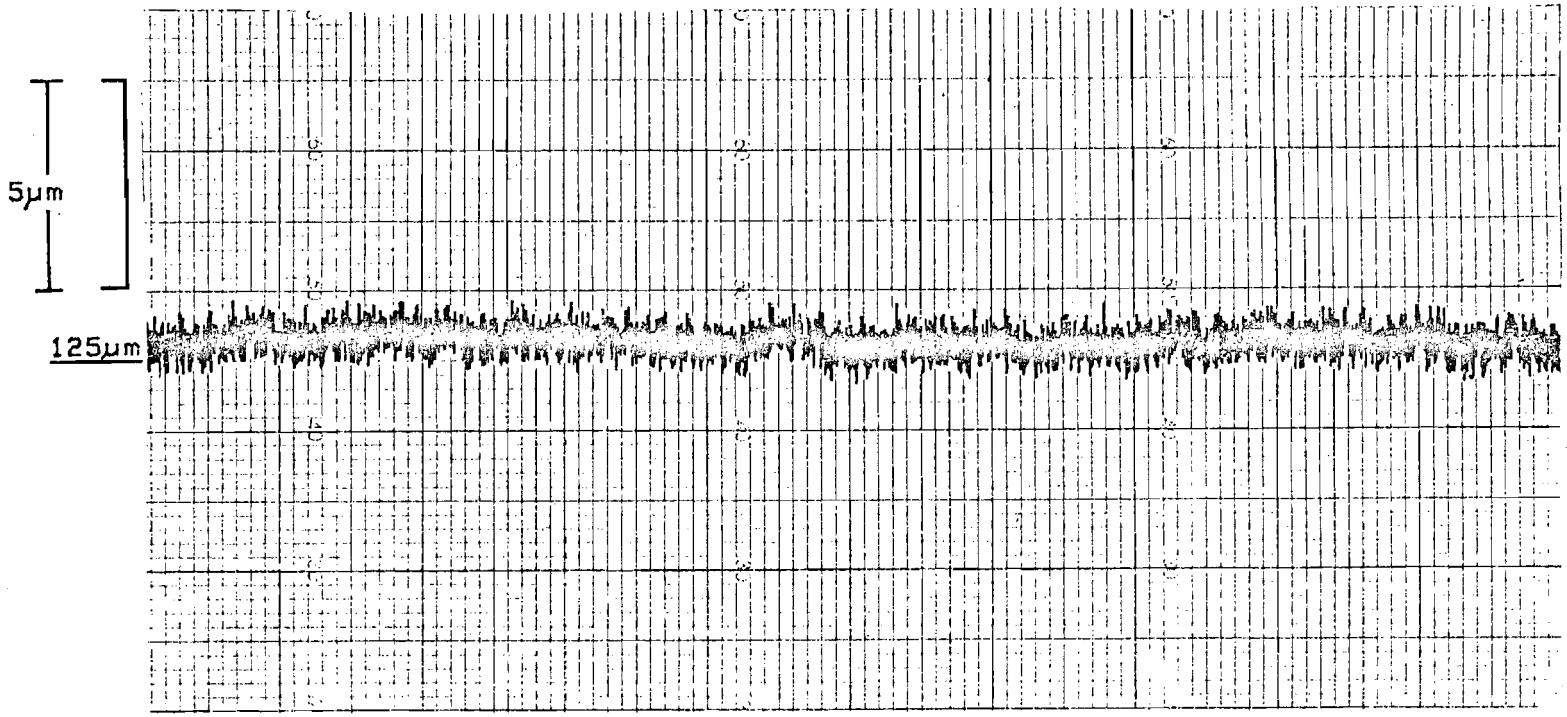

Nominal fibre diameter =125µm

DIAMETER VARIATIONS ALONG A 1km SECTION OF FIBRE VD244. The fibre was drawn from a preform which had been fabricated using an oxy-natural-gas deposition flame. The severe diameter variations found in earlier fibres (see figure 3.3) were not present in the 4km length of this fibre.

FIGURE 3.6

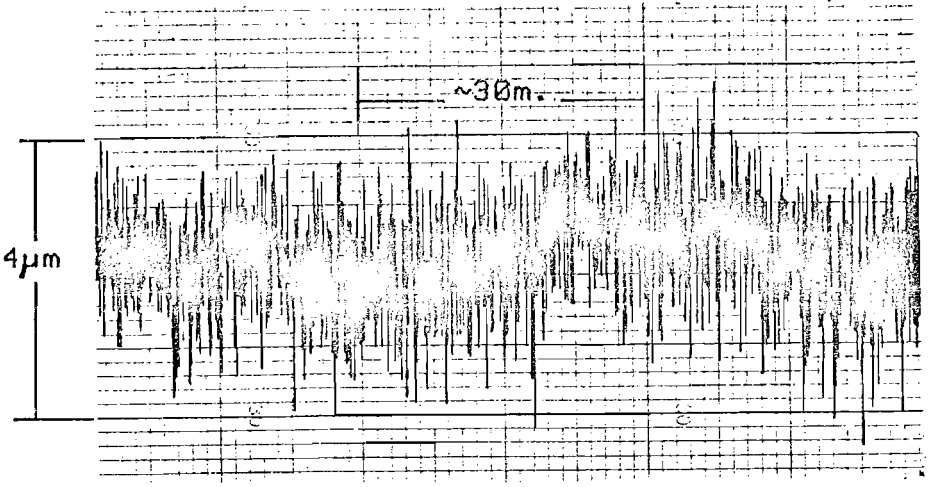

A. Fibre diameter noise with forced-air cooling of upper iris-housing

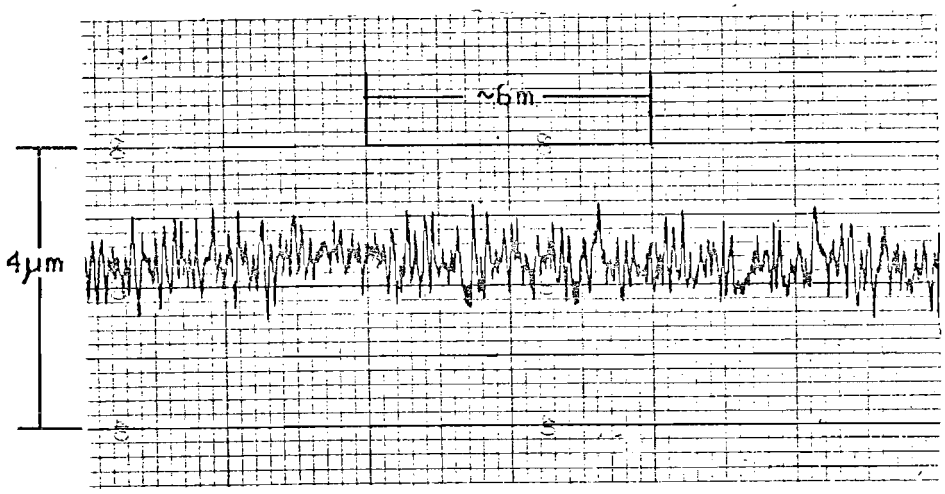

B. Fibre diameter noise after ceasing forced-air cooling of upper iris-housing.

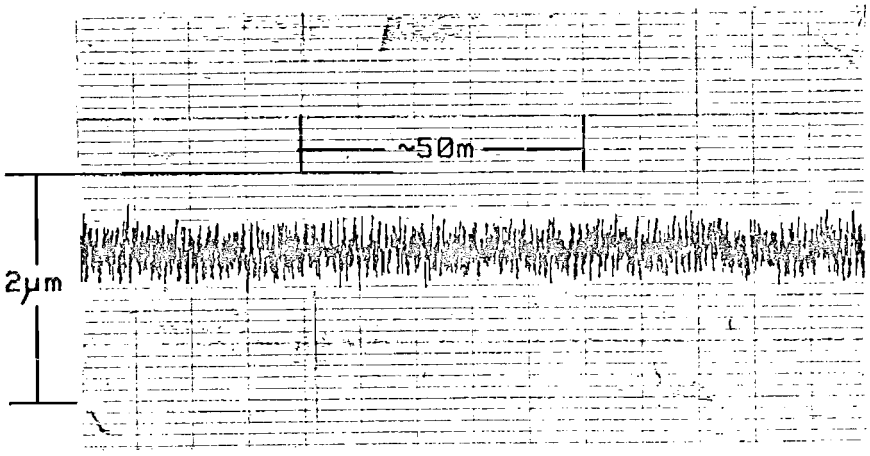

C. Fibre diameter noise using modified furnace with improved gas-sealing arrangements.

ILLUSTRATION OF THE INFLUENCE OF GAS-FLOW CONDITIONS WITHIN THE GRAPHITE FIBRE-DRAWING FURNACE UPON FIBRE DIAMETER NOISE.

In the original furnace design (figure 3.2) it was found that the fibre diameter was being modulated by a cooling-fan which was intended to cool the upper iris-housing.

FIGURE 3.7

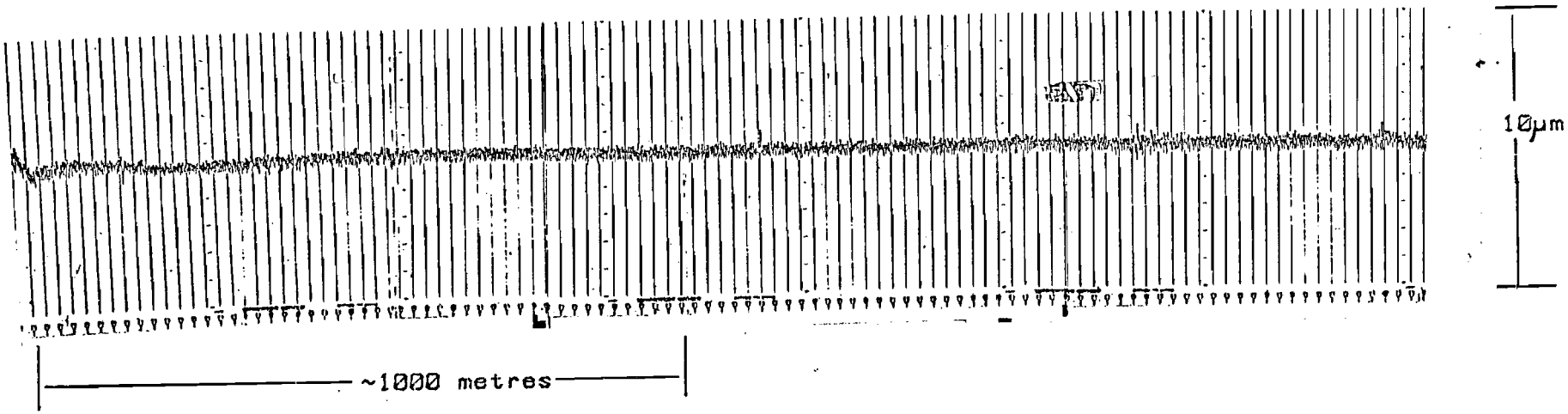

DIAMETER VARIATIONS ALONG THE LENGTH OF FIBRE VD281. The diameter plot is shown for the first 2km section of the 5km length of fibre. Over the entire 5km length, the fibre diameter was maintained within ± 0.5µm of the 125µm nominal diameter. The result was achieved by employing feedback control of the fibre-drawing speed to eliminate long-term fibre diameter variations due to preform taper.

FIGURE 3.8